



CHALMERS
UNIVERSITY OF TECHNOLOGY



Design criteria for seakeeping and stability of fishing vessels in regular waves

Master's thesis in the Nordic Master in Maritime Engineering – Ship Design track

NESTOR J. GÓMEZ ROJAS

DEPARTMENT OF MECHANICS AND MARITIME SCIENCES

CHALMERS UNIVERSITY OF TECHNOLOGY
Gothenburg, Sweden 2021
www.chalmers.se

MASTER'S THESIS IN THE NORDIC MASTER IN MARITIME ENGINEERING
– SHIP DESIGN TRACK

Design Criteria for Seakeeping and Stability of Fishing Vessels in Regular Waves

A systematic study of the seakeeping and dynamic stability of a stern trawler fishing vessel to determine specific design criteria.

Nestor Juan de Dios Gómez Rojas

Department of Mechanics and Maritime Sciences
Division of Maritime Technology

CHALMERS UNIVERSITY OF TECHNOLOGY
Gothenburg, Sweden 2021

Design Criteria for Seakeeping and Stability of Fishing Vessels in Regular Waves
A systematic study of the seakeeping and dynamic stability of a stern trawler fishing vessel to determine specific design criteria.

Nestor Juan de Dios Gómez Rojas

© Nestor Juan de Dios Gómez Rojas, 2021-06-04

Master's Thesis 2021:81
Department of Mechanics and Maritime Sciences
Division of Maritime Technology

Chalmers University of Technology
SE-412 96 Gothenburg
Sweden
Telephone: + 46 (0)72 - 869 6405

Cover:
Fishing vessel Stella Nova IX, picture taken by Magnus Wikander (SSPA Sweden AB).

Department of Mechanics and Maritime Sciences
Gothenburg, Sweden 2021-06-04

Design Criteria for Seakeeping and Stability of Fishing Vessels in Regular Waves
A systematic study of the seakeeping and dynamic stability of a stern trawler fishing vessel to determine specific design criteria.

Master's thesis in the Nordic Master in Maritime Engineering – Ship design track.
Nestor Juan de Dios Gómez Rojas

Department of Mechanics and Maritime Sciences
Division of Maritime Technology
Chalmers University of Technology

Abstract

The design requirements for new fishing vessels tend to be mostly based on existing fishing vessels. The design stage normally does not include an initial study of the seakeeping and dynamic stability of the vessels, due to the lack of time and budget and of documented criteria for this vessel segment. This study focuses on the compliance of a selected stern trawler fishing vessel with general existing seakeeping and parametric rolling criteria (e.g., ISO, 1997; Lewis, 1989; Nordforsk, 1987) to (a) select suitable seakeeping criteria for fishing vessels and (b) propose an assessment methodology to optimize such criteria, using the software SHIPFLOW Motions.

To test compliance, a set of typical working conditions (e.g., trawling, lightship, fully loaded) for the selected fishing vessel has been computed employing a commercial computational fluid dynamics (CFD) software tool, SHIPFLOW, which is based on non-linear potential flow theory. The results (ship responses or motions) have been post-processed through a code developed in MATLAB (RBSMC). Both seakeeping and the second-generation IMO stability criteria (specifically parametric roll due to its occurrence in this type of vessel despite its geometrical characteristics that differ from tankers and container vessels, which are the most susceptible to the phenomenon) have been assessed through a systematic study of the influence of the centre of gravity over the ship responses under different working conditions. This approach allowed to understand the behaviour of this vessel, where its responses were highly dependent on the working conditions and wave characteristics.

It was seen that the resonance of the studied motions (heave, pitch, and roll) take place at longer wavelengths than a tanker or a container. The centre of gravity location highly influences the responses. It was found that the trawling condition was one of the most affected ones, presenting high amplitudes of pitch and roll. Instead of applying an external force for modelling the trawling force, the trawling condition was modelled through shifting the position of the centre of gravity. Under this working condition, the vessel showed high pitch and roll angles of low acceleration that surpassed the acceptable limits. Meanwhile, in other conditions, the responses complied with the criteria. The lightship condition was the most sensitive condition in terms of parametric roll, where the variation of GM (metacentric radius) is susceptible to the occurrence of parametric roll, and the right waves could trigger the phenomenon. In general, the roll damping coefficient of a fishing vessel is high enough to prevent parametric rolling.

The selected criteria often resulted in margins which were larger than the responses of the vessel except for the trawling condition for which the limiting values of the criteria were smaller than the obtained responses. The presented methodology and the customized criteria in this work can be used for evaluation of fishing vessels in the design stage.

Keywords: Seakeeping; Regular Waves; Fishing Trawlers; Parametric Rolling; SHIPFLOW; IMO Second Generation Intact Stability Criteria.

Content

Abstract	I
Content.....	III
Preface.....	V
1 Introduction.....	1
1.1 Background	1
1.2 Study objectives	2
1.2.1 Scope and delimitations	2
2 Theory	3
2.1 Seakeeping	3
2.1.1 Waves.....	4
2.1.2 Numerical predictions for seakeeping	13
2.2 Stability	16
2.2.1 Intact stability.....	16
2.2.2 Second generation intact stability criteria.....	16
3 Fishing vessels	23
3.1 Main characteristics and definitions.....	23
3.2 Stern trawler fishing vessel	23
3.2.1 Fishing procedure.....	24
3.2.2 Fishing vessel of interest.....	26
4 Methodology	30
4.1 Methodological overview.....	30
4.1.1 Studied conditions.....	30
4.1.2 Considerations.....	32
4.2 Methods and tools	37
5 Results and discussion	45
5.1 Ship responses	45
5.2 Seakeeping results	48
5.2.1 Light ship conditions.....	54
5.2.2 Trawling conditions	58
5.2.3 Fully loaded conditions.....	60
5.3 Parametric Rolling.....	67
5.4 Questionnaire	69
6 Conclusions.....	70
6.1 Suggestions for further research.....	71
7 References.....	73
Appendix A.....	75

Appendix B	77
Appendix C	79
RBSMC.....	79
Code for parametric rolling evaluation	93
Code for triggering parametric rolling	97
Appendix D	104
Criteria analyses.....	104
Light ship working conditions	104
Trawling working conditions	112
Fully loaded working conditions	116

Preface

In this study, the chosen fishing vessel has been analysed under regular waves of frequent characteristics encountered by such vessels when sailing. These simulations also considered the real working conditions of the fishing vessel. The report is part of the research project “ASK – Arbetsbåtars Sjöegenskapskriterier”. This project is financed by Trafikverket (The Swedish Transport Administration) and carried out by SSPA Sweden AB along with KTH as a partner, and concerns seakeeping criteria in the design stage of work boats up to 75m in length.

This thesis has been carried out under the supervision of Arash Eslamdoost (Associate Professor at Chalmers University of Technology) and Ulrik Dam Nielsen (Associate Professor at Technical University of Denmark) as well as under the co-supervision of Nicole Costa (Senior Researcher) and Magnus Wikander (Business Development Manager) at SSPA Sweden AB, in the “ASK” research project.

I would also like to thank Martin Kjellberg (SSPA Sweden AB) and Francesco Coslovich (Chalmers University of Technology) for their support with the understanding of SHIPFLOW, Axel Hörteborn (SSPA Sweden AB) who provided critical information regarding the sea characteristics of the working zones, and Nicolas Bathfield (SSPA Sweden AB) for his input to this report. All the computational simulations were carried out by using a student license of SHIPFLOW Motions Potential Flow Code at Chalmers University of Technology with data obtained from ERA5 from Copernicus Products.

The information related to the fishing vessel used in this study was provided by JEA Marine Consulting AB (the ship designer). Fredrik Gustafsson, one of the former skippers of the ship, is also acknowledged for sharing his experience of working on this vessel.

Gothenburg 2021-06-04

Nestor Juan de Dios Gómez Rojas

1 Introduction

1.1 Background

Modern vessel procurement is often specified in terms of the vessel's power performance and speed in a certain sea area and state. This is unclear in terms of measurable seakeeping criteria/properties e.g., rolling angles, acceleration, frequencies of the motions, dimensioning of structure with regards to slamming, risk of broaching, water on deck, perceived comfort, possibility to perform given tasks in the intended operating environment, physiological load, and the ship's course-keeping. Establishing these seakeeping criteria is difficult since ships have different purposes and dimensions. There are already some established criteria, which are considered in this study (e.g., ISO, 1997; Lewis, 1989; Nordforsk, 1987), but they apply mainly to large ships. Displacement and semi-displacement workboats (considering particularly those with <75 meters in length), e.g., fishing vessels, are traditionally designed and built based on existing vessels since there is often a lack of time and budget to develop them and to run an initial study of the seakeeping and dynamic stability of the vessels. So, well-established criteria for these vessels are lacking, and so is the categorization of how different work operations are influenced by the ship's motions. Hence, it becomes difficult to assess in the design stage whether a vessel has sufficiently good seaworthiness compared to others of its kind or if the design needs to be further iterated.

There are some studies focused on the evaluation of different hull shapes of fishing vessels (Sayli et al., 2006), where the importance of a seakeeping assessment in the early design stages is pointed out. Other studies assess performance concerning sea conditions, also for fishing vessels (e.g., Guedes Soares, Tello, & Ribeiro e Silva, 2010), where pre-defined criteria are implemented to analyse fishing vessel responses. However, these are limited to certain regions and for a limited range of vessels and conditions.

Fishing vessels' responses are highly dependent on their varying loading conditions when operating (caused by the fishing procedure). These loading conditions lead to another important variable, which is the changing centre of gravity during the operation due to the increase of the cargo (fish). The changing centre of gravity, along with the fishing procedure and the sea state, impact the ship with accelerations, forces, and moments of different magnitude all over the structure. In turn, the motions affect the work environment, the crew members, and even the installed equipment on deck (Riola & Arboleya, 2006). On this matter, seakeeping becomes a topic of importance for the safety of the vessel and for the phenomenon known as parametric rolling. Parametric rolling in fishing vessels was first studied by Neves et al. (1999) and then assessed by different authors. In the studies by Rodrigues et al. (2011) and by Mantari et al. (2011), the fishing procedure was a key part of the analysis due to the previously mentioned changing displacement, stability, and ship responses.

1.2 Study objectives

This report is part of the research project “ASK – Arbetsbåtars Sjöegenskapskriterier” financed by Trafikverket (The Swedish Transport Administration) and coordinated by SSPA Sweden AB.

The present thesis focuses on the compliance of a selected, well-documented, stern trawler fishing vessel (Stella Nova IX) with general existing seakeeping (see sub-section 2.1.1.3) and parametric rolling criteria with the purpose of (a) selecting criteria suitable for this type of ship and (b) proposing an assessment methodology to optimize such criteria, using the software SHIPFLOW Motions.

To achieve these objectives, the following steps were followed:

- A systematic analysis on how different parameters (common wave characteristics) influence the seakeeping characteristics of the fishing vessel model, assessing specifically the changing centre of gravity (see section 4.1.2) to select from existing criteria suitable ones for stern trawler fishing vessels.
- Test the vessel model for compliance with the IMO second generation intact stability criteria, regarding the parametric roll phenomenon (see sections 2.2.2), followed by an evaluation of the triggering conditions of the phenomenon.
- Feasibility and efficiency commentary about the SHIPFLOW Motions Potential Flow code for determining the motion of a fishing vessel in moderate seas and under different wave conditions.

1.2.1 Scope and delimitations

Due to time constraints, the study was based on one stern trawler fishing vessel, that operates in the Baltic Sea and the North Sea. The selection of the fishing vessel was made by SSPA Sweden AB given that this ship is a well-documented representative case of the region due to its characteristics and fishing procedure.

To frame the study, the wave characteristics were based on the most frequent sea states in the zones of study (see section 4.1.2) and the working conditions on the stability booklet provided by the ship designer (section 3.2.2). The sea states were statistically chosen from the data source ERA5, from the record of 2019 and 2020 (ECMWF, 2021).

The seakeeping criteria were selected based on the studied literature concerning their relevance and applicability to fishing vessels (Guedes Soares et al., 2010; Papanikolaou, 2001; Sayli et al., 2006). As established in section 2.1.1.3, the criteria used were selected from common criteria from the studied literature, according to its suitability for fishing vessels (see Table 2-6).

The results are evaluated with the selected seakeeping criteria and with the IMO Second Generation Intact Stability Criteria.

2 Theory

The literature covered in this report takes into consideration an introduction of the concepts of seakeeping and stability as well as its seakeeping criteria.

In the seakeeping subsection, an overview of waves systems, spectral analysis and numerical methods is presented as background for the justification of the numerical method and software chosen.

The subsection regarding intact and dynamic stability shows the same approach as the seakeeping subsection.

2.1 Seakeeping

Seakeeping ability or seaworthiness refers to the capability of a vessel to perform its mission at sea. Seakeeping takes into consideration different aspects, like wave characteristics and the ship's particulars. From these, it is possible to predict the different phenomena the vessel experiences at sea i.e., motions, wetness, slamming, etc. (Lewis, 1989; Graham, 1990; O'Hanlon & McCauley, 1974).

These phenomena are studied according to the degrees of freedom a vessel presents when floating freely, see Figure 2-1.

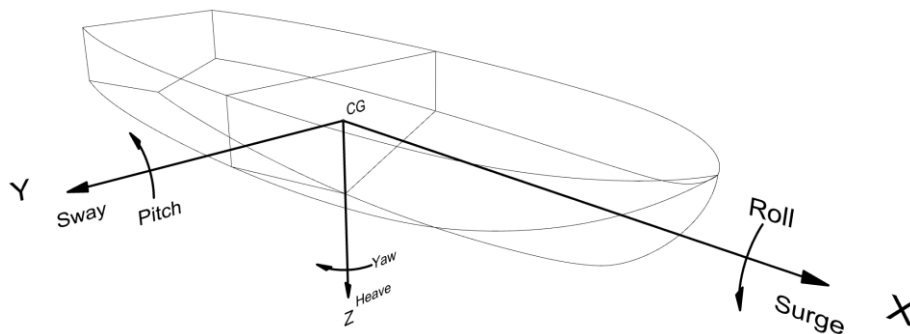


Figure 2-1: 6 Degrees of freedom of ship motions (Made in Rhinoceros 3D)

Each motion is described in Table 2-1. These motions measured relative to the vessel itself.

Table 2-1: Ship motions description

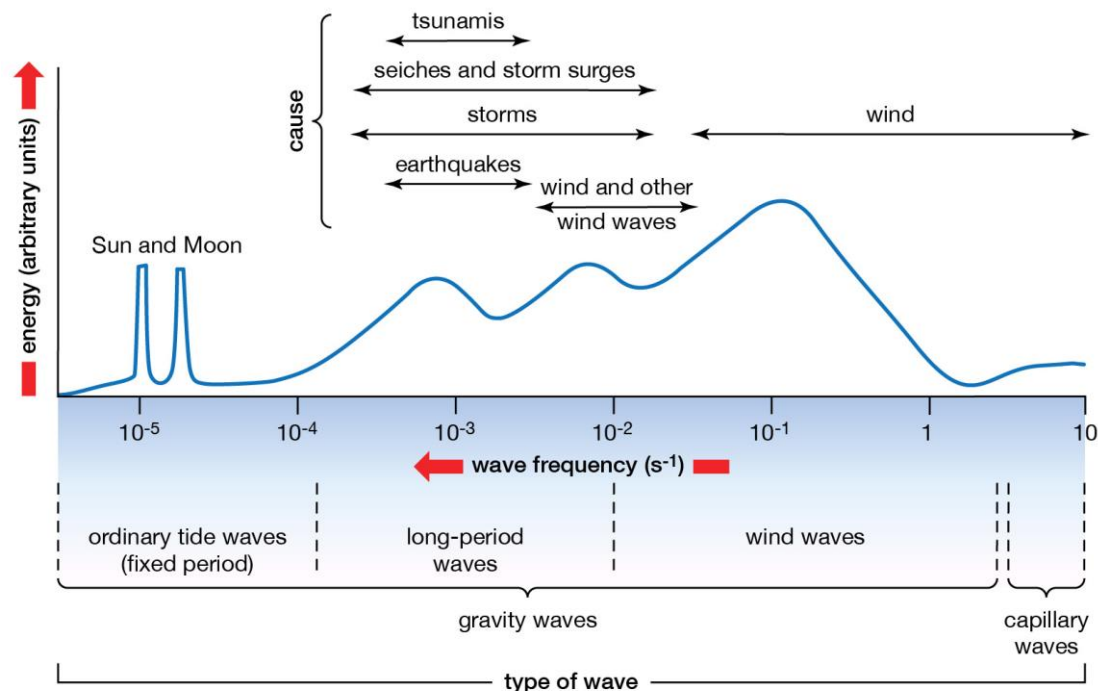
<i>Motion</i>	<i>Axis</i>	<i>Type</i>
<i>Surge</i>	<i>Along x</i>	<i>Translation</i>
<i>Roll</i>	<i>About x</i>	<i>Rotation</i>
<i>Sway</i>	<i>Along y</i>	<i>Translation</i>
<i>Pitch</i>	<i>About y</i>	<i>Rotation</i>
<i>Heave</i>	<i>Along z</i>	<i>Translation</i>
<i>Yaw</i>	<i>About z</i>	<i>Rotation</i>

2.1.1 Waves

Wave's characteristics are important inputs to consider when analysing a vessel at sea. It depends on the taken approach and wave theory adopted for the analysis of the vessel on how the results may vary.

Since there are several wave theories to consider, this section presents a theoretical background on the wave's physical models and its properties. Linear wave theory and Stokes waves are of interest due to their modelling possibility on many commercial software.

Surface gravity waves can be classified in short-term waves and long-term waves, see Figure 2-2.



© 2012 Encyclopædia Britannica, Inc.

Figure 2-2: Surface gravity wave types (Britannica, 2012)

Regular and irregular waves are the ones of interest for the purpose of the thesis. These are described in the following subsections.

2.1.1.1 Regular waves

Regular waves are normally created by wavemakers in basins for study purpose and cannot be found in oceans due to the controlled environment needed. These waves are characterized by its amplitude and frequency.

The governing theories behind these types of waves can be linear or non-linear. Each of those model waves, consider the orbital motion of the water particles, see Figure 2-3.

One of the most well-known linear approaches is the Airy wave's theory, which is also used for modelling random sea states (Goda, 2000) under this approach the modelled fluid flow is inviscid, incompressible and irrotational.

The equations governing the sinusoidal waves in deep water are shown in Table 2-2.

Table 2-2: Regular Airy wave's governing equations

<i>Properties</i>	<i>Symbol</i>	<i>Governing equation</i>
<i>Potential</i>	ϕ	$\phi = \zeta_a \left(\frac{g}{\omega} \right) \mu_1 \sin(kx - \omega t)$
<i>Wave elevation</i>	ζ	$\zeta = \zeta_a \cos(kx - \omega t)$
<i>Angular velocity</i>	ω	$\omega = \sqrt{kx}$
<i>Wave phase</i>		$kx - \omega t$
<i>Wavelength</i>	L	$L = \frac{gT^2}{2\pi}$
<i>Wave celerity</i>	c	$c = \sqrt{\frac{g}{k}}$
<i>Dynamic pressure</i>	P_d	$P_d = \zeta_a \rho g e^{kz} \cos(kx - \omega t)$
<i>Particle horizontal velocity</i>	u	$u = \zeta_a \omega e^{kz} \cos(kx - \omega t)$
<i>Particle vertical velocity</i>	w	$w = \zeta_a \omega e^{kz} \sin(kx - \omega t)$
<i>Particle horizontal acceleration</i>	\dot{u}	$\dot{u} = \zeta_a \omega^2 e^{kz} \cos(kx - \omega t)$
<i>Particle vertical acceleration</i>	\dot{w}	$\dot{w} = -\zeta_a \omega^2 e^{kz} \cos(kx - \omega t)$

On the non-linear approach, Stokes's theory assesses the modelling of the fluid flow with acceptable accuracy for intermediate and deep water, where the wavelengths are not large compared to the depth of the water (Fenton, 1985).

Ship in regular waves

When in regular waves, a concept of interest is the encounter frequency, ω_e . This frequency is the one that the ship experiences from the waves when moving at certain speed and direction relative the waves. This is the frequency that later be of use when carrying out the spectral analysis.

The presented eq.(2.1) can be better understood in Figure 2-4 where the ship sails at a given speed (U) and experiences the waves from each possible direction, μ . (Molland, 2008).

$$\omega_e = \omega - \frac{\omega^2}{g} U \cos \mu \quad (2.1)$$

The “negative” frequencies are projected on the positive region of the y axis. As negative frequencies are not physically possible and are a mathematical result.

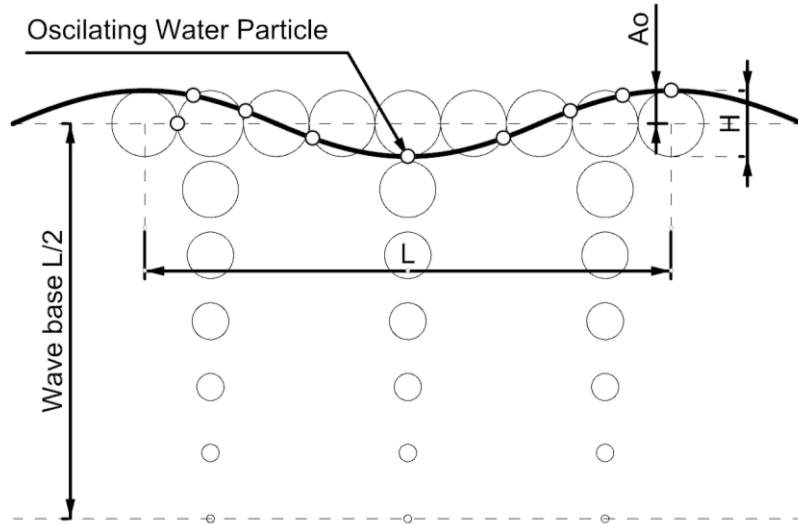


Figure 2-3: Orbital motion of water particles

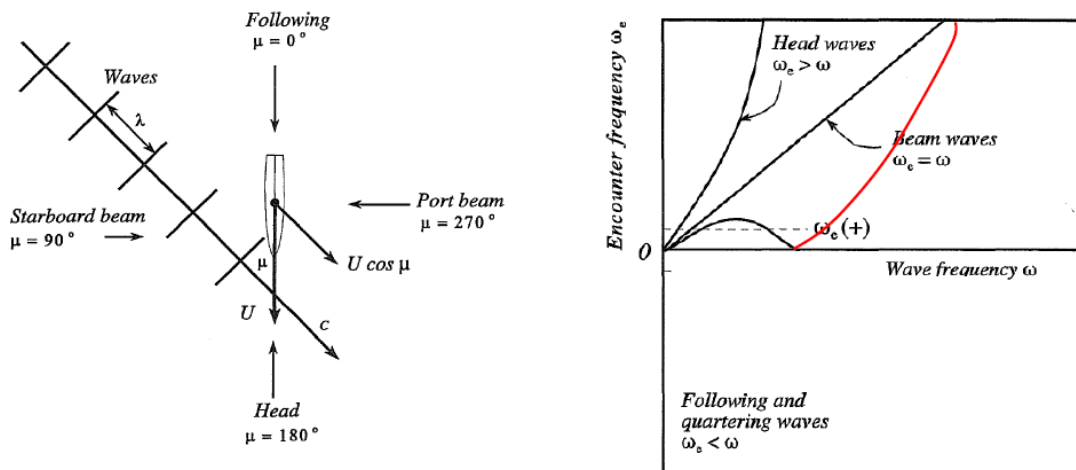


Figure 2-4: Encounter frequency behaviour (Nielsen, 2010)

2.1.1.2 Irregular waves

Ocean waves are irregular and for simplification they are considered to be the result of a superposition of different sinusoidal waves with random frequencies and properties. This superposition is theoretically applicable for moderate sea-states that can be linearized. However, this superposition has been demonstrated to be accurate enough for more extreme conditions (Molland, 2008).

The assumptions for this superposition to take place are the following:

- Stationary conditions, i.e., probability distribution of the wave elevation does not change in each period.
- The wave elevation is Gaussian distributed.
- The wave heights are Rayleigh distributed.

Equation (2.2) and (2.3) represent the summation of each wave component i and the wave spectrum respectively. Where k is the wave number, and ε the phase of the wave component.

$$\zeta(x, t) = \sum_{i=1}^n \zeta_i \cos(k_i x - \omega_i t + \varepsilon_i) \quad (2.2)$$

Where ζ_i is the amplitude of the wave component i .

$$S_{\zeta\zeta_i} = \frac{(\zeta_i)^2}{2\delta\omega} \quad (2.3)$$

Wave energy spectrum

The main characteristics of these irregular waves i.e., significant wave height, period and direction can also be estimated and of particular interest are the spectral value these waves present.

The seaway spectrum ($S_{\zeta\zeta}$) is defined by the energy distributed (m_0) with respect of the circular frequency (ω). Mathematically speaking, m_0 is the integral of $S_{\zeta\zeta}$ over the positive frequencies.

$$m_0 = \int_0^{\infty} S_{\zeta\zeta}(\omega) d\omega \quad (2.4)$$

The general form of the spectral moments is given by eq.(2.5) and from them some important characterizations of the wave system can be obtained, see Table 2-3.

$$m_n = \int_0^{\infty} \omega^n S_{\zeta\zeta}(\omega) d\omega \quad (2.5)$$

Table 2-3: Wave spectral properties

<i>Properties</i>	<i>Symbol</i>	<i>Expression</i>
<i>Significant wave height</i>	$H_S = H_{1/3}$	$4\sqrt{m_0}$
<i>Mean period</i>	T_1	$2\pi \frac{m_0}{m_1}$
<i>Zero-upcrossing period</i>	\bar{T}_Z	$2\pi \sqrt{\frac{m_0}{m_2}}$

On this matter, there are a few parametrised spectrums that rely on theoretical and measured wave spectra. For instance, see Bretschneider, JONSWAP and Pierson-Moskowitz wave spectrums (Molland, 2008; Nielsen, 2010).

Spectral analysis

The spectral analysis is a study of the energy transmitted from the waves to the ship and its responses i.e., motions, accelerations, forces, moments. As pictured in Figure 2-5, this analysis is done for a given vessel with certain weight distribution and speed.

From these first conditions, the RAO (Response Amplitude Operator) is obtained for later combining it with the wave encounter spectrum to finally get the response spectrum. The response spectrum corresponds to a certain position of the ship and to a specific motion. This information is useful to determine the effect of these responses over the crew or installed machinery and structures on the vessel. In order to evaluate the capability of the ship to withstand the environment and perform its mission, some criteria are applied, obtaining operators limit boundaries. These operator limit boundaries work as safety measures that can safeguard the vessel and the crew from potential danger. By using a wave scatter diagram of the sea where the ship operates it is possible to obtain a percentage operability of the ship, that depending on the criteria it can be translated in habitability, working conditions, etc.

A further mathematical explanation is as follows:

From eq.(2.4) and by using the encounter frequency, the encounter wave spectrum is obtained.

$$S_{\zeta\zeta}(\omega)d\omega = S_{\zeta\zeta_E}(\omega_E)d\omega_E \quad (2.6)$$

By applying eq.(2.1) the following relationship is obtained:

$$S_{\zeta\zeta_E}(\omega_E) = S_{\zeta\zeta}(\omega) \frac{d\omega}{d\omega_E} = \frac{S_{\zeta\zeta}(\omega)}{1 - 2\omega \frac{U \cos \mu}{g}} \quad (2.7)$$

The transfer function Y_n is the square root of the RAO, which depends on the wave velocity, heading and amplitude. This RAO is denoted by complex number. Then:

$$Y_E = Y(\omega_E) = \frac{\rho_{a,n}}{\zeta_{a,n}} \quad (2.8)$$

Where, $\rho_{a,e}$ is the amplitude of response corresponding to the n-wave component and by using eq. (2.3), the following expression for the response spectrum is obtained:

$$S_\rho(\omega_E) = Y(\omega_E)^2 S_{\zeta\zeta_E}(\omega_E) \quad (2.9)$$

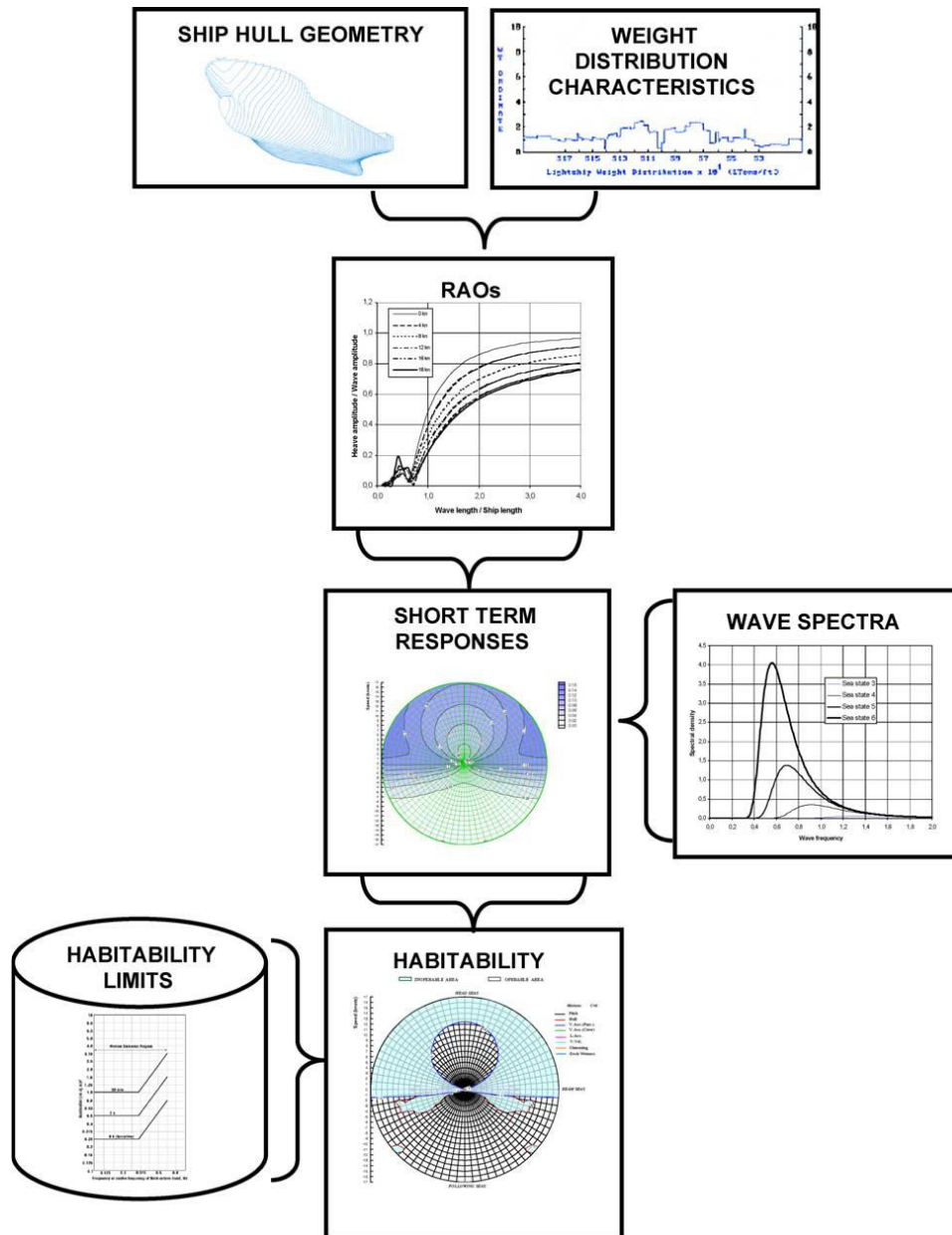


Figure 2-5: Seakeeping analysis (Sariöz & Narli, 2005)

2.1.1.3 Seakeeping criteria

These limiting criteria are quantitative and qualitative measurements that show whether the vessel withstand the environment where is carrying out its mission while performing it successfully. These criteria consider crew habitability, safety, and operability in correlation with the motions the vessel experiences according to Riola & Arboleya (2006) and Sayli, et al. (2006).

Given the importance of these criteria, it is necessary to implement standardized acceptance limits that guarantee a safe operability and overall mission. However, this is not an easy task as every ship possess its own behaviour according to its mission, zone of operation and operability conditions. Hence this study analyses a sole vessel (fishing vessel) under a range of conditions that are frequently encountered and produce critical ship responses.

Accelerations, forces and moments are of particular interest in this thesis as they affect directly the working conditions of the crew. Some zones of interest are the bridge and the working deck Tello et al., (2011), Rusu & Soares (2014). The ISO standards assess the motions and accelerations impact from the ship responses over the people on board (ISO 2631-1, 1997). Some criteria presented on Lewis (1989) are used along with those presented on Nordforsk (1987) and Ghaemi & Olszewski (2017). By combining these 3 criteria, shown on Table 2-4 and Table 2-5, Table 2-6 is customized as a criteria for fishing vessels, where RMS stands for Root Mean Square of the response and SSA stands for Single Significant Amplitude. The limiting values of SSA specified in Table 2-6 should be interpreted as twice the RMS.

Most of the values established on the criteria are taken from existing studies that fit commercial vessels (including fishing vessels). Where the MSI and MII are probabilistic indices that determine the occurrence of passenger sickness and interruption of activities carried by passenger or crewmembers, respectively. It is necessary to determine the values that trigger these indices. The MSI can be determined by following the procedure established by O'Hanlon & McCauley (1974) and the MII can be estimated by following Graham (1990).

Comfort can be compared with magnitudes suggested by the ISO 2631 – 1(1997) according to the values presented on Figure 2-6.

Less than 0.315m/s ²	Not uncomfortable
0.315 m/s ² to 0.63 m/s ²	A little uncomfortable
0.5 m/s ² to 1 m/s ²	Fairly uncomfortable
0.8 m/s ² to 1.6 m/s ²	Uncomfortable
1.25 m/s ² to 2.5 m/s ²	Very uncomfortable
Greater than 2 m/s ²	Extremely uncomfortable

Figure 2-6: Comfort assessment in vibrating environments (ISO, 1997)

The frequency of deck wetness is calculated according to (Papanikolaou, 2001). In this documentation the stability is assessed in a further study from the seakeeping criteria. It is also important to point out that these criteria are strongly linked with the fishing procedure, which leads to high frequency of deck wetness.

Table 2-4: General operability limiting criteria for ships (Ghaemi & Olszewski, 2017)

Ref. Criterion	NATO STANAG 4154	U.S. Coast Guard Cutter Certification Plan	Tasaki et al. (Japan)	NORDFORSK 1987			Cruikshank & Landsberg (USA)
				Merchant ships	Naval vessels	Fast small craft	
Vertical acceleration at forward perpendicular	0.2g RMS	0.4g SSA	0.80g @ P=0.001	0.275g (L≤100 m) or 0.05g (L≥330m)	0.275g	0.65g	0.25g
				0.20g for light manual work			
				0.15g for heavy manual work			
				0.10g for intellectual work			
				0.05g for transit passengers			
				0.02g for cruise liner			
Vertical acceleration at bridge	0.1g RMS	0.2g SSA		0.15g	0.2g	0.275g	0.20g
Lateral acceleration at bridge	0.10g RMS	0.2g SSA	0.60g @ P=0.001	0.12g	0.1g	0.275g	
				0.10g for light manual work			
				0.07g for heavy manual work			
				0.05g for intellectual work			
				0.04g for transit passengers			
				0.03g for cruise liner			
Motion Sickness Incidence (MSI)	20% of the crew in 4 hours	5% in a 30 minute exposure					
Motion Induced Interruption (MII)	1 tip per minute	2.1 tip per minute					
Roll Amplitude	4.0 deg RMS	8.0 deg SSA	25 deg @ P=0.001	6 deg	4 deg	4 deg	15 deg
				6.0 deg for light manual work			
				4.0 deg for heavy manual work			
				3.0 deg for intellectual work			
				2.5 deg for transit passengers			
				2.0 deg for cruise liner			
Pitch Amplitude	1.5 deg RMS	3.0 deg SSA					
Slamming (probability)			0.01	0.03 (L ≤ 100 m) or 0.01 (L ≥ 300 m)	0.03	0.03	0.06
Deck wetness (probability)			0.01	0.05	0.05	0.05	0.07
Propeller emergence (probability)			0.01				0.25

Table 2-5: Examples of seakeeping criteria (Lewis, 1989)

Index	Seaway Performance Criteria	Affected elements	Performance Degradation
(a)	Absolute Motion Amplitude		
1	Roll angle.	People, mission, and platform mission.	Personnel injury, reduced task proficiency, and mission and hull system degradation.
2	Pitch angle.		
3	Vertical displacement of points on flight deck.	People and Mission system.	Injury to personnel handling aircraft.
			Inability to safely launch or recover aircraft.
(b)	Absolute Velocities and Accelerations		
4	Vertical acceleration.	People and mission system.	Personnel fatigue, reduced task proficiency and mission system degradation.
5	Lateral acceleration.		
6	Motion sickness incidence.	People	Reduced task proficiency.
7	Slam acceleration (vibratory, vertical).	People, mission, and platform systems.	Personnel injury reduced task proficiency, and mission and hull system degradation. Preclusion of towed sonar operation.
(c)	Motions relative to sea		
8	Frequency of slamming (reimmersion and velocity threshold).	Mission systems.	Hull whipping stresses and damage to sensors on the masts.
		Platform systems.	Slamming damage to bottom forward hull structure.
9	Frequency of emergence of sonar dome.	Mission systems.	Reduced efficiency of sonar.
10	Frequency of deck wetness.	People	Injury or drowning personnel.
		Mission systems.	Damage to deck-mounted equipment.
11	Probability of propeller emergence.	Platform systems.	Damage to the main propulsion plant
(d)	Motions relative to aircraft		
12	Vertical velocity of aircraft relative to the flight deck	Mission systems.	Damage to aircraft landing gear and/or loss of aircraft.

Table 2-6: Designed seakeeping criteria for fishing vessels

Index	Seaway Performance Criteria	Affected elements	Criteria Value
(a)	Absolute Motion Amplitude		
1	Roll amplitude	People, mission, and platform mission.	6.0 deg for light manual work
			4.0 deg for heavy manual work
			3.0 deg for intellectual work
			2.5 deg for transit passengers
			2.0 for cruise liner
2	Pitch amplitude		1.5 deg (R.M.S.)
(b)	Absolute Velocities and Accelerations		
3	Vertical acceleration	People and mission system.	0.2g for light manual work
			0.15g for heavy manual work
			0.1g for intellectual work
			0.05g for transit passengers
			0.02g for cruise liner
4	Lateral acceleration	People and mission system.	0.10g for light manual work
			0.07g for heavy manual work
			0.05g for intellectual work
			0.04g for transit passengers
			0.03g for cruise liner
5	Motion sickness incidence (MSI)	People	20% of crew in 4 hours
6	Motion induced interruption (MII)	People	1 tip per minute
7	Slamming acceleration (vertical)	People, mission, and platform systems.	Vertical acceleration when slamming taking place TBD
(c)	Motions relative to sea		
8	Frequency of slamming (reimmersion and velocity threshold)	Mission and platform systems.	0.03 (L ≤ 100)
			TBD
9	Frequency of deck wetness	People	0.05
		Mission systems.	

2.1.2 Numerical predictions for seakeeping

Given the non-linearity of the natural environment in which a vessel sails, it is necessary to make use of numerical methods to facilitate the result generation with sufficient accuracy.

There are many approaches to carry out numerical simulations. In general, the Navier-Stokes's equations and continuity equations comply with the requirements for solving the problems considered in seakeeping, however due to the time and capability for solving every aspect of the phenomena, this does not seem feasible. Similar problems are perceived when applying the RANS model for simplified models or the Euler solvers, which do not solve the boundary layer due to the no consideration of the viscosity (Molland, 2008).

From the previously stated reasons, Potential flow is the approach mostly used for solving the seakeeping phenomena.

2.1.2.1 Potential flow analysis and panel method

The potential flow approach has the following characteristics:

- Inviscid flow assumption.
- Assumes an irrotational flow.
- Typically, much faster than Euler and RANS solver because the mathematical problem is smaller (less equations).
- Based on BEM (Boundary Element Method), this means that it only discretizes the boundary of the domain and not the whole volume.
- Not capable of simulating breaking waves and splashes.

The governing equation of the potential flow is the Laplace equation for the velocity potential ϕ :

$$\nabla \cdot \nabla \phi = 0 \quad (2.10)$$

Numerous potential flow methods for the seakeeping problem can be found in the literature. In many of them, the velocity potential is divided into different components, e.g.

$$\phi = (-Vx + \phi^S) + (\phi^w + \phi^I) \quad (2.11)$$

where the first term describes the steady flow, and the second term describes the periodic flow induced by the waves:

- Vx is the potential of (downstream) uniform flow with ship speed V .
- ϕ^S is the potential of the steady flow disturbance.
- ϕ^w is the potential of the undisturbed wave.
- ϕ^I is the remaining unsteady potential.

The following are some methods used for solving ϕ^I and ϕ^S :

- Strip Theory: Which approach reduces the 3D problem to a 2D one by dividing the ship in cross-sections of given thickness and a simplification of the free surface condition. This method carries some inaccuracies because of the simplification, i.e., not accurate for solving bulbous bows, usable for slender ships ($L/B > 5$ and $B/T > 4$), suitable for ships moving at low speeds ($F_n < 0.4$)

and long waves with small motions, added resistance needs to be corrected empirically.

- Unified theory: It also relies on the slenderness of the ship to justify a 2D approximation for the analysis in the near-field but coupled with a 3D approach for the far-field, however, is not as accurate as Strip theory method.
- Green Function Method: Depending on the approach of the equation solving, the implementation of this method varies significantly, and it could derive to large errors due to the omission of ϕ^S .

Even though linear methods are quite useful from time-computation perspective, the inaccuracies carry large errors, and the application is highly limited. In the cases of large and slender ships, these methods tend to be somehow accurate for linear regular waves. However, for the case of smaller and not so slender vessels these errors tend to be significant (Molland, 2008). From this, that a non-linear approach is more suitable for fishing vessels, where the discretization of the hull and free surface is done by panels like in the Rankine Singularity Method (Molland, 2008).

One of the commercial software that implements a numerical code with a nonlinear approach that is still faster than a corresponding RANS model is SHIPFLOW. This software presents a package dedicated to seakeeping named SHIPFLOW Motions, which performs the added resistance, resistance, sinkage, and motions in both regular and irregular waves calculations.

The code in charge of the calculations of the physics is called XPTD which is a time accurate potential flow panel method solver, for fully non-linear free surface conditions which implicitly captures the effects of incoming waves and waves due to forward speed, radiation, reflection, and diffraction as well as their interaction. (SHIPFLOW, 2021).

The approach used by SHIPFLOW 6 still simplifies the mathematical problem by assuming potential flow and the simplifications result in a series of limitations. As explained paragraphs above, the viscosity is not considered under this model, hence the damping coefficients corresponding to the viscous effects need to be known beforehand for obtaining an accurate result.

There are different theories and approaches to calculate the damping coefficients, through linearization, non-linear and approaches, these methods are explained in more detail by Himeno, 1981. Other methods are through the use of CFD analysis by simulating a roll decay motion or controlled roll motion (ITTC, 2011), these can be also carried out with experimental procedures in towing tanks.

Particularly, Watanabe and Inoue present an interesting approach that is simple to implement, though the accuracy can be discussed (Watanabe, Inoue, & Murahashi, 1964). This method seems to be the most suitable for the implementation procedure and due to that this study does not focus on the calculation of the most accurate parameter, but on the influence of the motions on the seakeeping performance. For a more accurate damping coefficient calculation, an experimental test or a CFD RANS simulation can be employed.

2.2 Stability

The stability assessment of ships has been extensively studied through time in a vast literature (Molland, 2008). In the last 20 years a topic of interest that compromises ship's stability from a different approach is being assessed by IMO. This is the dynamic stability of ships, related to parametric rolling, pure loss of stability, broaching and surf-riding, and dead ship condition. On this matter, it is of interest to analyse and understand how certain working conditions can lead to the occurrence of a phenomena as parametric rolling of small ships as fishing vessels (understand small as length below 75 m) which can lead to capsize of the vessel or loss of control (Second generation intact stability criteria).

To understand this phenomenon properly, a brief introduction to the intact stability of a vessel is explained and from there, the theory behind the Second-generation intact stability criteria is assessed.

2.2.1 Intact stability

This concept refers to the stability of a vessel or naval structure in no damage conditions. The study of the stability of a ship is of great importance to guarantee the integrity of it on seas, even though some considerations and approximations are considered when performing this study i.e., non-changing hydrostatic curves for small angles of roll and pitch, small angles of motion, calm water, and geometrical considerations. See Molland (2008) & Lewis (1989). This approach requires that certain regulations and criteria be satisfied. IMO plays an important role on this matter by presenting guidance and concepts backed up by several studies related to ship's stability i.e., Belenky et al., (2011).

However, certain conditions escape from the scope of these assumptions and it is logical to happen because ships do not sail under these ideal conditions, but under rough and extreme conditions depending on the route (Molland, 2008).

The mathematical values that characterize the stability of a ship are the Metacentric radius (GM) and the righting lever or curve of statical stability (GZ).

2.2.2 Second generation intact stability criteria

The IMO second generation intact stability criteria assess phenomena as broaching, parametric roll, and surfing, trying to comprehend, explain and predict its occurrence to prevent accidents, damages, and the loss of the ship.

For the sake of this thesis, only the parametric rolling phenomena is studied to determine design criteria related to seakeeping performance. (Belenky, Bassler, & Spyrou, 2011).

2.2.2.1 Parametric rolling

Parametric rolling is a special condition of resonance characterized by large rolling angles under specific wave characteristics. This phenomenon happens due to the change

on the stability (varying GM) caused by the incident waves that alters the submerged geometry and waterplane area. This behaviour is strictly conditioned by the frequency range and wavelength and as these conditions do not happen constantly, the amplified response decays in time. See Belenky et al., (2011).

Figure 2-7 shows the variation of the GZ curve (restoring arm). On one hand the encountered waves affect the submerged geometry shape, affecting the KB (vertical centre of buoyancy) location. On the other hand, the affected waterplane is also affected (constantly increasing and decreasing), this can be observed in the waterplane projected blue and red lines. Where the blue waterplane is the varying one and the red waterplane is the static one, this way the BM (metacentric radius) changes constantly. These constant changes derive finally in the variation of GM (Metacentric height) and GZ, triggering then the phenomenon known as parametric rolling.

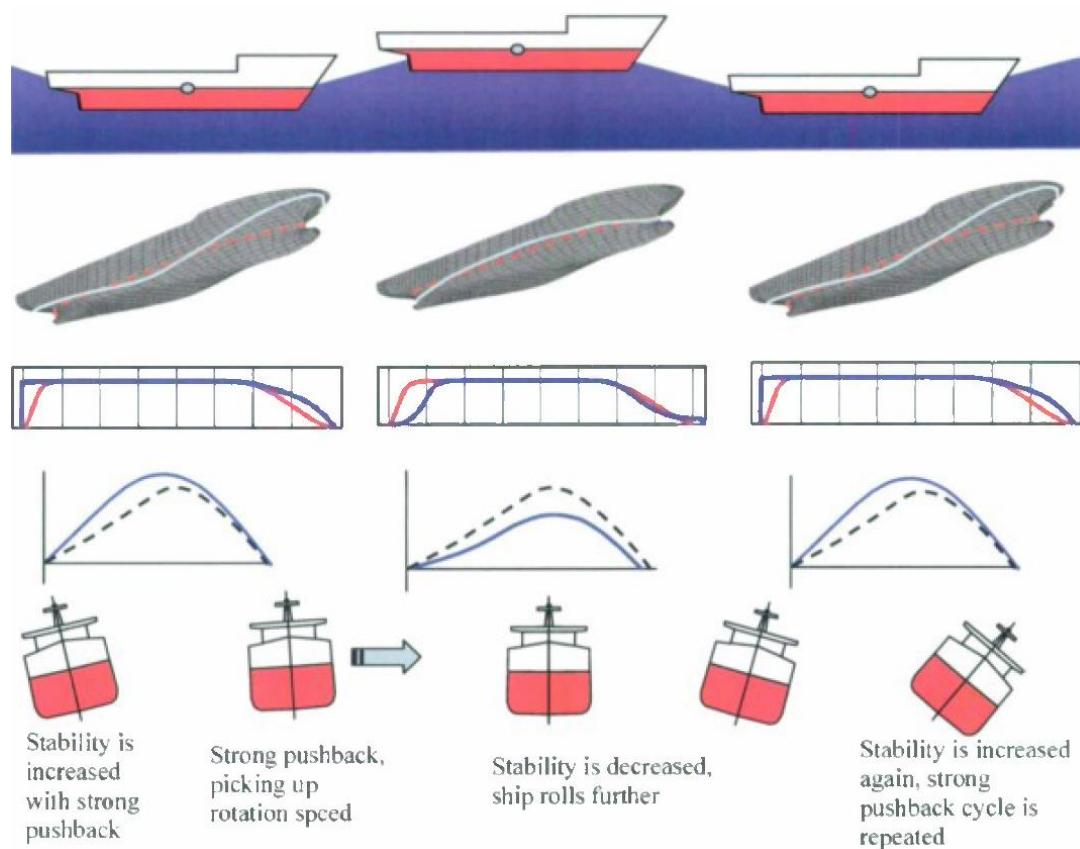


Figure 2-7: Development of parametric rolling phenomena. See Belenky et al., (2011)

For the mathematical interpretation of the phenomena, the Mathieu-Type equation is used (Mathieu, 1868). The damping coefficient is also of importance as this one can prevent the phenomenon to happen.

To “reach” the parametrical rolling condition, certain vulnerability criteria need to be fulfilled. Only the first vulnerability criteria are presented and studied on this thesis. The mentioned criteria, approaches the phenomenon through the Mathieu-Type equation and states the need of a frequency condition, damping condition, magnitude of stability change and wave parameters. The numerical model is explained in the following sub-section.

2.2.2.2 Numerical predictions for stability

A numerical code was developed in MATLAB to estimate the occurrence of parametric rolling. The code is based on the Mathieu-Type equation.

Derivation of Mathieu-Type Equation

This equation is a simple mathematical non-forced rolling model under following or head seas, the following equation represents a simple model of the motion. (Belenky et al., 2011).

$$(I_{44} + \delta I_{44})\ddot{\phi}_4 + N_{44}\dot{\phi}_4 + S_{44}\phi_4 = 0 \quad (2.12)$$

The presented equation of roll motion shows the hydrodynamic coefficients explained on sub-section 4.1.2.2.

Where the restoring moment S_{44} can be approximated by the hydrostatic curves to eq.(2.13).

$$S_{44} = g \cdot \Delta \cdot GM \quad (2.13)$$

Here g is the gravity acceleration, Δ is the mass displacement and GM is the metacentric radius of the ship that at the same time can be presented with a sinusoidal representation as eq. (2.14).

$$GM = GM_m + GM_a \cos(\omega_e t) \quad (2.14)$$

Where:

$$GM_m = 0.5(GM_{max} + GM_{min}) \quad (2.15)$$

$$GM_a = 0.5(GM_{max} - GM_{min}) \quad (2.16)$$

Being GM_{max} the GM value when the ship is on the wave trough and GM_{min} the GM value when the ship is on the wave crest. This approximation is not completely precise as it formulates a shifted changing GM respect to the exact one.

By substituting eq. (2.12) to eq. (2.15) in eq. (2.11) a new form based on normalised frequencies that represent the variation of the GM is obtained,

$$\ddot{\phi}_4 + 2\delta\dot{\phi}_4 + (\omega_m^2 + \omega_a^2 \cos(\omega_e t))\phi_4 = 0 \quad (2.17)$$

where:

$$\omega_m^2 = \sqrt{\frac{\Delta \cdot GM_m}{I_{44} + \delta I_{44}}}; \quad \omega_a^2 = \sqrt{\frac{\Delta \cdot GM_a}{I_{44} + \delta I_{44}}}; \quad \delta = \frac{1}{2} \frac{N_{44}}{I_{44} + \delta I_{44}} \quad (2.18)$$

The differential equation is solved in the MATLAB developed in Appendix C by applying a change of variable to later solve a system of first order differential equations.

Later a non-dimensionalisation on time, followed by non-dimensionalisation of the roll frequency and damping with respect to the wave frequency of encounter can be implemented as follows:

$$\mu = \frac{\delta}{\omega_e}; \quad \bar{\omega}_m = \frac{\omega_m}{\omega_e}; \quad \bar{\omega}_a = \frac{\omega_a}{\omega_e}; \quad \phi(\tau) = x(\tau) \cdot \exp(-\mu\tau) \quad (2.19)$$

A final expression on terms of the Mathieu-type equation is obtained:

$$\frac{d^2x}{d\tau^2} + (p + q \cos(\tau)) \cdot x = 0 \quad (2.20)$$

Here:

$$p = (\bar{\omega}_m^2 - \bar{\mu}^2); \quad q = \bar{\omega}_a^2 \quad (2.21)$$

These parameters are now used to predict the occurrence of the parametric rolling phenomena.

For the interpretation of these values, there are 2 types of solutions, the bounded or “stable” and the unbounded or “unstable”. These two results are represented on the Ince-Strut diagram shown in Figure 2-8, where the white zones represent the bounded regions and the red one the unbounded ones.

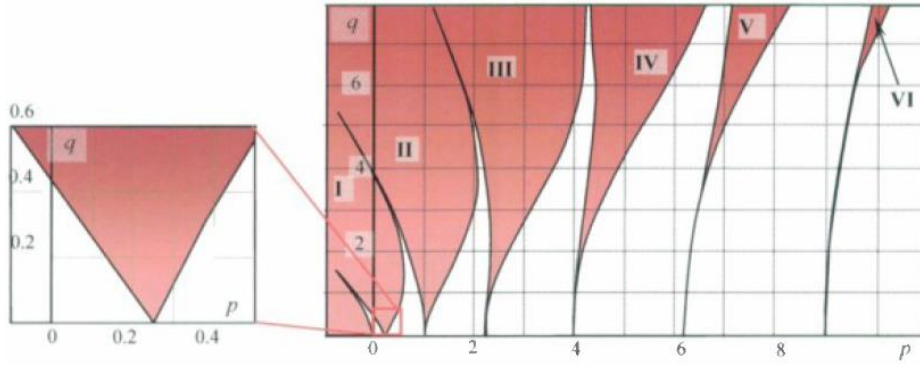


Figure 2-8: Ince-Strut diagram (Belenky, Bassler, & Spyrou, 2011)

One of the more common and studied zones are where $p = 0.25$, which corresponds to the first instability zone.

From the developed code, Figure 2-9 and Figure 2-10 show the behaviour of the roll motion under the bounded and unbounded solution for the given combination of values of p and q .

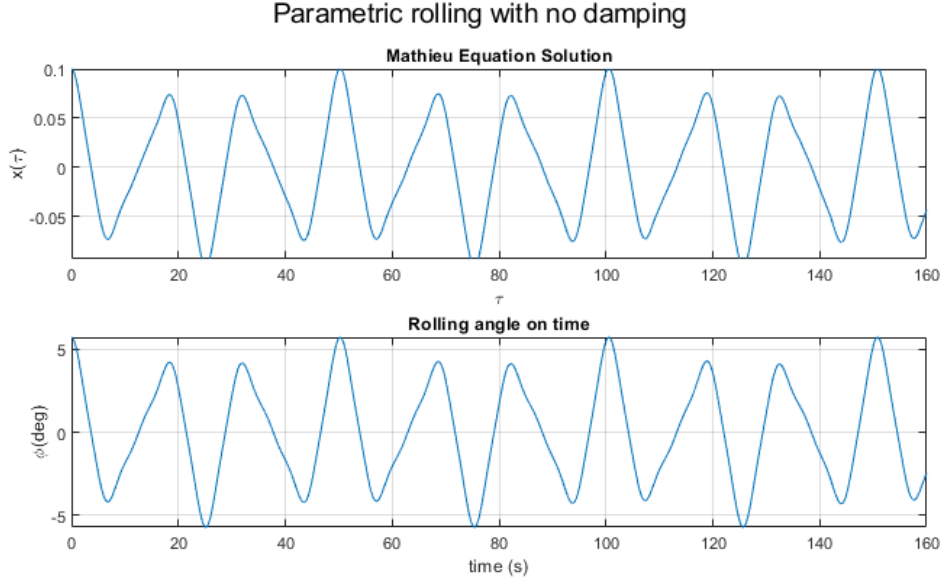


Figure 2-9: Bounded solution, $p=0.1$ & $q=0.2$

Figure 2-9 shows the bounded or “stable” solution, that represents a non-dimensional and a dimensional rolling response on time. Meanwhile Figure 2-10 shows the unbounded or “unstable” solution, that represents a non-dimensional and dimensional constantly growing rolling response.

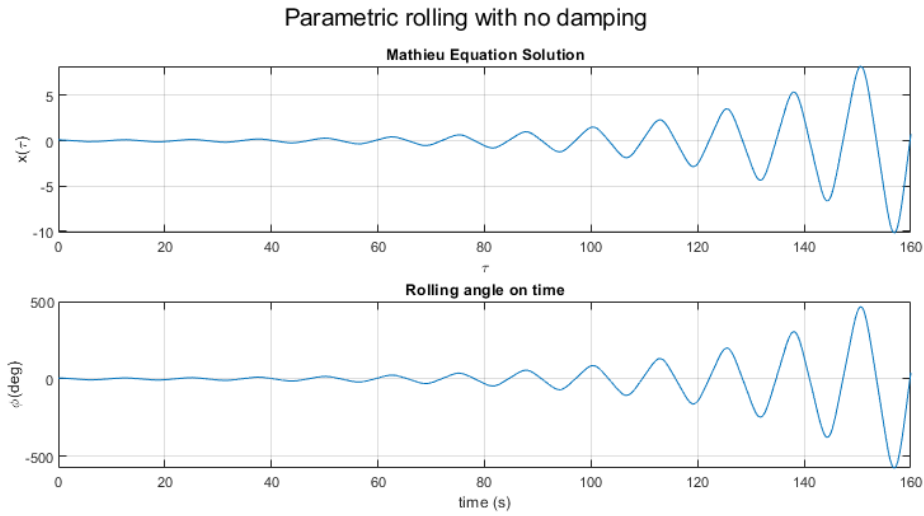


Figure 2-10: Unbounded solution, $p=0.15$ & $q=0.2$

The influence of the damping and non-linearity will play an important role. As seen on Figure 2-10, the amplitude keeps growing indefinitely, which is not realistic. The non-linearity of the stiffness (GZ curve) plays the role of regulator, resulting in decreased oscillation in time. By implementing a GZ as cubic parabola as eq.(2.22) , eq.(2.27) takes the shape of eq.(2.23).

$$GZ(\phi) = GM \cdot \phi(1 - \phi^2) \quad (2.22)$$

$$\ddot{\phi}_4 + 2\delta\dot{\phi}_4 + (\omega_m^2 + \omega_a^2 \cos(\omega_e t))\phi_4(1 - \phi_4^2) = 0 \quad (2.23)$$

GZ is a function of roll angle as shown on Figure 2-11:

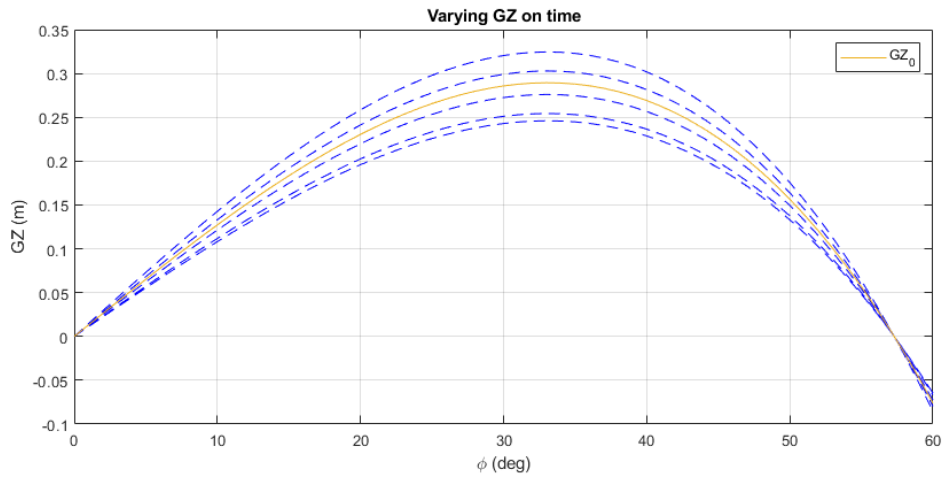


Figure 2-11: Changing GZ curve

And the unbounded solution takes the new shape shown on Figure 2-12, which is now being affected by the non-linear behaviour of GZ.

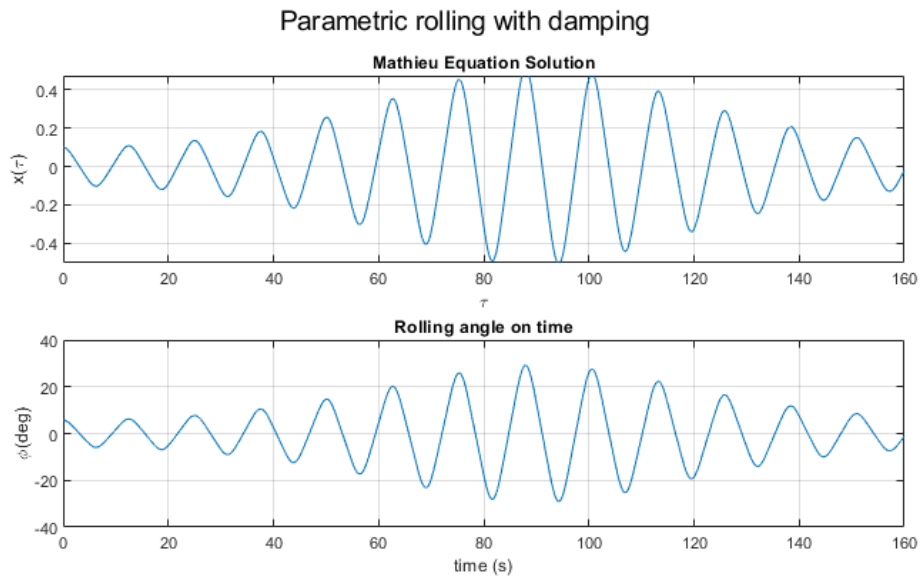


Figure 2-12: Unbounded solution with non-linear behaviour.

As the Mathieu equation only shows if the phenomenon takes place or not, and not if the phenomenon decays, the non-linearity accounts for this. When the energy from the excitation meets the frequency requirements, the parametric resonance is reached. Also, the oscillator reaches a balance, and the parametric roll is stabilized with a specific roll amplitude when this energy reaches its limit. However, once the energy required for the resonance is not supplied, the rolling amplitude starts to decay.

An important observation is that the effect of the changing GM can show that the parametric rolling is triggered in frequencies that should not do it when accounting for the non-linearity of GZ.

Vulnerability criteria

There are 2 levels of vulnerability criteria on this phenomenon, where the first level criteria are applied for regular waves with a more conservative approach and the second

level criteria is of higher friability and applied for irregular waves. However only the first one is presented in this report.

As mentioned before, there are some conditions needed to be fulfilled in order trigger the parametric rolling. (Belenky et al., 2011)

- a. Frequency condition: Related to the value of p and q , the range shown below is an initial condition that can trigger the phenomena. If the condition is fulfilled, the next condition must be calculated.

$$p_{B1,B2} = \frac{1}{4} \pm \frac{q}{2} \quad (2.24)$$

- b. Damping Threshold condition: This condition is based on Hayashi (1953) and adjusted for a more precise evaluation. The result shows if the ship is susceptible or not to parametric rolling if the formulation surpasses the damping coefficient.

$$\mu_{ABS} < qk_1k_2\sqrt{1 - k_3^2} \quad (2.25)$$

$$k_1 = 1 - 0.1875q^2; \quad k_2 = 1.002p + 0.16q + 0.759; \quad k_3 = \frac{q^2 - 16 + \sqrt{q^4 + 352q^2 + 1024p}}{16q} \quad (2.26)$$

- c. Magnitude of stability change: This condition compares the change on the GM values and amplification factor (f) after a given number of encountering waves (n). Where this ratio must be higher or equal to 0.49 according to Belenky et, al. (2011) and ABS (2004), in order to satisfy the condition of stability change.

$$\frac{GM_a}{GM_m} \geq 2 \frac{\ln(f)}{\pi n} + \frac{4\delta}{\omega_m} \quad (2.27)$$

3 Fishing vessels

This section provides an overview of fishing vessels and the related technology used for fishing that characterize a vessel to understand the main problems presented during the ship's journey and fishing procedures.

3.1 Main characteristics and definitions

Fishing vessels are a particular kind of ships that presents a quite large variation of shapes and dimensions. These particulars are dependant of the following considerations:

- Fish and seafood type.
- Hold capacity.
- Refrigeration type.
- Capture method and machinery.
- Zone of operation.

Some of the most common fishing vessels are the following:

- Seine fishing vessel.
- Trawler fishing vessel.
- Dredger fishing vessel.
- Trawler – purse seiners.
- Gillnetter fishing vessel.
- Lift netter fishing vessel.
- Trap setter fishing vessel.
- Handliner fishing vessel.
- Multipurpose fishing vessel.

Each type of vessel mentioned has its own fishing procedure (FAO, Fishing Vessel type, 2021). The main variation can be seen on the working deck (machinery and hold location) and by the location of the bridge (at forward or aft). Depending on the location of the machinery and habitability zone, the induced forces and accelerations need to be studied to minimize the effects of the crew and cargo. Some fishing procedure may be more affected by some type of motions than others. Take for example the beam trawler fishing vessels or the typical American seine fishing vessel that carry the fishing procedure by starboard. This procedure is more compromised by roll motions than any other. However, due to the location of the bridge on seine fishing vessels, some of the main interesting motions to study are pitch and slamming.

Due to the broad range of fishing vessels, this thesis focuses the study on stern trawlers only and the results presented are applicable for the specific ship of study. However, similar ships can be studied by following the applied methodology.

3.2 Stern trawler fishing vessel

In this type of vessels, the trawl is located over the stern and the design of the ship itself can vary largely. It can count with a ramp or not and it may be possible for the ship to

work in pairs with another vessel to carry one large trawl or a double trawl (FAO, Fishing vessel types - Stern trawlers, 2021). Figure 3-1 shows a representative vessel of this type.

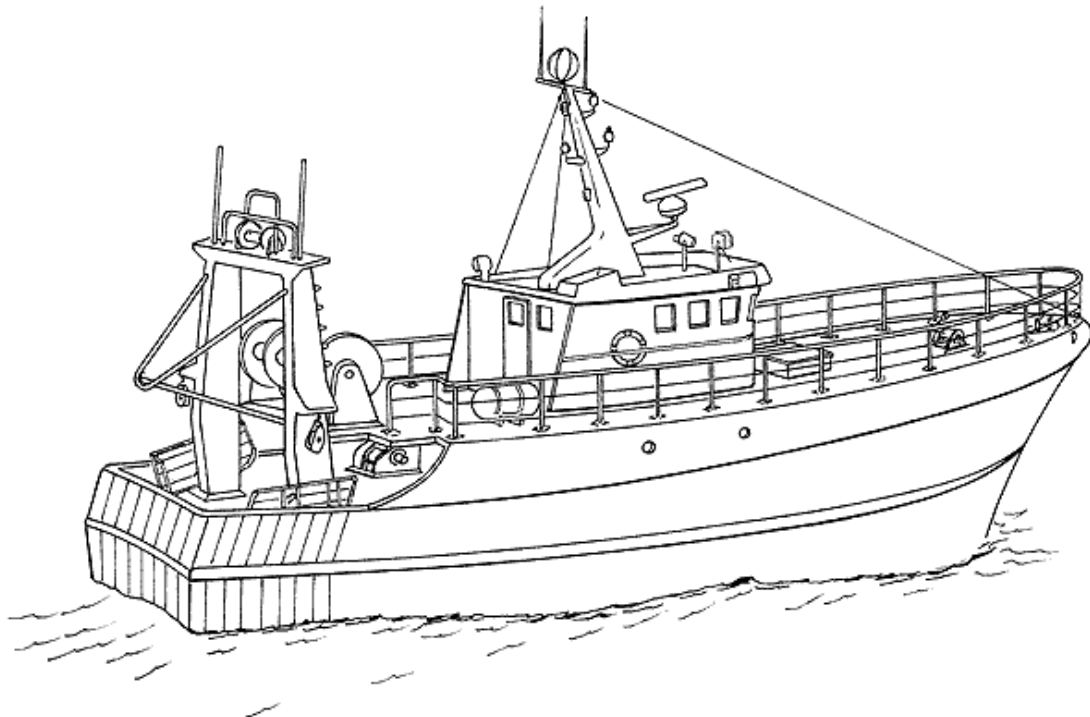


Figure 3-1: Typical stern trawler fishing vessel. (FAO, Fishing vessel types - Stern trawlers, 2021)

3.2.1 Fishing procedure

For a better understanding of the condition under which the vessel performs a brief description of the fishing procedure is specified in the chapter.

These vessels present an equipment called trawler above the stern which drops a net that later forms a purse that capture the fish by a dragging manoeuvre. Later a fishing pump is submerged along with its hose to transport the fish from the purse to the holds through a system of gutters that distribute the fish to the holds. Mainly, the equipment involved are purely cranes and pulleys systems. In this case there is no static equipment under extreme forces apart from the gantry that may be subject of strong forces due to the dragging force of the purse. On this matter, the foundation of the gantry may be of interest for a next study. Figure 3-2 to Figure 3-5 show the described procedure. These pictures were extracted from the official video of fishing procedure of the Stella Nova IX (Ex-Carmona) (Dyrön, 2016).



Figure 3-2: Net dropping



Figure 3-3: Purse dragging.



Figure 3-4: Fishing pump and hose immersion



Figure 3-5: Fish distribution through the gutters

3.2.2 Fishing vessel of interest

The fishing vessel selected for the study is the STELLA NOVA IX (ex-Carmona). Is a 510 - stern trawler monohull type vessel of Danish flag that operates in the Baltic Sea and North Sea.

The ship was built in 2014 by the owner and manager Fiskeriselskabet STELLA NOVA ApS.



Figure 3-6: Stella Nova IX

The vessel counts with the certifications shown in Table 3-1.

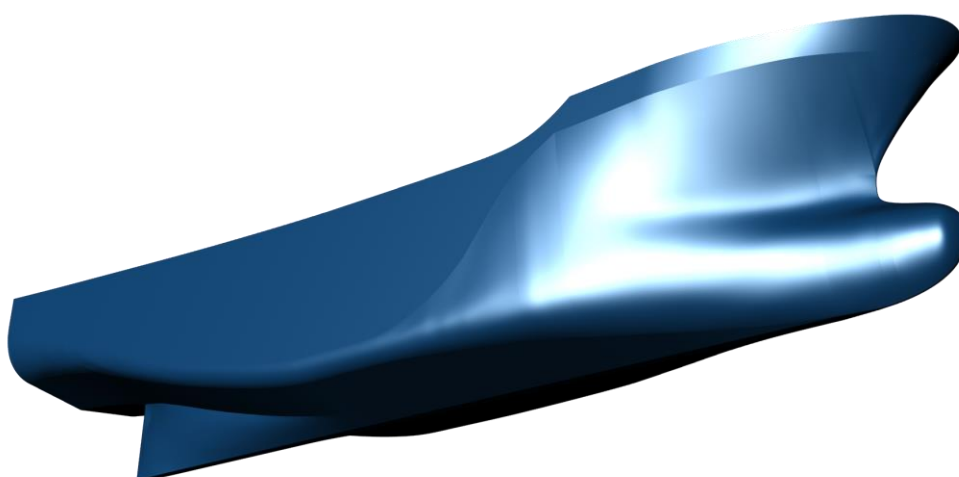


Figure 3-7: 3D hull rendering of stella Nova IX (Made in Rhinoceros 3D ver.7.0)

Table 3-1: Stella Nova IX Certificates

Code	Certificate	Type	Term
AFS-IC	International Anti-Fouling System Certificate	Statutory	Full
BWM-E	Ballast Water Management Certificate - Exchange Method	Statutory	Full
CLCE	Classification Certificate	Class	Full
EEC	Energy Efficiency Certificate	Statutory	Full
FVSC	Fishing Vessel Safety Certificate	Statutory	Full
IAPP	Air Pollution Prevention Certificate	Statutory	Full
OPP-A-IC	International Oil Pollution Prevention Certificate, Type A	Statutory	Full
SPP-IC	International Sewage Pollution Prevention Certificate	Statutory	Full

3.2.2.1 Hull main particulars

Figure 3-7 shows a 3D rendering of the hull. It was built from the lines plan provided by the Ship Owner and its main characteristics are shown in Table 3-2. This 3D model shows the hull plus the bulbous bow and the keel. Neither the rudder or the propeller was included in the modelling or analysis.

Table 3-2: Stella Nova IX main properties

Main particulars	Dimension	Unit
Loa	49.84	m
Lpp	43.30	m
Breath (B)	11.00	m
Depth (D)	7.60	m
Draught (T)	6.50	m
Gross tonnage (GT)	1023	
Dead weight tonnage (DWT)	1289	Ton

3.2.2.2 Stability study summary

To evaluate the computational model of the Stella Nova IX, it is necessary to review the stability booklet to have knowledge about the critical conditions the vessel is performing under. Table 3-4 shows the considered conditions by the designer. This information was provided by the designer JEA Marine Consulting.

The Table 3-3 show the description of the conditions and trimming and heeling status in which the vessel was studied.

Table 3-3: Stability conditions description

Cond.	Description	Trim (m)	Heel (deg)
1	Light ship	3.046	0
2	Departure to fish ground, 100% Bunkers and stores Salt/Ballast 100% and in RSW1C&1PS o1S, 50% 3S o 3PS	0.013	0.2
2.1	+ Icing	0.013	0.15
3	Fully loaded 100%, BUNKERS and STORES, 100% cargo holds.	-1.526	0.17
3.1	+ Icing	-1.526	0.21
4	Fully loaded, Full load 40% bunkers	-1.812	-0.25
4.1	+ Icing	-1.811	-0.23
5	Arrival fully loaded 10% BUNKERS and STORES, 100% cargo, technical water in ballast tanks.	-1.679	0.19
5.1	+ Icing	-1.68	0.18
6	Arrival 20% load inside tanks 10% BUNKERS and STORES, Technical water in ballast tanks.	1.64	-0.13
6.1	+ Icing	1.64	-0.22
7	10% BUNKERS and STORES, Technical water in ballast tanks, and 30% in RSW 1 SB&PS, RSW1	2.254	-0.17
7.1	+ Icing	2.256	-0.16
8	DOCKING condition, deadweight ab.410t	-0.063	0.1

Table 3-4: Summary of stability conditions - Stella Nova IX

Cond.	Weight (ton)	Draft AP (m)	Draft M (m)	Draft FP (m)	LCG (m)	TCG (m)	VCG (m)	GM (m)
1	851.9	4.773	3.25	1.727	17.169	-0.006	5.796	0.81
2	1562.8	5.068	5.062	5.055	19.936	0.015	4.871	0.708
2.1	1588.15	5.068	5.062	5.055	19.901	0.014	4.949	0.631
3	2121.48	5.659	6.422	7.185	20.132	0.013	4.933	0.845
3.1	2145.28	5.659	6.422	7.185	20.098	0.013	4.989	0.789
4	1998.83	5.272	6.178	7.084	20.519	0.007	5.105	0.574
4.1	2022.63	5.273	6.178	7.084	20.479	0.007	5.162	0.517
5	1944.57	5.211	6.05	6.89	20.51	0.012	5.191	0.486
5.1	1968.37	5.21	6.05	6.89	20.469	0.012	5.249	0.429
6	1164.35	4.88	4.06	3.24	18.854	0.015	5.254	0.609
6.1	1189.76	4.88	4.06	3.24	18.83	0.015	5.349	0.516
7	1051.7	4.895	3.768	2.641	18.148	0.017	5.333	0.722
7.1	1077.1	4.896	3.768	2.64	18.138	0.016	5.436	0.619
8	1260.75	4.345	4.381	4.408	20.66	0.016	5.077	0.418

From these conditions the representative scenarios for the analysis are selected. According to the designer, the stability of the ship enters a critical stage when trawling. During the trawling activity, the vessel is being affected by a moment due to the fishing purse of around 158 m-MT. The approach for simulating this condition is later explained in sub-section 4.1.2.

The conditions where ice is present are discarded from the analysis and from this the representative cases to study correspond to the conditions where the GM reaches its minimum value. These scenarios take place when docking and when the vessel is fully loaded (condition 4 and 8), see Table 3-4 and Table 3-3. As the docking condition is of no interest for the seakeeping performance of the vessel, the condition is also discarded. Instead, the departure condition is selected as the vessel spends a considerable amount of time under this one when sailing to the fishing zone. Another condition of interest is the trawling under the departure characteristics. These 3 conditions are the selected ones for the study of the motions of the vessel.

4 Methodology

In this chapter, the followed procedure for studying the topic is presented and explained. As stated before, in section 1.2, the focus is on the compliance of a fishing vessel with existing seakeeping criteria and parametric rolling criteria to (a) select the seakeeping criteria suitable for this type of vessel and (b) propose an assessment methodology to optimize such criteria, using SHIPFLOW Motions.

An overview of the methodologies in the studied literature is presented as background for establishing the specific methodology utilised in this thesis.

4.1 Methodological overview

There are two main topics of study in this thesis. The first one is the seakeeping behaviour of a fishing vessel operating in regular waves and the second one is the effects on the stability regarding dynamic parameters (parametric rolling). Given these two different but related subjects, the approach has taken into consideration both, for a later particular evaluation of results.

In general it is necessary to first reduce the scope of study to a certain type of fishing vessels with similar characteristics, this was done in section 3 as these type of vessels (trawlers) are the most representative and of interest in the region (North Sea and Baltic Sea) and fall into the delimitations of work boats under 75m in length of the project “Arbetsbåtars Sjöegenskapskriterier (ASK)” conducted by SSPA Sweden AB in cooperation with KTH. The used vessel is later specified in section 3.2.2.

To assess the described objectives, it is necessary to investigate the motion responses of the selected vessel, under the selected conditions of study. It was decided to simulate the closest to real conditions the ship encounters. These conditions are characterized by both the environment characteristics and the working conditions of the vessel. The environment characteristics are defined by the wave characteristics (wave height, wavelength, and wave direction), which are obtained from the database ERA5 (ECMWF, 2021) and the working conditions are defined by the ship’s displacement, speed, trim, heeling angle, etc (see Table 4-1 and Table 4-2).

Once the working conditions and environment characteristics were obtained, these were implemented in SHIPFLOW along with the geometry of the respective vessel (Figure 3-7).

The parametric rolling conditions are also assessed by the corresponding evaluation with the vulnerability criteria explained in section 2.2.2.

4.1.1 Studied conditions

The studied conditions for the seakeeping analysis and dynamic stability assessment are established according to the studied cases specified in section 3.

4.1.1.1 Conditions for seakeeping analysis

In this section, the following conditions are specified:

- Ship velocity.
- Trimming, heeling and displacement.
- Ship heading direction with respect to the waves, wave height and wavelength (or sea state).

The simulated ship speed is in correlation with the real speed experienced by the ship when operating in the corresponding working condition. In the same way, the trimming and heeling status in concordance with the displacement and working condition.

The angles of incidence, wave height, and wavelength of the encountered waves are set according to the conditions presented in the working zone the selected ship operates in. This data was obtained from the records of the years 2019 and 2020 provided by ERA5 (ECMWF, 2021). The working zones were selected according to the common route where the vessel operated during these 2 years. Two of these zones are located where the vessel fishes and the other two, where the ship navigates from or to the fishing zone (Figure 4-1 and Table 4-1). These four points were crossed with the vessel working conditions and sea states, then an evaluation of occurrence was executed to obtain the most frequent states. This statistical evaluation considered the mean values around each month for each one of the variables (see Appendix A, p.75).

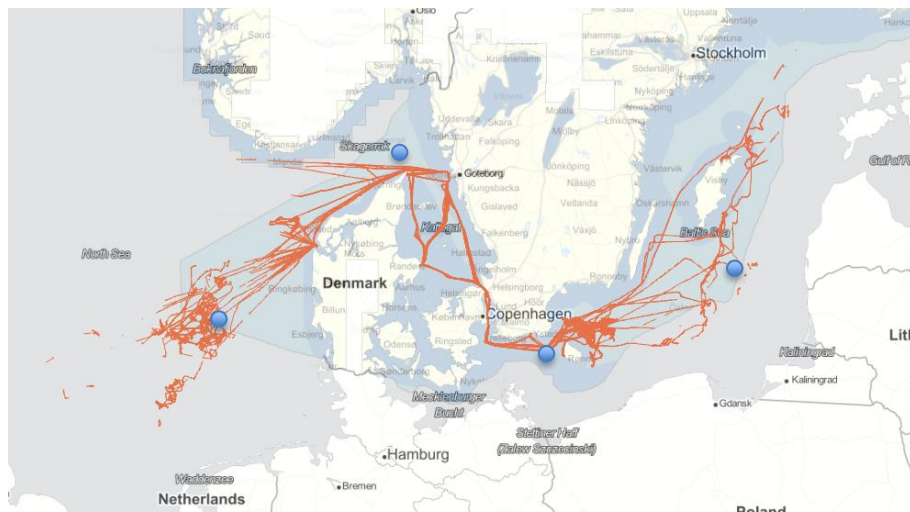


Figure 4-1: Historic route – Stella Nova IX (Extracted from AIS data from the Swedish Maritime Administration and the Danish Maritime Authority)

Table 4-1: Ship orientation on each point (direction in degrees)

P. 01 (55.5, 6)		P. 02 (58, 10.6)				P. 03 (54.6, 14.4)				P. 04 (56, 19.3)	
dir 1	dir 2	dir 1	dir 2	dir 3	dir 4	dir 1	dir 2	dir 3	dir 4	dir 1	dir 2
245	65	245	65	145	325	145	325	55	235	55	235

From here a series of cases are established in Table 4-2:

Table 4-2: Condition combination list

Analysis combination for frequent conditions					
Condition	Working condition	Speed (knots)	wave height (m)	wavelength (m)	wave direction (deg)
01	Departure	12	0.85	24.11	163.54
02	Departure	12	0.85	24.11	263.54
03	Departure	12	0.6	19.9	240.85
04	Departure	12	0.6	19.9	330.85
05	Trawling	3	1.78	61.38	177.45
06	Trawling	3	1.07	33.18	327.98
07	Loaded	11.75	1.78	61.38	357.45
08	Loaded	11.75	0.85	24.11	343.54
09	Loaded	11.75	0.85	24.11	83.54
10	Loaded	11.75	0.6	19.9	60.85
11	Loaded	11.75	0.6	19.9	150.85
12	Loaded	11.75	1.07	33.18	147.98

Because of limitations within SHIPFLOW 6.0, analysis 02 and 09, that are beam seas, will not be able to be simulated.

4.1.1.2 Second generation intact stability conditions

The boundary conditions established for this analysis are the following:

- Ship speed.
- Trimming, heeling and displacement.
- Rolling condition due to trawling moment applied on the ship.
- Heading wave conditions (wave height, wavelength).

To investigate the apparition of parametric rolling, certain conditions need to be fulfilled (see chapter 2.2.2). After assessment of the vulnerability criteria, the apparent condition that triggers parametric rolling is simulated later SHIPFLOW.

4.1.2 Considerations

4.1.2.1 Centre of gravity

Both the longitudinal centre of gravity (LCG) and the vertical centre of gravity (VCG) can be specified in SHIPFLOW, and this will set a specific trimming condition as the code calculates the centre of buoyancy by the given draft.

If the longitudinal centre of gravity is not specified, then the code locates this coordinate right below the longitudinal centre of buoyancy (LCB) to maintain the initial trimming and heeling condition of the imported hull.

Given these features and that the buoyancy centre can only change to compensate the weight by altering the trimming conditions, the draft is set free to change according to the variation of the centre of gravity.

A particular case of study is the trawling condition. In this condition the vessel is under an external load (purse drag force) that affect the trimming of the ship. As SHIPFLOW Motions 6 does not have a feature to account for external loads, it was seen necessary to recreate the condition by shifting the centre of gravity by virtually adding a weight at the appropriate location that will produce the same sink, trim, and heel.

4.1.2.2 Hydrodynamic coefficients

On another matter, SHIPFLOW motions, being a potential flow solving code, does not take in consideration the viscosity of the fluid for the solution of the flow. This means that recirculation and changing vorticity, that may be of relevance due to the hull shape (big keel, bulbous bow, and wet transom), will not be considered when solving the fluid flow. Such effects are partially responsible for the damping effects which now will be neglected if is not calculated separately. To obtain accurate results, it is first necessary to calculate the additional damping coefficients to account for the absence of viscous roll damping and input them in SHIPFLOW to carry out the simulations.

By expressing the roll motion of the ship by 1-DOF equation as eq. (4.1), the hydrodynamic coefficients need to be investigated and input in SHIPFLOW for a correct prediction of motions of the ship.

$$(I_{44} + \delta I_{44})\ddot{\phi}_4 + N_{44}\dot{\phi}_4 + S_{44}\phi_4 = M_{E44}(t) \quad (4.1)$$

There are different approaches that can be taken for determining the hydrodynamic coefficients, restoring coefficient (S_{44}), damping coefficient (N_{44}), and added mass moment of inertia ($I_{44} + \delta I_{44}$). ME_{44} represents the external load. The hydrodynamic coefficients for roll and pitch motion can be estimated by a decay motion analysis with an initial condition for each motion. However, this must be carried with a viscous solver code (Coslovich, 2020). The estimation of the hydrodynamic coefficients can be done by following the procedure presented in (Kianejad S. , Enshaei, Duffy, & Ansarifard, 2020), (Kianejad S. S., Enshaei, Duffy, Ansarifard, & Ranmuthugala, 2018) and (Sadra Kianejad, Hossein Enshaei, Jonathan Duffy, & Nazanin Ansarifard, 2019). It is also important to mention that this procedure is time consuming and more computational demanding.

In Coslovich (2020) two main methods for the calculation of the damping coefficient are assessed, one related to the ship's geometry and another to experimental results.

As explained on section 2.1.2.1, Watanabe and Inoue approach (Himeno, 1981) is used to estimate the damping coefficient, this coefficient is only considered on the quadratic term (eq. 4.2 – 4.5), as the linear one is considered already by the software.

$$B_q = h \left[1.42 \frac{C_b T}{L} + 2 \frac{A_{bk} \sigma_0}{L^2} + 0.01 \right] f(Fn, \Lambda) \quad (4.2)$$

Where:

$$h = \left[\left(\frac{KG - T/2}{B} \right)^3 + \left(\frac{T}{B} \right)^2 \frac{L}{4B} + \frac{cB}{64T} \right] \frac{\rho \nabla B^2 180}{4\pi^3 C_B} \quad (4.3)$$

$$c \approx 1.994 C_{wp}^2 - 0.1926 C_{wp} \quad (4.4)$$

$$f(Fn, \Lambda) = 1 + 0.8 \frac{1 - e^{-10Fn}}{\Lambda^2} \quad (4.5)$$

And Λ represents the natural frequency and wave frequency ratio, where the natural frequency is calculated according to Molland, Anthony F. (2008). C_b and C_{wp} are hydrostatic properties (block coefficient and waterplane coefficient respectively). Fn is the Froude number at the studied speed. L , B and T are the main dimensions of the vessel (length, beam, and draught). Finally, ∇ is the volumetric displacement and KG is the vertical centre of gravity.

By using the data from Table 3-4 to Table 4-2, on equations (4.1) to (4.5) the damping coefficients are estimated and later non-dimensionalised by $(\rho \cdot Lpp^5)$ as shown on Table 4-3. This normalisation of the damping coefficient is done for the quadratic component of the linearized expression of the damping coefficient and is specifically done for its use in SHIPFLOW.

Table 4-3: Estimated damping coefficients.

Condition	Damping coefficient	
	Dimensional	Non-dimensional
01	1.36×10^7	6.14×10^{-5}
02	1.44×10^7	6.50×10^{-5}
03	1.37×10^7	6.20×10^{-5}
04	1.53×10^7	6.90×10^{-5}
05	1.47×10^7	6.66×10^{-5}
06	1.49×10^7	6.71×10^{-5}
07	7.32×10^7	3.55×10^{-4}
08	3.60×10^8	1.75×10^{-3}
09	3.10×10^7	1.50×10^{-4}
10	3.74×10^7	1.81×10^{-4}
11	2.79×10^7	1.35×10^{-4}
12	2.87×10^7	1.39×10^{-4}

4.1.2.3 Zones of study

In fact, if the study were to focus on the entire ship, it would have to assess every part of the vessel. Given that this is not feasible, it was seen coherent to focus on the most important areas inside and on the vessel. To do so, the approach considered had the objective of assessing the effect of the ship response on the crew, and for this a short questionnaire was created and sent to a previous skipper of the Stella Nova IX (Carmona at that time). The questionnaire is further described in section 4.2, p. 41, and presented in Appendix B, p.77.

The mentioned areas were selected based on the time spent on it by the skippers and where it is expected to be important to have established limits of vibrations and motions in correlation with the existing criteria applied for seakeeping assessment. The following list specifies the zones of interest, which are equally specified on the questionnaire filled by the skippers.

- Habitability
 - Quarters
 - Common areas (kitchen, bathroom, etc)
 - Bridge
- Working deck
 - Aft zone
 - Mid ship
 - Forward zone
- Other zones
 - Engine room
 - Bow

The specified zones are delimited as mentioned in Table 4-4 and measured from the aft perpendicular and base line.

Table 4-4: Delimitation of zones of study

		Aft end (m)	Forward end (m)	Bottom end (m)	Top end (m)	RBSMC Level.
Habitability	Quarters	11.90	20.30	7.60	10.10	8 – 10
	Common areas	11.90	20.30	10.10	12.50	10 – 12
	Bridge	11.23	19.50	12.50	15.35	12 – 13
Working Deck	Aft Zone	-2.20	11.30	5.30	12.50	5 – 12
	Mid ship	11.30	20.30	5.30	12.50	5 – 12
	Forward Zone	20.30	32.55	5.30	12.50	5 – 12
Other zones	Engine room	4.80	14.80	0.19	5.30	0 – 5
	Bow	32.50	46.60	8.15	11.05	8 – 11

RBSMC (see Appendix C) is the code used to calculate the responses at different points on the vertical levels of the geometry. A more detailed explanation of the code is given in section 4.2.

Certain results are expected in each zone, depending on the location on the ship, such as high pitch on the bow or rolling on the sides of the bridge and working decks.

By taking into consideration the same type of coordinate system as for the ship motions to the human body to identify the degrees of freedom, the motions experienced by the crew can be characterized numerically and compared with the established criteria. Table 4-5 shows the criteria of importance on each zone of the ship.

Table 4-5: Criteria application for each studied zone

Zone	Seaway Performance Criteria
Habitability	
Quarters	(a.1), (a.2), (b.3), (b.4), (b.5), (b.6)
Common areas	
Bridge	(a.1), (a.2), (b.3), (b.4), (b.5), (b.6), (b.7)
Working deck	
Aft zone	(a.1), (a.2), (b.3), (b.4), (b.5), (b.6)
Mid ship	
Forward zone	(a.1), (a.2), (b.3), (b.4), (b.5), (b.6), (b.7)
Other zones	
Engine room	(b.3), (b.4), (b.5), (b.6)
Bow	(b.2), (b.3), (b.6), (c.8), (c.9)

4.1.2.4 Study variants

As the main interest is to study the influence of the location of the centre of gravity of the vessel on the seakeeping and intact stability, a variation in the longitudinal and vertical coordinates of the centre of gravity of is achieved by analysing the different conditions specified on Table 4-2.

In the case of the analysis of the intact stability, as only the parametric rolling is assessed, this will be studied on the corresponding frequencies that will trigger this condition after the identification of possibility of occurrence of the phenomena. To do this, only the first vulnerability criteria is analysed by following the steps specified on section 2.2.2.1.

The results obtained from the simulations are later postprocessed in section 5 by evaluating them in comparison to the criteria chosen and explained on section 2.1.1.3.

4.1.2.5 Seakeeping criteria considerations

The evaluation of the results presented on section 5 is done by taking into consideration the four parameters specified by the ISO 2631 – 1(1997) as health, comfort, perception and motion sickness. These are at the same time divided in two groups, depending of their frequency of occurrence.

- 0.5 Hz to 80 Hz for health, comfort, and perception.
- 0.1 Hz to 0.5 Hz for motion sickness.

Only comfort and motion sickness, in addition to motion induced interruption (MII) (specified in section 2.1.1.3), are considered for the evaluation of the results presented in section 5.

The measurement of the accelerations is suggested to be done according to the basicentric axes specified by ISO 2631 – 1 (1997) and as shown on Figure 4-2. As the regulation specifies, the measurement should be done on the contact surface between the human body and the vibrating body (Ship). In order to comply with this requirement, the measurement needs to be done at the contact interface between the

located deck and human body part (feet, back, head, etc). However, due to the amount of simulations, and given that the distances from the different human body parts to evaluate are rather small compared to the tolerance of the code RBSMC, it is decided to simplify the evaluation by studying only the “vertical levels”.

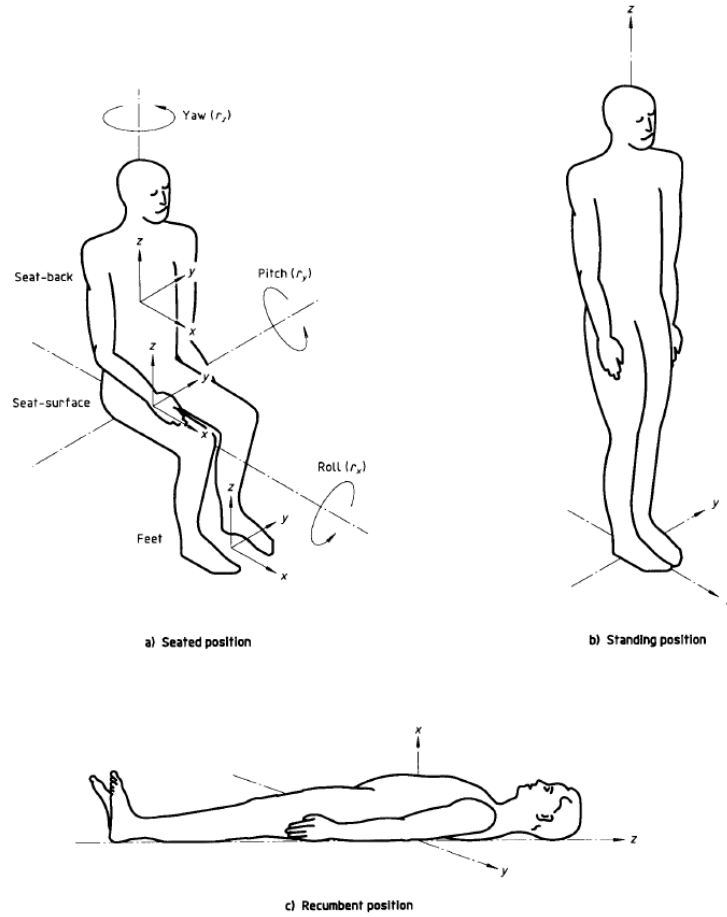


Figure 4-2: Basicentric axes of the human body (ISO 2631 – 1, 1997).

4.2 Methods and tools

Due to the conditions and characteristics that fishing vessels present, the results obtained do not apply to other fishing vessels. However, the methodology follows a flexible approach that can be replicated not only for similar vessels but for different fishing vessels within a range of characteristics that the computational tools allow. As Figure 4-3 and Figure 4-4 show, the workflow is characterised by a succession of steps that can be replicated for different hull shapes, working conditions and environmental characteristics.

As an initial step for the study of the behaviour of the Stella Nova IX (Ex-Carmona), it was seen proper to develop a study of the responses of the vessel under a range of conditions. The selected condition is the departure condition at 12 knots with a wave height of 0.85 m (0.0184 Lpp) and a range of wavelengths from 0.25Lpp to 7Lpp. The study is carried out under head waves to study heave and pitch motions and under beam-waves to study roll motions. Along with this, a study of the heave, pitch and roll decay motion is performed to obtain the natural period for each motion (a general damping

coefficient was assumed in this procedure). Under this initial study it is expected to understand the resonance frequencies of the vessel. Results of this first study are presented in section 5.1.

Once the initial study is finished, the working conditions and parametric rolling are evaluated as shown in figures Figure 4-3 and Figure 4-4.

The 3D model of the fishing vessel is created using Rhino 3D student license ver.6. To avoid any problem with how SHIPFLOW generates the panelization from the geometry, it is necessary to simplify some “complicated shapes”. The modifications are not expected to affect the results to a large degree and to accelerate the convergence of the simulation. In this way the aft part of the keel was softened, and the transom was made completely vertical. The complications take place due to how SHIPFLOW’s Potential code approaches the geometry and how the code solves the flow behind the transom of the vessel. This is further explained in section 5.

The wave characteristics were obtained through the data provided by ERA5 and with help from SSPA by gathering the data referred.

Once the information from the vessel and the wave characteristics are obtained, it is possible to proceed with the computational analysis in SHIPFLOW for the seakeeping assessment. With help of the developed code RBSMC the final responses in different zones of the ship are obtained and possible to be evaluated through the customized criteria.

On the side of the parametric rolling assessment, the evaluation is done mathematically through the vulnerability criteria specified in sub-section 2.2.2.2 (Belenky, Bassler, & Spyrou, 2011).

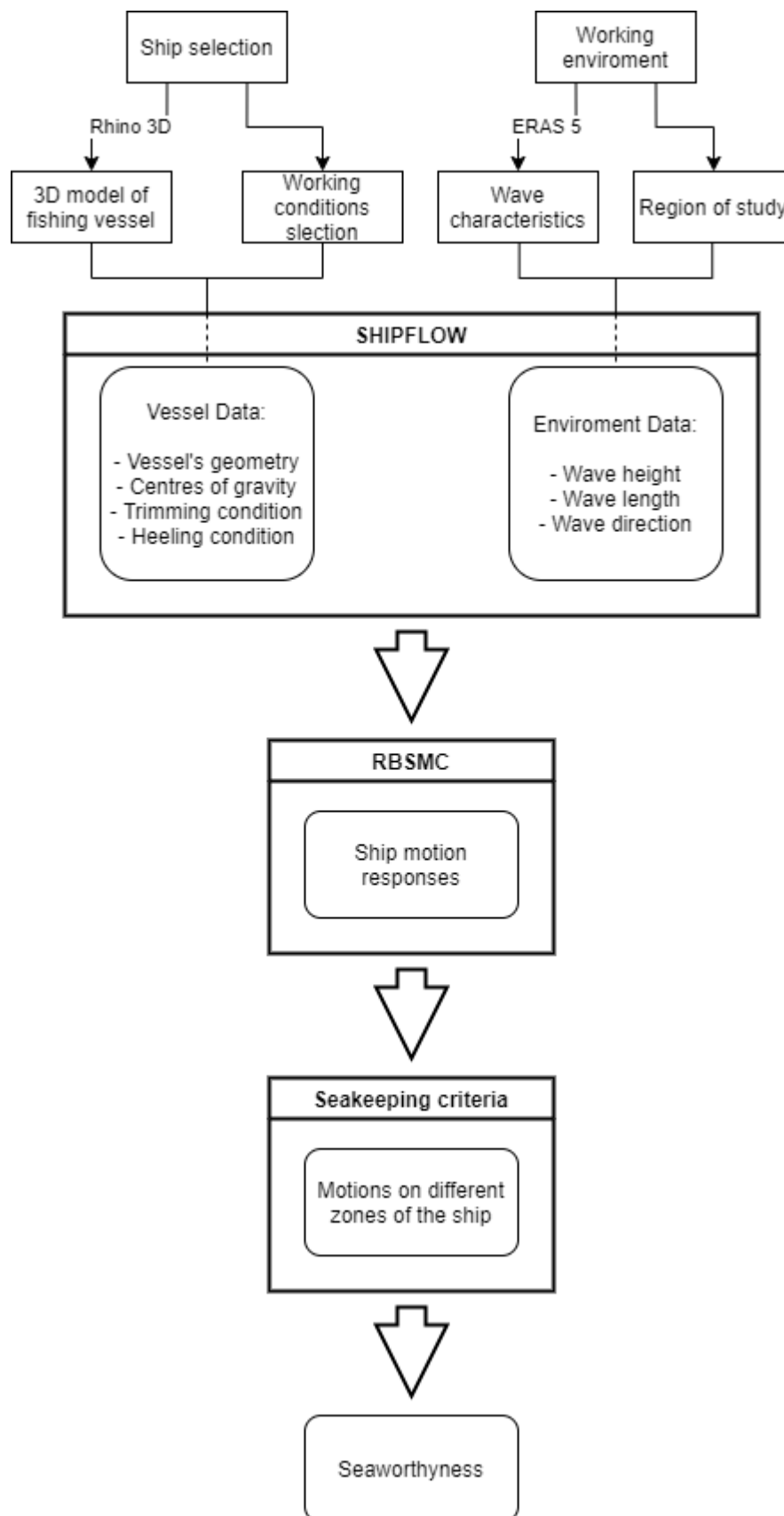


Figure 4-3: Working flow method for Seakeeping assessment

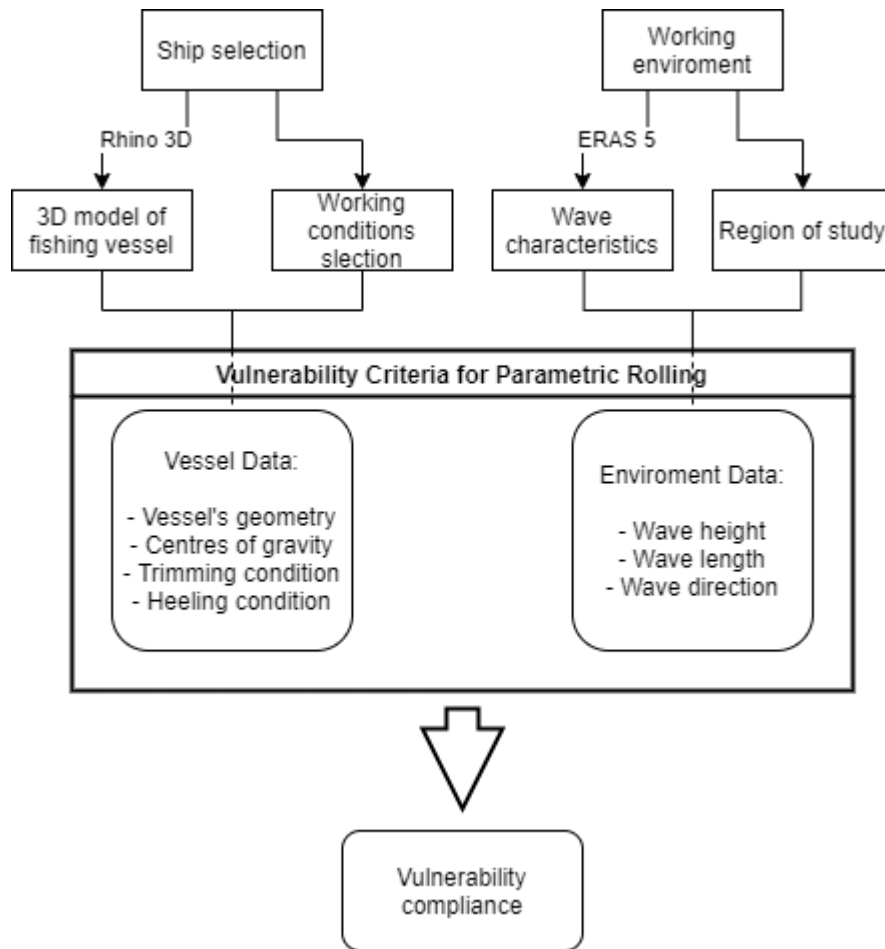


Figure 4-4: Working methodology for Parametric rolling assessment

CAD modelling

From AutoCAD, the lines plan was exported to Rhinoceros 3D to create the 3D surface of the hull. See Figure 4-5. Figure 4-6 shows the modification of the transom and keel's aft part.

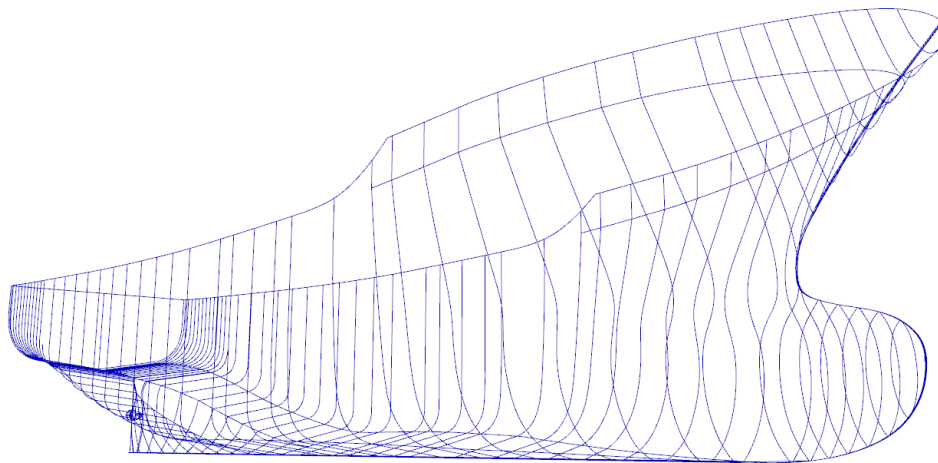


Figure 4-5: 3D lines plan exported to Rhinoceros 3D.

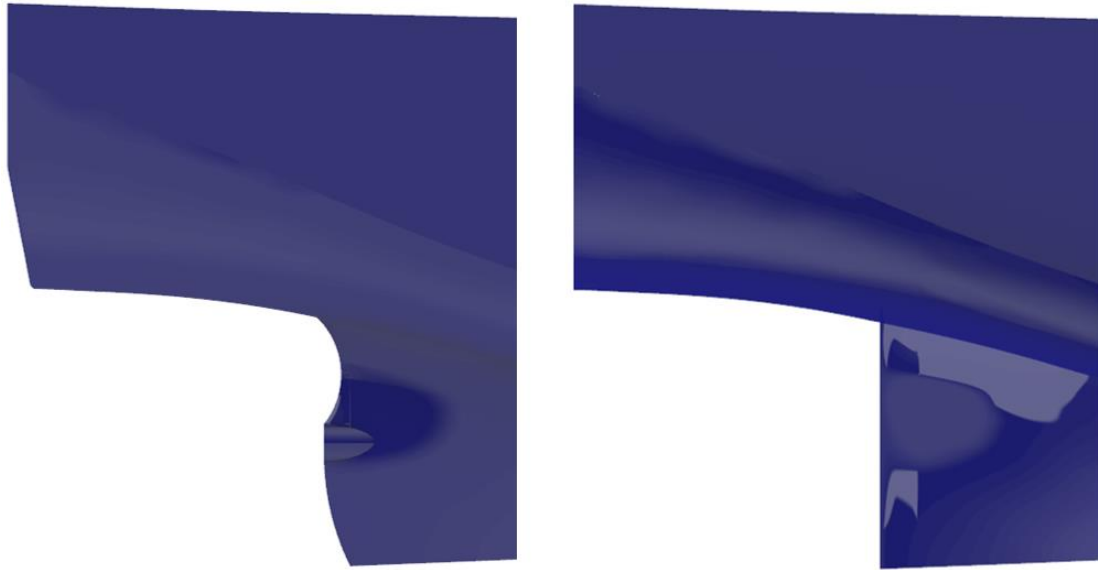


Figure 4-6: Transom and keel modification

SHIPFLOW computation

SHIPFLOW discretize the geometry using quadrilateral panels. The panelization of the hull was set to a medium range value to which the convergence of the solution was successful. A finer refinement showed problems in convergence due to the high density of elements in edges and at the transom.

Even though SHIPFLOW is a useful and versatile software that allows for the computation of a potential solver to simulate the responses of a ship in calm water and in waves, some limitations were identified when setting the different conditions to be analysed.

The main limitation falls in the approach the software computes the flow around the vessel's transom. This large transom is a challenging geometry that continuously sinks and emerges from the water. As potential flow does not consider the viscosity of the fluid (irrotational flow), the behaviour of the inviscid flow at the transom level is numerically challenging and not computed properly. More specifically, the constant change between wet and dry transom creates a flow recirculation at this region, which is not possible to be directly computed, unless certain considerations and adjustments are taken. SHIPFLOW is capable of approximate these effects to some extent, but this is still under development.

Regarding the panelization at the transom, it had a topology that concentrated the elements towards the lower point of the centerline. This arrangement resulted in a strong concentration of singularities which caused numerical problems for the solver. In turn, this resulted in a diverging solution on the nearby free surface which eventually led to a stop of the computations.

To avoid this complication, the panel density at the transom was reduced, as well as the damping factor governing the transom flow model. As Table 4-6 shows, the panel density of the hull gets reduced as the L_{pp} grows and the panel density of the free surface grows with the vessel speed.

Table 4-6: Panelization per condition

Condition	No. Elements			No. Nodes		
	Hull	Free Surface	Total	Hull	Free Surface	Total
Condition 01	12104	34506	46610	12690	35148	47838
Condition 02	12104	34506	46610	12690	35148	47838
Condition 03	12104	34506	46610	12690	35148	47838
Condition 04	12104	34506	46610	12690	35148	47838
Condition 05	11580	17710	29290	12154	18196	30350
Condition 06	11580	17710	29290	12154	18196	30350
Condition 07	12432	33760	46192	13024	34396	47420
Condition 08	12432	33760	46192	13024	34396	47420
Condition 09	12432	33760	46192	13024	34396	47420
Condition 10	12432	33760	46192	13024	34396	47420
Condition 11	12432	33760	46192	13024	34396	47420
Condition 12	12432	33760	46192	13024	34396	47420

Another challenge is found during the panelization of the aft-keel zone. When trying to panelize the quite complex aft end of the keel, SHIPFLOW compresses the element excessively and even overlaps them. These cannot be computed.

Then it was seen proper to simplify the geometries as seen in Figure 4-6. This modification allowed for a faster convergence and more even distribution of the panel in the geometry.

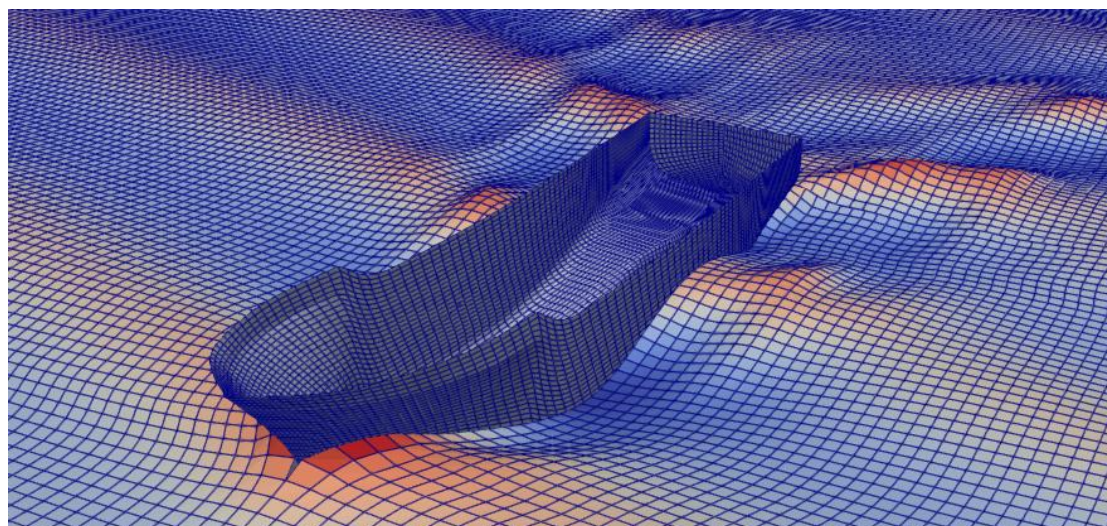


Figure 4-7: Panelization observed in PARAVIEW for condition 01.

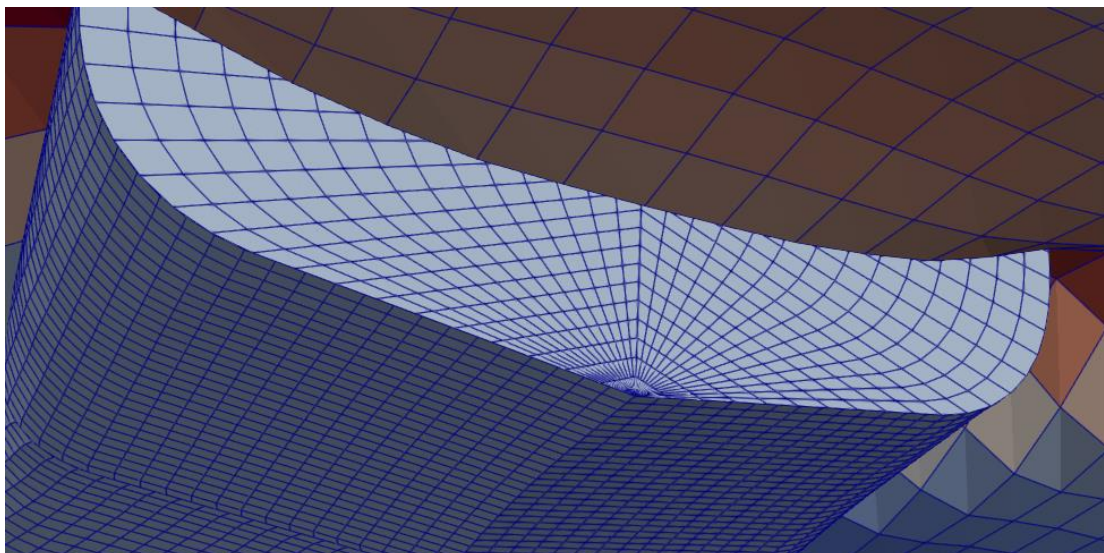


Figure 4-8: Panelization at transom, below free surface for condition 07.

As explained in sub-section 4.1.2.1, there is no implemented feature that can simulate an external load on the vessel for which it was necessary to recreate the same effects in an approximated way. The external load was simulated as an added weight (11.3 tons) on the main deck and located at the same longitudinal and horizontal position of the acting force. The extra weight produced the same trim and heel angles that the load will cause in static conditions. At the same time, the added weight was simulated but shifting the centre of gravity of the vessel according to the required trim and heel angle in static conditions.

Regarding the wall-time of the computations, this was dependent of the condition simulated. Some lasted for 12 h and others surpassed the 24 hours. The dependency was due to the convergence criteria specified in sub-section Methods and tools 4.2. In some conditions the convergence was reached when the error in the resistance had a value of 1%. In other cases, the solution converged at 100 encountered waves and the longest simulations lasted for a total of 10000 iterations (time steps). To set an appropriate amount of data, several encountered waves was set depending on the wavelength and angle of incidence. This was also done for reaching enough repetitions in the responses.

On behalf of the convergence criteria for the simulations, three conditionals were established. Either the simulation stops when a total of 100 waves were encountered, when the simulation reached 10000 iterations or when the added resistance reached an error of 1% or lower. Also, a number of encountered waves was set depending on the wavelength and angle of incidence. This is done to obtain enough data for the post-processing stage.

Finally, there was an interesting observation when studying the RAO's under different wavelengths. Due to limited size of the computational domain employed in SHIPFLOW Motions, the longer wavelengths cannot be imposed correctly at the wave forcing zone (starting part of the domain). Therefore, the encountered waves have lower wave height than their nominal values. This observation was communicated to the developer who agreed with the statement. In order to resolve the issue a longer domain (at least half the wavelength) should be employed to capture the correct wave profile. However, this approach increases the cost of the computations. Instead, the issue was

resolved by calculating the RAO's by the actual wave height that was observed by the ship instead of the nominal wave height defined at the inlet boundary.

RBSMC

As SHIPFLOW output are the ship responses (motions, velocity, accelerations, forces, and moments) around the centre of gravity, it was necessary to build a code which could extend the values to different parts of the ship. This code was created in MATLAB, and it is attached in Appendix C, p.79. The code was built with the following considerations:

- Assumption that the ship behaves as a rigid body.
- Model and full-size output results. Hence, the output results can be expressed nondimensionalized, scaled or on real values.
- Inputs are the results from SHIPFLOW Motions and geometrical values of the ship such as length, beam, draft, decks, etc.
- The geometry of the vessel must be input as a series of points coordinates as three columns in a ".csv" file and it must be symmetric.
- The resolution of the results can be adjusted for better inspection.
- The output is a mapping of the motions, velocities, and acceleration on different "vertical levels" (vertical coordinates limited by the input geometry that work as "water planes").
- The different levels are considered as continuous waterplanes.

Given these characteristics, the code is referred as RBSMC (Rigid Body Ship Motions Computation).

Questionnaire

A short questionnaire was created and sent to a previous skipper of the Stella Nova IX (Carmona at that time). This questionnaire was of a qualitative nature, with a combination of open-ended questions (e.g., what were the most critical working conditions encountered during the operations) and closed-ended questions with a 5-point Likert scale to assess the level of comfort perceived by the skipper in different zones of the vessel. The questionnaire is presented in Appendix B, p.77. The overall objective of the questionnaire was to capture information from an experienced skipper to help to understand the responses of the vessel and assess them against the results obtained from the simulations.

5 Results and discussion

In this section, the results obtained from the simulations and their corresponding post-processing are presented. First a section presenting the responses of the vessel is shown, followed by the seakeeping analysis and the parametric rolling assessment.

5.1 Ship responses

Under the conditions specified in sub-section 4.2, a systematic study of the vessel is carried out in order to understand the heave, pitch and roll motions of the vessel. The condition used for this analyses is the light-ship condition.

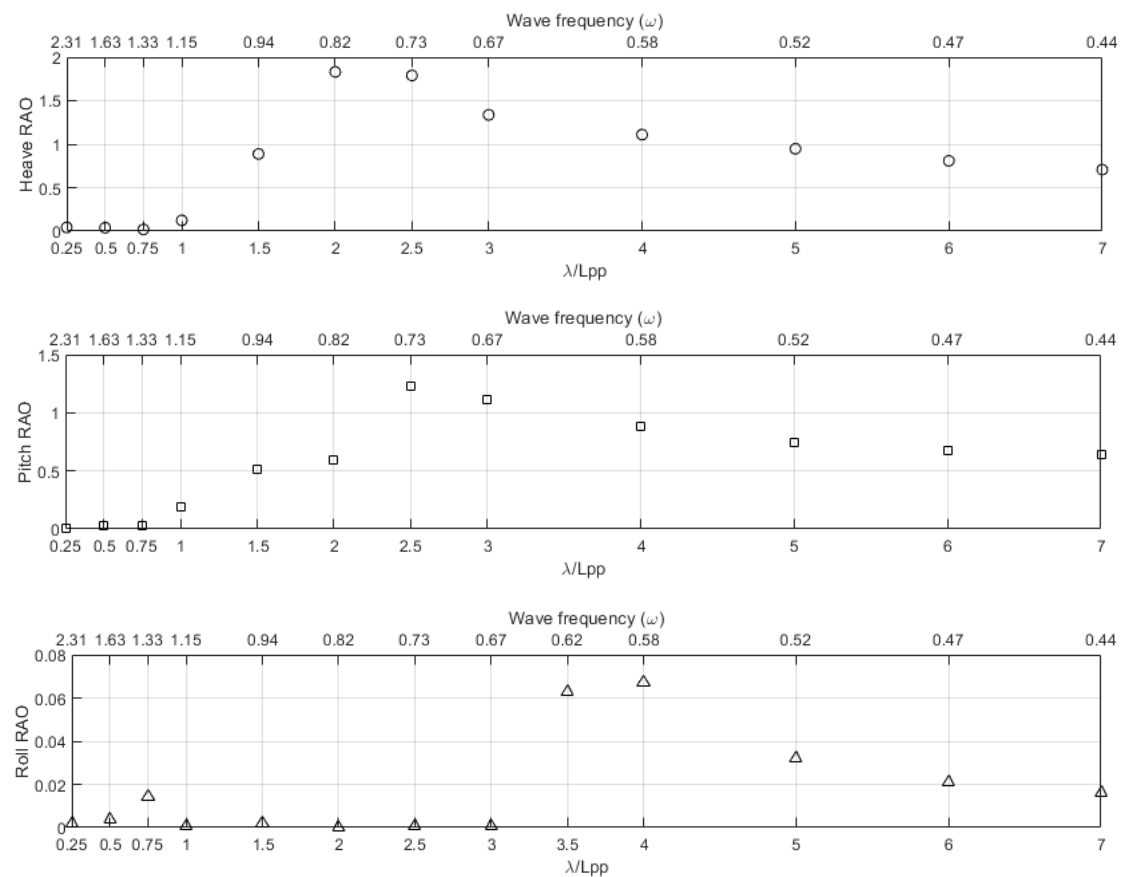


Figure 5-1: RAO at 12knots (head waves, wave height $0.0184L_{pp}$ and light-ship condition)

It is important to mention that SHIPFLOW had certain limitations when trying to compute large waves. To simplify, the code was not able to “sustain” larger than the domain waves, this caused the vessel to encounter smaller wave heights than the input ones. The responses of the vessel then, are smaller than what it should be. This behaviour is noted in Figure 5-1, where the asymptotic value of the RAO’s for Heave and Pitch are smaller than the 1. Such responses are not physically possible as in reality a vessel’s response follows the wave motion at long wave lengths. Hence, the normalization of the responses should be the unity.

To correct for this error during the non-dimensionalisation, it was necessary to measure the “actual” wave-height computed by SHIPFLOW, this was done through the Open-source software PARAVIEW ver. 5.9. A correction on the non-dimensionalisation of the RAO, Figure 5-4, was done by re-scaling the wave height according to the measured value (see Figure 5-2 and Figure 5-3).

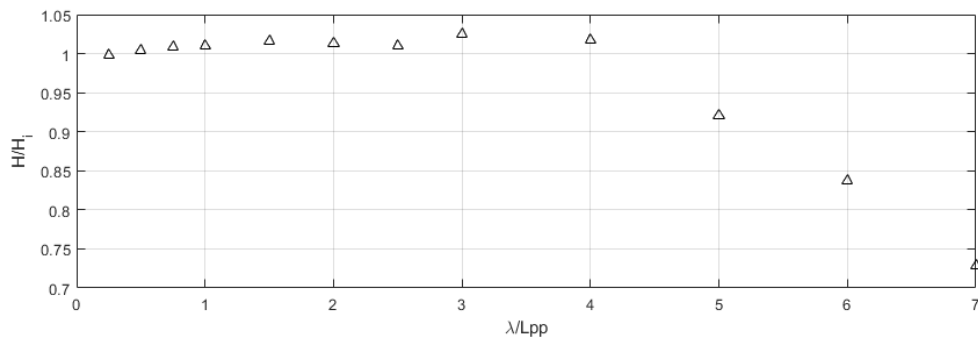


Figure 5-2: Pitch and Heave wave height ratio (wave height computed by SHIPFLOW/ wave height input).

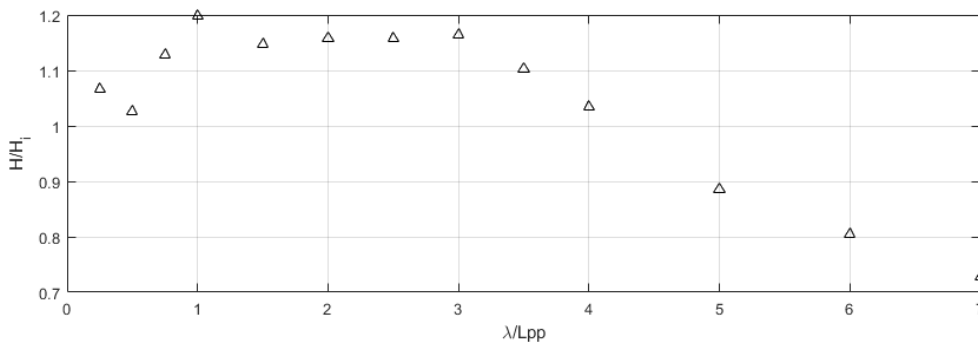


Figure 5-3: Roll wave height ratio (wave height computed by SHIPFLOW/ wave height input).

Figure 5-4 shows the corrected RAOs of the vessel in head waves for heave and pitch motions and beam waves, for roll motion. A particular and interesting observation is the minor motions the vessel experiences under small wavelengths, specially in the roll motion, where the resonance is not triggered until after a λ/L_{pp} larger than 3.

To estimate the natural frequencies of the vessel, three decay simulations were carried out, one for each motion at 12 knots. The natural period for each motion was obtained from these ones and later compared with the natural frequencies of wave encounter to understand what wavelengths will trigger the highest motions on the ship at this speed (See Table 5-1).

Table 5-1: Frequency, periods, and wavelengths

	Encounter period (s)	Encounter frequency (rad/s)	Wave period (s)	Wave length (λ/L_{pp})
Heave	6.06	1.037	8.79	2.6
Pitch	6.32	0.994	9.08	2.78
Roll	10.41	0.604	10.41	3.65

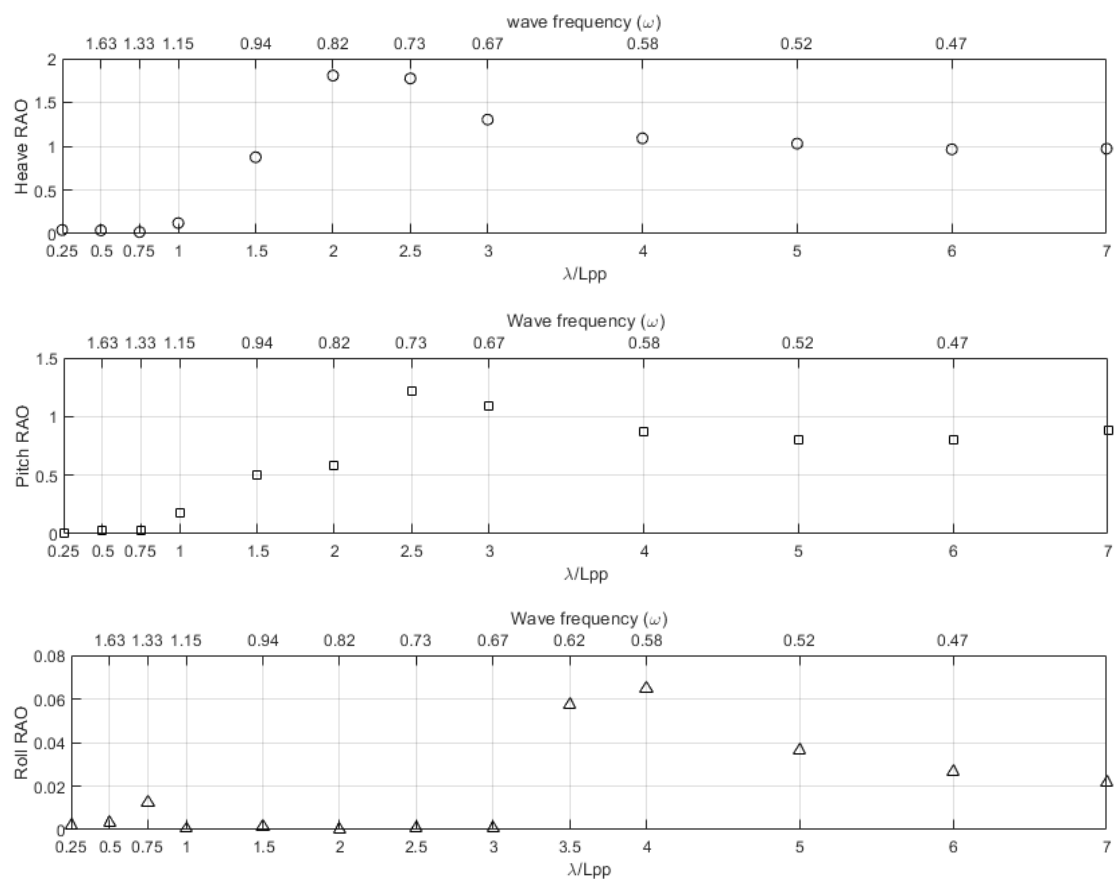


Figure 5-4: corrected RAO's for 12 knots.

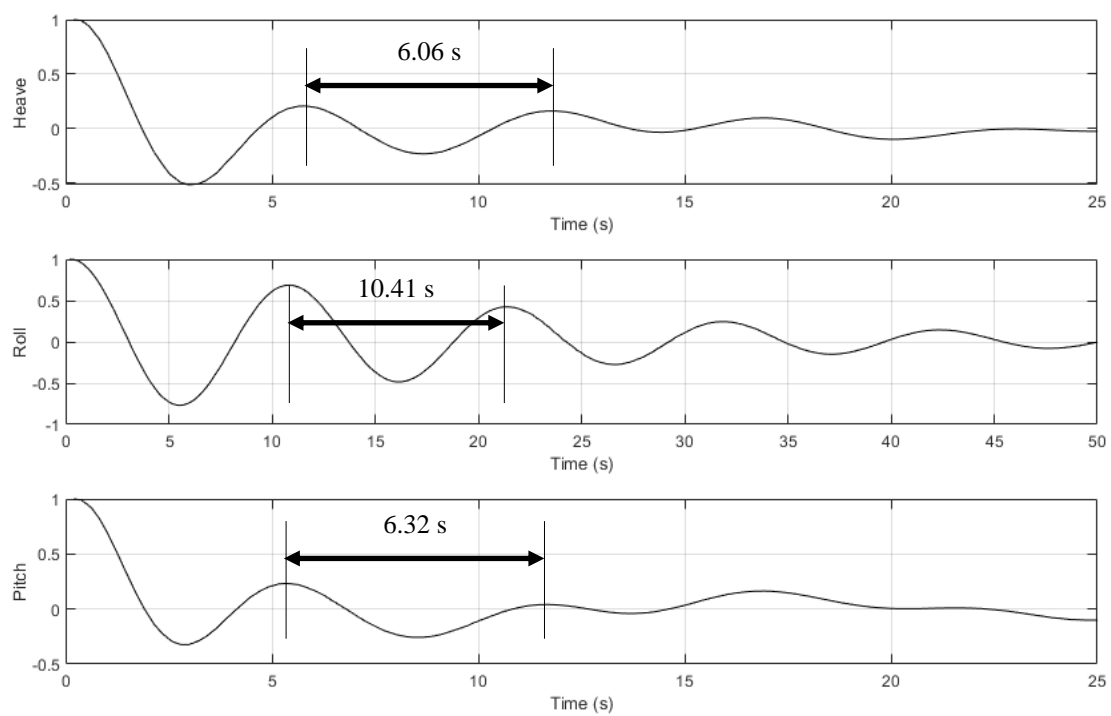


Figure 5-5: Motion decay simulation

The natural periods are consistent with the RAO curves for each motion, where the resonance is reached at large wave lengths, especially for roll motion.

On this matter, fishing vessels seem to differ in behaviour from tankers and container vessels. The studied vessel presents a response to waves quite different of what could be expected from larger ships. As Figure 5-4 shows, the resonance takes place at large wavelengths, especially for the roll motion, with a minor increase in the motions at high frequency waves.

As these analyses are carried out under lightship condition, they are not generalizable for all the remaining conditions. Its constantly changing displacement and speed, increase the range of possibilities for an optimal design. These different and variable working conditions, along with the environmental characteristics, create a series of different possible scenarios to study.

A good way to approach the large number of possibilities would be to perform the same systematic analysis under irregular waves and for each main working condition. However, there is a limited number of computational tools that can be used to simulate this type of vessels without incurring in high uncertainties.

5.2 Seakeeping results

In this section the results for the simulations of each condition are presented along with the compliance to the customized criteria. For the visualisation of all the results from RBSMC, refer to Appendix D, p.104.

Table 5-2 shows the comfort evaluation of each condition in the quarters zone, in comparison with Figure 2-6. From this, it is seen that the vessel is comfortable in most of the scenarios studied, according to ISO 2631 – 1 (1997). Again, the trawling condition seems to escape from the trend of the other results. (See Table 5-2).

Table 5-2: Evaluated comfort in working deck, quarters, and bridge.

Cond.	Working deck		Quarters		Bridge	
	Value (m/s ²)	Comfort	Value (m/s ²)	Comfort	Value (m/s ²)	Comfort
1	0.22	Below the range	0.175	Below the range	0.175	Below the range
2	0.61	A little uncomfortable	0.57	A little uncomfortable	0.59	A little uncomfortable
3	0.225	Below the range	0.125	Below the range	0.15	Below the range
4	0.042	Below the range	0.032	Below the range	0.032	Below the range
5	2.1	Very uncomfortable	1.1	Uncomfortable	1.1	Uncomfortable
6	0.45	A little uncomfortable	0.32	A little uncomfortable	0.335	A little uncomfortable
7	0.11	Below the range	0.082	Below the range	0.084	Below the range
8	0.12	Below the range	0.085	Below the range	0.145	Below the range
9	0.65	Fairly uncomfortable	0.39	A little uncomfortable	0.41	A little uncomfortable
10	0.13	Below the range	0.09	Below the range	0.12	Below the range
11	0.13	Below the range	0.1	Below the range	0.12	Below the range
12	0.51	A little uncomfortable	0.27	Below the range	0.31	Below the range

From Figure 5-7 to Figure 5-14 the results obtained from the extrapolation calculated by RBSMC for condition 05 and 07 at waterplanes 00 and 10 each are presented as a series of colour plots.

This contour plots show the RMS values of the motions, velocities and accelerations obtained at different point of the waterplanes (see Figure 5-6). The components are calculated by extrapolation from motions, velocities, and accelerations from the centre of gravity to each coordinate specified in the RBSMC code. From the plots it is then possible to analyse the responses at each needed location on the ship with the customized seakeeping criteria, see Appendix D and tables from Table 5-3 to Table 5-14.

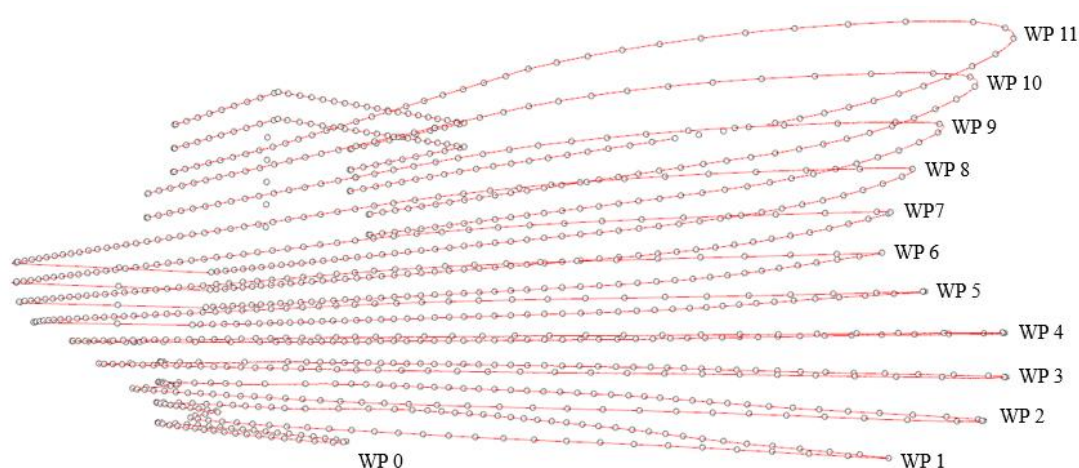


Figure 5-6: Waterplanes read by RBSMC

Figure 5-7 to Figure 5-14 show the results obtained by RBSMC in conditions 5 and 10 at the waterlines 0 and 10 respectively. These waterplanes are of special interest due to the high responses obtained at its furthest locations. The highest values of responses on these zones correspond to the engine room and forward part of the main deck, which is in correlation with the limits specified in the selected criteria.

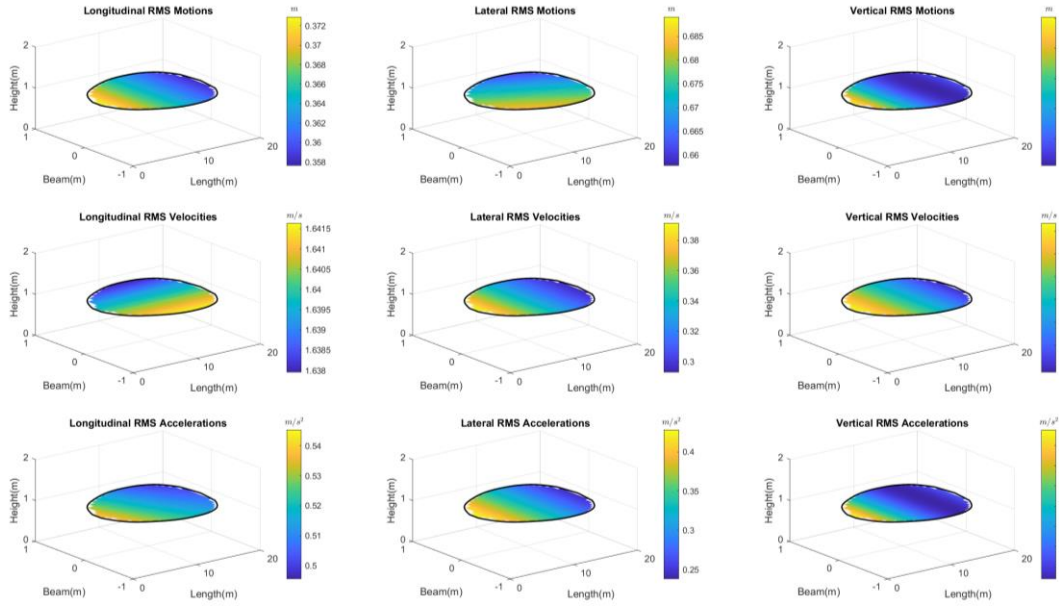


Figure 5-7: RMS components for motion, velocities and accelerations. Condition 05 - waterplane 00. Obtained by RBSMC code.

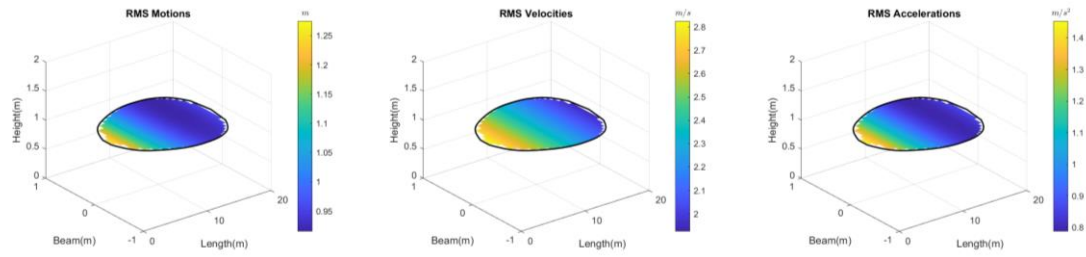


Figure 5-8: RMS for motion, velocities and accelerations. Condition 05 - waterplane 00. Obtained by RBSMC code.

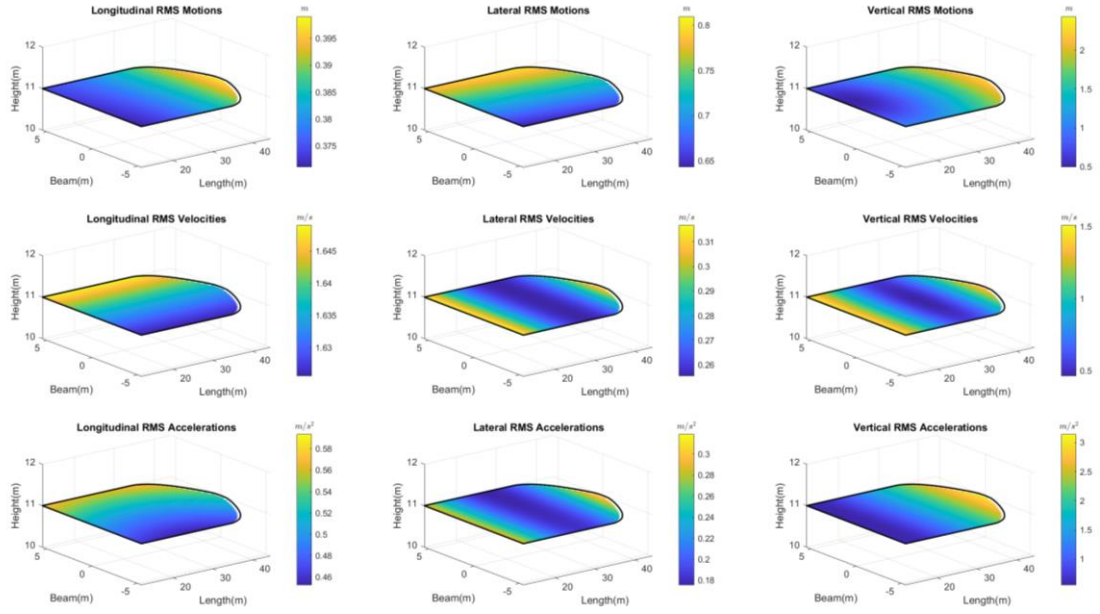


Figure 5-9: RMS components for motion, velocities and accelerations. Condition 05 - waterplane 10. Obtained by RBSMC code.

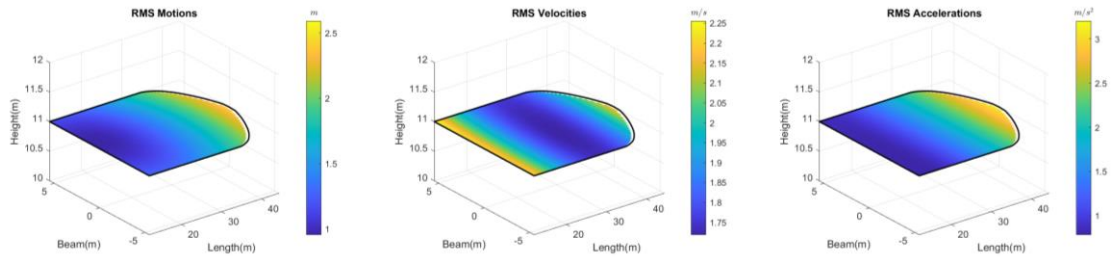


Figure 5-10: RMS for motion, velocities and accelerations. Condition 05 - waterplane 10. Obtained by RBSMC code.

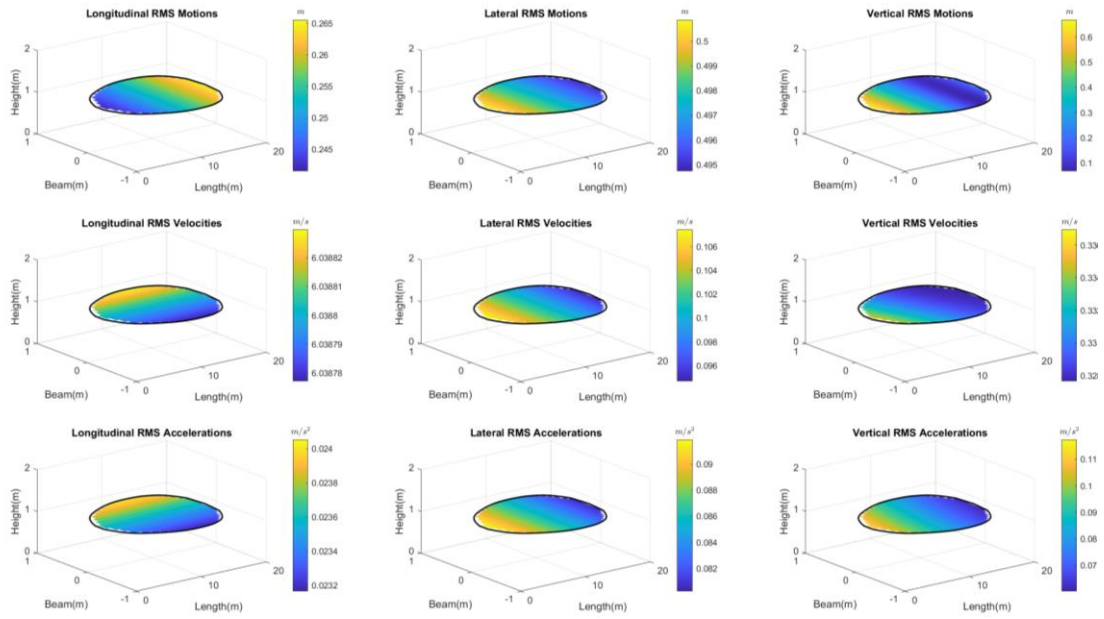


Figure 5-11: RMS components for motion, velocities and accelerations. Condition 10 - waterplane 00. Obtained by RBSMC code.

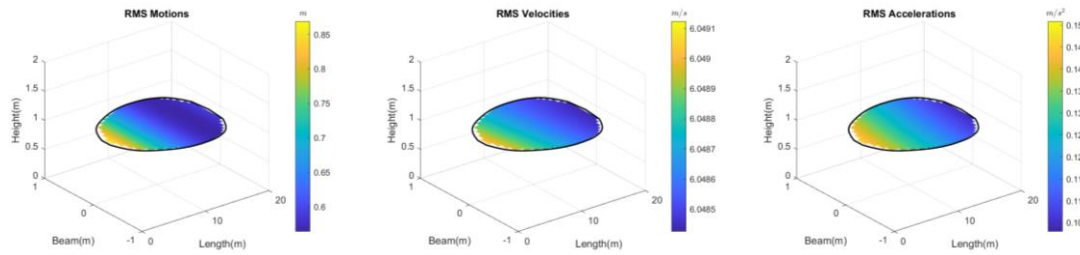


Figure 5-12: RMS for motion, velocities and accelerations. Condition 10 - waterplane 00. Obtained by RBSMC code.

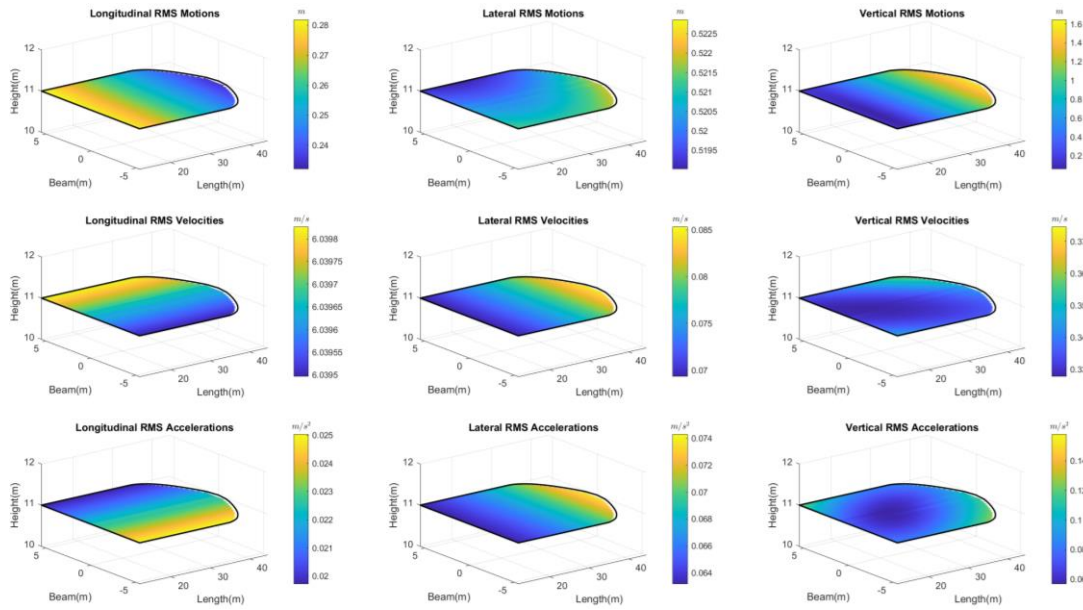


Figure 5-13: RMS components for motion, velocities and accelerations. Condition 10 - waterplane 10. Obtained by RBSMC code.

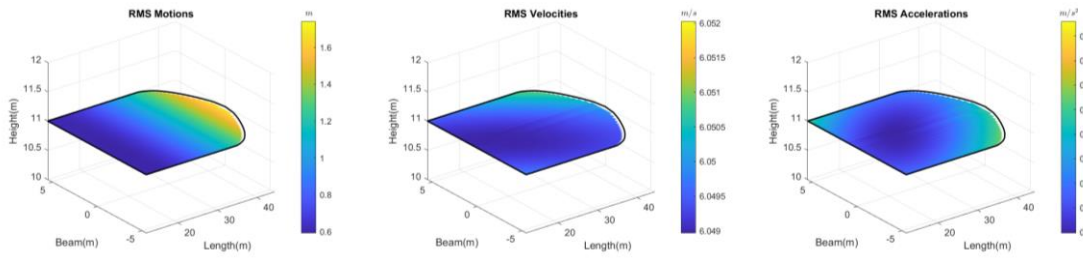


Figure 5-14: RMS for motion, velocities and accelerations. Condition 10 - waterplane 10. Obtained by RBSMC code.

5.2.1 Light ship conditions

Table 5-3: Condition 01

Index	Seaway Performance Criteria	Criteria Value	Actual Value	Compliance
(a)	Absolute Motion Amplitude			
1	Roll amplitude	6.0 deg for light manual work	0.72 deg	Below
		4.0 deg for heavy manual work		Below
		3.0 deg for intellectual work		Below
		2.5 deg for transit passengers		Below
		2.0 for cruise liner		Below
2	Pitch amplitude	1.5 deg (R.M.S.)	0.477 deg	Below
(b)	Absolute Velocities and Accelerations			
3	Vertical acceleration	0.2g for light manual work	0.02g	Below
		0.15g for heavy manual work		Below
		0.1g for intellectual work		Below
		0.05g for transit passengers		Below
		0.02g for cruise liner		Limit
4	Lateral acceleration	0.10g for light manual work	0.005g	Below
		0.07g for heavy manual work		Below
		0.05g for intellectual work		Below
		0.04g for transit passengers		Below
		0.03g for cruise liner		Below
5	Motion sickness incidence (MSI)	20% of crew in 4 hours	0 %	Below
6	Motion induced interruption (MII)	1 tip per minute	Roll – 0 tpm Pitch – 0 tpm	Below
7	Slamming acceleration (vertical)	Vertical acceleration when slamming taking place TBD	0	TBD
(c)	Motions relative to sea			
8	Frequency of slamming (reimmersion and velocity threshold)	0.03 (L <= 100)	0	Yes
		3.85 knots	12 knots	Higher
9	Frequency of deck wetness	0.05	0	Below

Table 5-4: Condition 02

Index	Seaway Performance Criteria	Criteria Value	Actual Value	Compliance
(a)	Absolute Motion Amplitude			
1	Roll amplitude	6.0 deg for light manual work	0.2 deg	Below
		4.0 deg for heavy manual work		Below
		3.0 deg for intellectual work		Below
		2.5 deg for transit passengers		Below
		2.0 for cruise liner		Below
2	Pitch amplitude	1.5 deg (R.M.S.)	0.573 deg	Bellow
(b)	Absolute Velocities and Accelerations			
3	Vertical acceleration	0.2g for light manual work	0.062g	Below
		0.15g for heavy manual work		Below
		0.1g for intellectual work		Below
		0.05g for transit passengers		Higher
		0.02g for cruise liner		Higher
4	Lateral acceleration	0.10g for light manual work	0.005g	Below
		0.07g for heavy manual work		Below
		0.05g for intellectual work		Below
		0.04g for transit passengers		Below
		0.03g for cruise liner		Below
5	Motion sickness incidence (MSI)	20% of crew in 4 hours	0 %	Below
6	Motion induced interruption (MII)	1 tip per minute	Roll – 0 tpm Pitch – 0 tpm	Below
7	Slamming acceleration (vertical)	Vertical acceleration when slamming taking place TBD	0	TBD
(c)	Motions relative to sea			
8	Frequency of slamming (reimmersion and velocity threshold)	0.03 (L <= 100)	0	Yes
		3.85 knots	12 knots	Higher
9	Frequency of deck wetness	0.05	0	Below

Table 5-5: Condition 03

Index	Seaway Performance Criteria	Criteria Value	Actual Value	Compliance
(a)	Absolute Motion Amplitude			
1	Roll amplitude	6.0 deg for light manual work	0.126 deg	Below
		4.0 deg for heavy manual work		Below
		3.0 deg for intellectual work		Below
		2.5 deg for transit passengers		Below
		2.0 deg for cruise liner		Below
2	Pitch amplitude	1.5 deg (R.M.S.)	0.097 deg	Bellow
(b)	Absolute Velocities and Accelerations			
3	Vertical acceleration	0.2g for light manual work	0.016g	Below
		0.15g for heavy manual work		Below
		0.1g for intellectual work		Below
		0.05g for transit passengers		Below
		0.02g for cruise liner		Below
4	Lateral acceleration	0.10g for light manual work	0.005g	Below
		0.07g for heavy manual work		Below
		0.05g for intellectual work		Below
		0.04g for transit passengers		Below
		0.03g for cruise liner		Below
5	Motion sickness incidence (MSI)	20% of crew in 4 hours	0 %	Below
6	Motion induced interruption (MII)	1 tip per minute	Roll – 0 tpm Pitch – 0 tpm	Below
7	Slamming acceleration (vertical)	Vertical acceleration when slamming taking place TBD	0	TBD
(c)	Motions relative to sea			
8	Frequency of slamming (reimmersion and velocity threshold)	0.03 (L <= 100)	0	Yes
		3.85 knots	12 knots	Higher
9	Frequency of deck wetness	0.05	0	Below

Table 5-6: Condition 04

Index	Seaway Performance Criteria	Criteria Value	Actual Value	Compliance
(a)	Absolute Motion Amplitude			
1	Roll amplitude	6.0 deg for light manual work	1.318 deg	Below
		4.0 deg for heavy manual work		Below
		3.0 deg for intellectual work		Below
		2.5 deg for transit passengers		Below
		2.0 for cruise liner		Below
2	Pitch amplitude	1.5 deg (R.M.S.)	0.309 deg	Bellow
(b)	Absolute Velocities and Accelerations			
3	Vertical acceleration	0.2g for light manual work	0.003g	Below
		0.15g for heavy manual work		Below
		0.1g for intellectual work		Below
		0.05g for transit passengers		Below
		0.02g for cruise liner		Below
4	Lateral acceleration	0.10g for light manual work	0g	Below
		0.07g for heavy manual work		Below
		0.05g for intellectual work		Below
		0.04g for transit passengers		Below
		0.03g for cruise liner		Below
5	Motion sickness incidence (MSI)	20% of crew in 4 hours	0 %	Below
6	Motion induced interruption (MII)	1 tip per minute	Roll – 0 tpm Pitch – 0 tpm	Below
7	Slamming acceleration (vertical)	Vertical acceleration when slamming taking place TBD	0	TBD
(c)	Motions relative to sea			
8	Frequency of slamming (reimmersion and velocity threshold)	0.03 (L <= 100)	0	Yes
		3.85 knots	12 knots	Higher
9	Frequency of deck wetness	0.05	0	Below

5.2.2 Trawling conditions

Table 5-7: Condition 05

Index	Seaway Performance Criteria	Criteria Value	Actual Value	Compliance
(a)	Absolute Motion Amplitude			
1	Roll amplitude	6.0 deg for light manual work	6.3 deg	Higher
		4.0 deg for heavy manual work		Higher
		3.0 deg for intellectual work		Higher
		2.5 deg for transit passengers		Higher
		2.0 for cruise liner		Higher
2	Pitch amplitude	1.5 deg (R.M.S.)	6.16 deg	Higher
(b)	Absolute Velocities and Accelerations			
3	Vertical acceleration	0.2g for light manual work	0.19g	Below
		0.15g for heavy manual work		Higher
		0.1g for intellectual work		Higher
		0.05g for transit passengers		Higher
		0.02g for cruise liner		Higher
4	Lateral acceleration	0.10g for light manual work	0.03g	Below
		0.07g for heavy manual work		Below
		0.05g for intellectual work		Below
		0.04g for transit passengers		Below
		0.03g for cruise liner		Limit
5	Motion sickness incidence (MSI)	20% of crew in 4 hours	77 %	Higher
6	Motion induced interruption (MII)	1 tip per minute	Roll - 1.33 Pitch - 0.93	Limit
7	Slamming acceleration (vertical)	Vertical acceleration when slamming taking place	TBD	TBD
(c)	Motions relative to sea			
8	Frequency of slamming (reimmersion and velocity threshold)	0.03 (L <= 100)	0.0835	Higher
		3.896 knots	3 knots	Below
9	Frequency of deck wetness	0.05	0.154	Higher

Table 5-8: Condition 06

Index	Seaway Performance Criteria	Criteria Value	Actual Value	Compliance
(a)	Absolute Motion Amplitude			
1	Roll amplitude	6.0 deg for light manual work	7.16 deg	Higher
		4.0 deg for heavy manual work		Higher
		3.0 deg for intellectual work		Higher
		2.5 deg for transit passengers		Higher
		2.0 for cruise liner		Higher
2	Pitch amplitude	1.5 deg (R.M.S.)	1.82 deg	Higher
(b)	Absolute Velocities and Accelerations			
3	Vertical acceleration	0.2g for light manual work	0.027g	Below
		0.15g for heavy manual work		Below
		0.1g for intellectual work		Below
		0.05g for transit passengers		Below
		0.02g for cruise liner		Higher
4	Lateral acceleration	0.10g for light manual work	0.015g	Below
		0.07g for heavy manual work		Below
		0.05g for intellectual work		Below
		0.04g for transit passengers		Below
		0.03g for cruise liner		Below
5	Motion sickness incidence (MSI)	20% of crew in 4 hours	0 %	Below
6	Motion induced interruption (MII)	1 tip per minute	Roll - 2.8 tpm Pitch – 0 tpm	Higher
7	Slamming acceleration (vertical)	Vertical acceleration when slamming taking place	TBD	TBD
(c)	Motions relative to sea			
8	Frequency of slamming (reimmersion and velocity threshold)	0.03 (L <= 100)	0	Below
		3.896 knots	3 knots	Below
9	Frequency of deck wetness	0.05	0	Below

5.2.3 Fully loaded conditions

Table 5-9: Condition 07

Index	Seaway Performance Criteria	Criteria Value	Actual Value	Compliance
(a)	Absolute Motion Amplitude			
1	Roll amplitude	6.0 deg for light manual work	0.745deg	Below
		4.0 deg for heavy manual work		Below
		3.0 deg for intellectual work		Below
		2.5 deg for transit passengers		Below
		2.0 for cruise liner		Below
2	Pitch amplitude	1.5 deg (R.M.S.)	1.92 deg	Higher
(b)	Absolute Velocities and Accelerations			
3	Vertical acceleration	0.2g for light manual work	0.012g	Below
		0.15g for heavy manual work		Below
		0.1g for intellectual work		Below
		0.05g for transit passengers		Below
		0.02g for cruise liner		Below
4	Lateral acceleration	0.10g for light manual work	0.001g	Below
		0.07g for heavy manual work		Below
		0.05g for intellectual work		Below
		0.04g for transit passengers		Below
		0.03g for cruise liner		Below
5	Motion sickness incidence (MSI)	20% of crew in 4 hours	0 %	Below
6	Motion induced interruption (MII)	1 tip per minute	Roll – 0 tpm Pitch – 0 tpm	Below
7	Slamming acceleration (vertical)	Vertical acceleration when slamming taking place	TBD	TBD
(c)	Motions relative to sea			
8	Frequency of slamming (reimmersion and velocity threshold)	0.03 (L <= 100)	0	Below
		3.83 knot	11.75 knot	Higher
9	Frequency of deck wetness	0.05	2.76	Higher

Table 5-10: Condition 08

Index	Seaway Performance Criteria	Criteria Value	Actual Value	Compliance
(a)	Absolute Motion Amplitude			
1	Roll amplitude	6.0 deg for light manual work	1.432 deg	Below
		4.0 deg for heavy manual work		Below
		3.0 deg for intellectual work		Below
		2.5 deg for transit passengers		Below
		2.0 for cruise liner		Below
2	Pitch amplitude	1.5 deg (R.M.S.)	0.123 deg	Below
(b)	Absolute Velocities and Accelerations			
3	Vertical acceleration	0.2g for light manual work	0.01g	Below
		0.15g for heavy manual work		Below
		0.1g for intellectual work		Below
		0.05g for transit passengers		Below
		0.02g for cruise liner		Below
4	Lateral acceleration	0.10g for light manual work	0.007g	Below
		0.07g for heavy manual work		Below
		0.05g for intellectual work		Below
		0.04g for transit passengers		Below
		0.03g for cruise liner		Below
5	Motion sickness incidence (MSI)	20% of crew in 4 hours	0 %	Below
6	Motion induced interruption (MII)	1 tip per minute	Roll – 0tpm Pitch – 0 tpm	Below
7	Slamming acceleration (vertical)	Vertical acceleration when slamming taking place	TBD	TBD
(c)	Motions relative to sea			
8	Frequency of slamming (reimmersion and velocity threshold)	0.03 (L <= 100)	0	Below
		3.83 knot	11.75 knot	Higher
9	Frequency of deck wetness	0.05	0	Below

Table 5-11: Condition 09

Index	Seaway Performance Criteria	Criteria Value	Actual Value	Compliance
(a)	Absolute Motion Amplitude			
1	Roll amplitude	6.0 deg for light manual work	0.397 deg	Below
		4.0 deg for heavy manual work		Below
		3.0 deg for intellectual work		Below
		2.5 deg for transit passengers		Below
		2.0 for cruise liner		Below
2	Pitch amplitude	1.5 deg (R.M.S.)	0.928 deg	Below
(b)	Absolute Velocities and Accelerations			
3	Vertical acceleration	0.2g for light manual work	0.032g	Below
		0.15g for heavy manual work		Below
		0.1g for intellectual work		Below
		0.05g for transit passengers		Below
		0.02g for cruise liner		Higher
4	Lateral acceleration	0.10g for light manual work	0.02g	Below
		0.07g for heavy manual work		Below
		0.05g for intellectual work		Below
		0.04g for transit passengers		Below
		0.03g for cruise liner		Below
5	Motion sickness incidence (MSI)	20% of crew in 4 hours	0 %	Below
6	Motion induced interruption (MII)	1 tip per minute	Roll – 0 tpm Pitch – 0 tpm	Below
7	Slamming acceleration (vertical)	Vertical acceleration when slamming taking place	TBD	TBD
(c)	Motions relative to sea			
8	Frequency of slamming (reimmersion and velocity threshold)	0.03 (L ≤ 100)	0	Below
		3.83 knot	11.75 knot	Higher
9	Frequency of deck wetness	0.05	0	Below

Table 5-12: Condition 10

Index	Seaway Performance Criteria	Criteria Value	Actual Value	Compliance
(a)	Absolute Motion Amplitude			
1	Roll amplitude	6.0 deg for light manual work	1.29 deg	Below
		4.0 deg for heavy manual work		Below
		3.0 deg for intellectual work		Below
		2.5 deg for transit passengers		Below
		2.0 for cruise liner		Below
2	Pitch amplitude	1.5 deg (R.M.S.)	3 deg	Higher
(b)	Absolute Velocities and Accelerations			
3	Vertical acceleration	0.2g for light manual work	0.01g	Below
		0.15g for heavy manual work		Below
		0.1g for intellectual work		Below
		0.05g for transit passengers		Below
		0.02g for cruise liner		Higher
4	Lateral acceleration	0.10g for light manual work	0.007g	Below
		0.07g for heavy manual work		Below
		0.05g for intellectual work		Below
		0.04g for transit passengers		Below
		0.03g for cruise liner		Below
5	Motion sickness incidence (MSI)	20% of crew in 4 hours	0 %	Below
6	Motion induced interruption (MII)	1 tip per minute	Roll – 0 tpm Pitch – 0 tpm	Below
7	Slamming acceleration (vertical)	Vertical acceleration when slamming taking place	TBD	TBD
(c)	Motions relative to sea			
8	Frequency of slamming (reimmersion and velocity threshold)	0.03 (L ≤ 100)	0	Below
		3.83 knot	11.75 knot	Higher
9	Frequency of deck wetness	0.05	0	Below

Table 5-13: Condition 11

Index	Seaway Performance Criteria	Criteria Value	Actual Value	Compliance
(a)	Absolute Motion Amplitude			
1	Roll amplitude	6.0 deg for light manual work	0.06 deg	Below
		4.0 deg for heavy manual work		Below
		3.0 deg for intellectual work		Below
		2.5 deg for transit passengers		Below
		2.0 for cruise liner		Below
2	Pitch amplitude	1.5 deg (R.M.S.)	0.029 deg	Higher
(b)	Absolute Velocities and Accelerations			
3	Vertical acceleration	0.2g for light manual work	0.011g	Below
		0.15g for heavy manual work		Below
		0.1g for intellectual work		Below
		0.05g for transit passengers		Below
		0.02g for cruise liner		Higher
4	Lateral acceleration	0.10g for light manual work	0.006g	Below
		0.07g for heavy manual work		Below
		0.05g for intellectual work		Below
		0.04g for transit passengers		Below
		0.03g for cruise liner		Below
5	Motion sickness incidence (MSI)	20% of crew in 4 hours	0 %	Below
6	Motion induced interruption (MII)	1 tip per minute	Roll – 0 tpm Pitch – 0 tpm	Below
7	Slamming acceleration (vertical)	Vertical acceleration when slamming taking place	TBD	TBD
(c)	Motions relative to sea			
8	Frequency of slamming (reimmersion and velocity threshold)	0.03 (L ≤ 100)	0	Below
		3.83 knot	11.75 knot	Higher
9	Frequency of deck wetness	0.05	0	Below

Table 5-14: Condition 12

Index	Seaway Performance Criteria	Criteria Value	Actual Value	Compliance
(a)	Absolute Motion Amplitude			
1	Roll amplitude	6.0 deg for light manual work	0.261 deg	Below
		4.0 deg for heavy manual work		Below
		3.0 deg for intellectual work		Below
		2.5 deg for transit passengers		Below
		2.0 for cruise liner		Below
2	Pitch amplitude	1.5 deg (R.M.S.)	0.298 deg	Higher
(b)	Absolute Velocities and Accelerations			
3	Vertical acceleration	0.2g for light manual work	0.031g	Below
		0.15g for heavy manual work		Below
		0.1g for intellectual work		Below
		0.05g for transit passengers		Below
		0.02g for cruise liner		Higher
4	Lateral acceleration	0.10g for light manual work	0.009g	Below
		0.07g for heavy manual work		Below
		0.05g for intellectual work		Below
		0.04g for transit passengers		Below
		0.03g for cruise liner		Below
5	Motion sickness incidence (MSI)	20% of crew in 4 hours	0 %	Below
6	Motion induced interruption (MII)	1 tip per minute	Roll – 0 tpm Pitch – 0 tpm	Below
7	Slamming acceleration (vertical)	Vertical acceleration when slamming taking place	TBD	TBD
(c)	Motions relative to sea			
8	Frequency of slamming (reimmersion and velocity threshold)	0.03 (L ≤ 100)	0	Below
		3.83 knot	11.75 knot	Higher
9	Frequency of deck wetness	0.05	0.005	Below

In general, the studied vessel presents results below the customized criteria, except for the trawling working conditions, which seem to be highly affected by the shifted centre of gravity, producing roll motion of higher magnitude in comparison to the other conditions. This is supported by the comment of the skipper and from the designer. They both stated that the highest responses take place when the vessel is trawling.

The external force when trawling sets the initial condition for roll motion. This behaviour was only present during the trawling working condition and the rolling effects were not in the same magnitude when the vessel was simulated in lightship working condition or fully loaded working condition, even under beam waves.

Not only roll motions were higher when simulating the trawling condition. Pitch motion presented as well high values (see Figure D-19 and Figure D-23); this is also related to the position of the centre of gravity that was shifted to simulate the external force from the purse. In addition to this, conditions 7, 9 and 10 present larger pitch angles in comparison to other simulations. However, the vertical accelerations are low, which reflects slow pitch motions with mid-high amplitude. On this matter, a more forward centre of gravity seems to produce higher pitch motions. Another condition with mid-high pitch angles is the second one, which was analysed under the same waves as condition 09 and close speeds (12 and 11.75 knots), in this case it is possible to see that condition 09 presents higher responses of this motion, where the vessel working condition differs in the displacement with a further LCG from the transom. The wave direction is suspected to be the most important factor that differentiates the responses in these two simulations.

Other remarking responses, that were observed in every analysis, were the pitch angle and pitch acceleration in the engine room. It seems that because of location of the floatation centre, centre of gravity and the vertical location of the engine room deck, the responses in this zone are quite like the ones at the bow (close value responses). This is also supported by the skipper comments, who stated that there are rather strong motions in the engine room and in the bow.

On another note, the MSI and MII present small values as can be expected by the magnitude of the accelerations and only surpass the limiting criteria in conditions 5 and 6. The MII is estimated for both roll and pitch as both motions are large in these two conditions. Meanwhile the MSI reaches its maximum value in condition 5, where the pitch and roll motions are the highest.

Regarding the frequency of deck wetness, it is shown that the higher values take place when the vessel is trawling (see Table 5-7 and Table 5-8). This is due to the high vertical accelerations and motions. On this matter a match with the answers from the questionnaire was found, where the skipper stated that the trawling condition presented strong motions. It is also important to point out that fishing vessels present a feature called camber, which is a curvature in the deck that allows to drain the water through scuppers by the sides of the freeboard. This design is part of the concept of fishing vessels due to the high frequency of water on deck when operating. On this note the deck wetness probability are 1.5% and 27.6%. Condition 7 shows that at fully loaded working condition, when the freeboard is small, large waves are critical for the criteria.

From the questionnaire it is seen that the vessel presents low responses to large wavelengths and high roll responses in short waves, there was no comment related to

medium wavelengths. This is in correlation with Figure 5-5, where a similar behaviour is observed. At the same time, the responses of the vessel in fully loaded, when the vessel is characterised by a negative trim (forward draft deeper than aft draft), difficult the manoeuvring according to the skipper.

5.3 Parametric Rolling

To evaluate the possible scenarios according to the real conditions specified in subsection 4.1.1, a variety of simulations were performed with the same conditions used for the seakeeping assessment.

Table 5-15: Compliance of vulnerability criteria

Condition	Vulnerability criteria				
	Probable condition	Susceptibility criteria			Severity criterion
	Ahead speed (knots)	Frequency condition	Damping threshold condition	Magnitude of stability change	Restoring term
1	5.28	No	No	No	Not needed
2	5.28	No	No	No	Not needed
3	6.27	No	No	No	Not needed
4	6.27	No	No	No	Not needed
5	3	Yes	No	No	Not needed
6	2.56	Yes	No	No	Not needed
7	4.62	No	No	No	Not needed
8	6.83	No	No	No	Not needed
9	6.83	No	No	No	Not needed
10	7.57	No	No	No	Not needed
11	7.57	No	No	No	Not needed
12	4.7	No	No	No	Not needed

As seen in Table 5-15, none of the analysed conditions trigger the parametric rolling phenomena according to the criteria studied. However, conditions 5, 6 satisfy the frequency condition and the changing magnitude of GM is close to the limit of 0.49. (0.45 and 0.43 respectively). However, the damping coefficient is high enough to “close” the curve before the values of p and q enter the instability zone.

Since the interest is to assess the occurrence of parametric rolling, an extra study of the required conditions for the first instability zone is carried out.

To “reach” the parametric rolling phenomena, a specific condition is set, where the parameters p and q are placed in the instability regions of the Ince-strut diagram as follows:

$$p = 0.25; \quad q = 0.2$$

These limit values correspond to the first instability zone in the Ince-Strut diagram (See Figure 2-8).

To perform this simulation, 3 conditions are studied (light ship, trawling and fully loaded) that are conditions 1, 5 and 7 in Table 4-2.

Given an analysis in head waves and maintaining the damping coefficient of the vessel under this condition, to reach the threshold damping that corresponds it is possible to determine the factor $\mu = 0.1946$, which is an even higher value than the non-dimensional damping coefficient. Now the non-dimensional frequencies are calculated through eq. (2.21). From here it is possible to determine the parameters that trigger the parametric rolling event (see Table 5-17).

As the damping coefficients vary depending on the conditions and speeds, approximated damping coefficient, corresponding to head waves were used.

Table 5-16: Initial condition for evaluation

Condition	Speed (knots)	Displacement (kg)	Moment of Inertia	Static GM	ω_0	Damping coefficient
1	12	1.563E+06	3.026E+07	0.752	0.617	1.360E+07
5	3	1.574E+06	3.048E+07	0.752	0.617	1.473E+07
7	11.75	1.999E+06	3.870E+07	0.627	0.564	2.787E+07

Table 5-17: Parameters that trigger parametric rolling for $p = 0.25$ & $q = 0.2$

Condition	ω_e	ω_m	GM_m	ω_a	GM_a	Wave ω	Wavelength
1	1.155	0.620	0.758	0.516	0.526	0.776	2.21Lpp
5	1.242	0.666	0.876	0.555	0.609	1.064	1.15Lpp
7	1.850	0.993	1.945	0.827	1.351	1.102	1.11Lpp

There is a whole spectrum of conditions that, according to the vulnerability criteria, can trigger the phenomena as soon as the parameters lay in the instability zones of the Ince – Strut diagram. For example, a more appropriate wavelength under the trawling condition could have triggered the phenomenon, as the velocity requirement was fulfilled (see Table 5-15 and Table 5-16), and the GM presented a significant variation of almost 0.49 m (see Table 5-17). Or longer waves under the light-ship weight condition could have developed the event as these produce a higher variation of GM.

By studying the parameters presented in Table 5-17, the phenomenon is likely to happen at light-ship condition, where the damping coefficient is smaller due to a shallow draft and at smaller wavelengths, when the speed is lower and if the variation of GM is large enough. This can happen in high-stepped waves. However, at fully loaded condition, parametric rolling is less likely to take place as the damping coefficient is too large, influencing in the Ince-strut diagram and making the parameters p and q do not lay inside the first instability region.

Figure 5-15 shows the behaviour of the parametric rolling when the factors p and q are the mentioned ones.

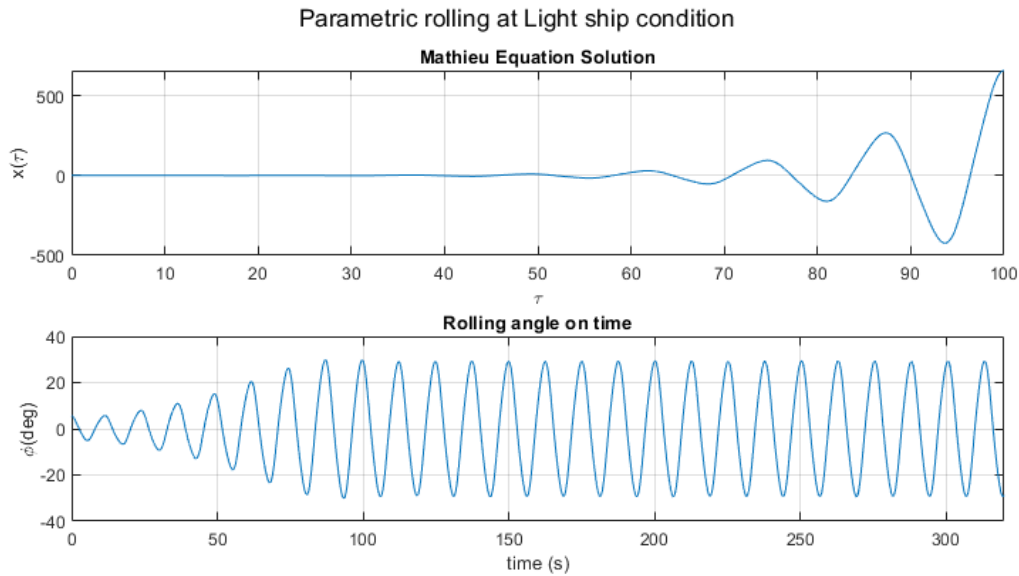


Figure 5-15: Parametric rolling at light-ship condition, $p=0.25$ and $q=0.2$.

5.4 Questionnaire

The results of the questionnaire are presented in Appendix B, and discussed in the subsequent section.

The questionnaire shows that the ship, in overall, is a comfortable fishing vessel for the crew.

The main problems regarding manoeuvring are related to the trawling condition and to a fully loaded with negative trim condition, to which the vessel responses are stronger.

The engine room, as well as the bow possess a less comfortable environment for the crew.

In general, the habitability zone presents a comfortable environment for the skippers. This is also in correlation with the results obtained from the simulations (see Appendix D).

6 Conclusions

The present thesis focuses on the compliance of a selected, well-documented, stern trawler fishing vessel (Stella Nova IX) with general existing seakeeping (see subsection 2.1.1.3) and parametric rolling criteria with the purpose of (a) selecting seakeeping criteria suitable for this type of ship and (b) proposing an assessment methodology to optimize such criteria, using the software SHIPFLOW Motions

To test compliance, a systematic analysis using SHIPFLOW, and the developed codes shown in Appendix C. was performed on how different parameters (common wave characteristics and working conditions) influence the responses of the fishing vessel. The study was focused specifically on the effect of the changing centre of gravity (see section 4.1.2) on ship responses, to select suitable seakeeping criteria for fishing vessels and to investigate the triggering conditions of parametric rolling for this vessel. This addressed objective (a) by comparing the ship responses with the selected criteria and obtaining results under the limits of such criteria, with exceptions that need further study.

To achieve the second objective (b), the methodology described in section 4 is built in a way that it can be applied to more vessels of similar characteristics. By replicating the methodology with similar fishing vessels and analysing the responses, it is possible to refine the selected criteria and adapt them to this type or other types of fishing vessels.

From this study, it is apparent that fishing vessels behave quite differently from large ships, e.g., larger vessels experience resonance at shorter wave lengths ratios than the studied vessel. The behaviour can be attributed to the high damping coefficients in relation to the weight displacement of the vessel and other proportion ratios. The estimation of the damping coefficient is done under assumptions and accepted uncertainties, given that the study of this parameter is a whole topic, and it escapes from the scope and intention of this thesis.

The customized criteria present high limiting values for most of the studied conditions with exception of the trawling condition. It is recommended to evaluate these conditions with a tool that can simulate an external force, so simplification of the problem through shifting of the CG can be skipped.

These criteria can be used for the study of more trawler fishing vessels to assess the responses under different working conditions. To refine the mentioned criteria, more studies of similar fishing vessels can be carried out. If the ship's responses are in the same magnitude as the ones presented in this report, then the limiting values can be adjusted depending on the working condition. The trawling condition needs to be specified as a particular scenario, where the limits of the criteria might change due to the nature of the operation.

The fishing vessel model was also tested for compliance with the second-generation IMO intact stability criteria, regarding the parametric roll phenomenon, followed by an evaluation of the triggering conditions of the phenomenon.

Parametric rolling is a phenomenon that can be triggered by a series of different scenarios and fishing vessels are not exempt from it. However, they are less likely to

experience it at fully loaded conditions, where the damping coefficients are high enough to prevent the phenomenon.

From the performed analysis, it is seen that the studied vessel is more vulnerable to experience parametric rolling when sailing in light-ship condition, if the wave conditions are met and if the damping coefficient of the vessel is low enough to not mitigate the phenomenon.

Lastly, in this study, the feasibility and efficiency of the SHIPFLOW Motions Potential Flow code for determining the motion of a fishing vessel in moderate seas and under different wave patterns, were tested. SHIPFLOW Motions 6 has room to improve. As stated before, the panelization of the hull can be improved to be able to capture more “complicated” geometries and a feature of a resizable domain could be of help when simulating long wavelengths.

Given the geometry of these type of vessels (large keels and large wet transoms in proportion to hull), potential flow codes seem challenged to solve and reach results as straightforward as with larger ships.

6.1 Suggestions for further research

More scenarios dependent of the wave characteristics should be studied to have a deeper understanding of the fishing vessel’s responses. As an extension of the study, not only common condition but also all possible scenarios should be analysed.

Another extension of this study could be done by analysing more types of hulls of different proportions (such as L_{pp}/B , B/T and C_b) to test the robustness of the methodology and to identify if the customized criteria suit more fishing vessels of similar and different characteristics. On this matter, the customized criteria can be refined by setting more accurate limiting values, ranges and making it dependent of the working condition.

A deeper investigation of the damping coefficient and its influence on the ship responses, specially roll motion can be carried out to understand its influence on the parametric rolling phenomenon.

As only the Parametric rolling phenomenon has been studied, a next step can be the assessment of the remaining phenomena specified in the Second-generation IMO stability criteria, such as pure loss of stability, broaching and surf-riding, and dead ship condition.

The code RBSMC was developed to extrapolate the responses from the centre of gravity of the vessel, obtained by SHIPFLOW. This code can be applied to different hull shapes. It will be interesting to develop an interphase with SHIPFLOW that allows a direct import of the results to the code.

The mapped responses on the “vertical levels”, obtained from RBSMC, can be used for structural analysis of the foundations of equipment.

New features and capabilities will be introduced into SHIPFLOW Motions in its upcoming release where major parts have been re-written completely (e.g., automatic, and adaptive unstructured meshing, adding external forces, extraction of motions and accelerations at arbitrary points, improved modelling of transom flow etc.). This new version of the code can be employed for resolving some of the issues observed in this study.

7 References

- Belenky, V., Bassler, C. C., & Spyrou, K. J. (2011). *Development of Second Generation Intact Stability*. United States Navy, Hydromechanics Department, Washington DC.
- Britannica, E. (2012). *Surface waves*. Retrieved from Encyclopædia Britannica: <https://www.britannica.com/science/wave-water#/media/1/637799/47257>
- Coslovich, F. (2020). *Towards 6 Degrees of Freedom Seakeeping Simulations Using a Fully Nonlinear Potential Flow Method*. THESIS FOR THE DEGREE OF LICENTIATE OF ENGINEERING, Chalmers University of Technology, Department of Mechanics and Maritime Sciences, Gothenburg.
- Dyrön, G. 3. (2016, October 27). Följ med Carmona ut på en fisketur. Retrieved from <https://youtu.be/8zk1JUpiHCg>
- ECMWF. (2021, April 15). *ERA5 hourly data on single levels from 1979 to present*. Retrieved from <https://cds.climate.copernicus.eu/cdsapp#!/dataset/reanalysis-era5-single-levels?tab=overview>
- FAO. (2021). *Fishing Vessel type*. Retrieved from Food and Agricultural Organization of the United Nations: <http://www.fao.org/fishery/vesseltype/search/en>
- FAO. (2021). *Fishing vessel types - Stern trawlers*. Retrieved from Food and Agriculture Organization of the United Nations: <http://www.fao.org/fishery/vesseltype/30/en>
- Fenton, J. D. (1985). A fifth-order Stokes theory for steady waves. *Waterway, Port, Coastal & Ocean Eng*, 216-234.
- Ghaemi, M. H., & Olszewski, H. (2017). Total ship operability – Review, concept and criteria. *POLISH MARITIME RESEARCH*, 24(93), 74-81.
- Goda, Y. (2000). Random Seas and Design of Maritime Structures. In *Advanced Series on Ocean Engineering* (Vol. 15).
- Graham, R. (1990). Motion-Induced Interruptions as Ship Operability Criteria. *ASNE Naval Engineer Journal*, 102(02).
- Guedes Soares, C., Tello, M., & Ribeiro e Silva, S. (2010). Seakeeping performance of fishing vessels in irregular waves. *Ocean Engineering*, 763-773.
- Himeno, Y. (1981, September). *Prediction of Ship roll damping - State of the art*. University of Michigan.
- ISO. (1997, 05 01). ISO 2631-1. *Mechanical vibration and shock evaluation of human exposure to whole-body vibrations, Part 1: General requirements*. Switzerland: ISO. Retrieved 1997
- ITTC. (2011). Numerical Estimation of Roll Damping. *28th ITTC Quality System Manual - Recommended Procedures and Guidelines*.
- Kianejad, S. S., Enshaei, H., Duffy, J., Ansarifard, N., & Ranmuthugala, D. (2018, August). Investigation of scale effects on roll damping through numerical simulations. *32nd Symposium on Naval Hydrodynamics*, (pp. 5-10). Hamburg, Germany. Retrieved August 2018
- Kianejad, S., Enshaei, H., Duffy, J., & Ansarifard, N. (2020). Calculation of ship roll hydrodynamic coefficients in regular beam waves. *Ocean Engineering*.
- Lewis, E. V. (1989). *Principles of Naval Architecture - Second Revision* (Vol. III). Jersey City: The Society of Naval Architects and Marine Engineers.
- Mantari, J., Ribeiro e Silva, S., & Guedes Soares, C. (2011). Loss of fishing vessel's intact stability in longitudinal waves. *International Journal of Small Craft Technology*, 153, 23-37.

- Molland, A. F. (2008). *The Maritime Engineering Reference Book, A Guide to Ship Design, Construction and Operation*. Elsevier Ltd.
- Neves, M. A., Perez, N. A., & Valerio, L. (1999). Stability of Small Fishing Vessels In Longitudinal Waves. *Ocean Engineering*, 26, 1389-1419.
- Nielsen, U. D. (2010). *Ship Operations - Engineering Analyses and Guidance*. Kgs. Lyngby, Denmark: TECHNICAL UNIVERSITY OF DENMARK.
- Nordforsk. (1987). *Assessment of Ship Performance in a Seaway: The Nordic Co-operative Project: "Seakeeping Performance of Ships"*. Nordforsk.
- O'Hanlon, J. F., & McCauley, M. E. (1974). Motion sickness incidence as a function of the frequency and acceleration of vertical sinusoidal motion. *Human Factor research*.
- Papanikolaou, D. S. (2001). On the stability of Fishing vessels with trapped water on Deck. *Ship Technology Research*, 48.
- Riola, J. M., & Arboleya, M. G. (2006). Habitability and personal space in Seakeeping behaviour. *Journal of Maritime Research*, III, 41-54.
- Rodrigues, J. M., Perera, L. P., & Soares, G. (2011). Decision support system for the safe operation of fishing vessels in waves. *1st Int. Conf. on Maritime Engineering and Technology*. Lisbon.
- Rusu, L., & Soares, C. G. (2014). Forecasting fishing vessel responses in coastal areas. *Journal of Marine Science and Technology*, 215-227.
- Sadra Kianejad, Hossein Enshaei, Jonathan Duffy, & Nazanin Ansarifard. (2019). Prediction of a ship roll added mass moment of inertia using numerical simulation. *Ocean Engineering* 173, 77-89.
- Sariöz, K., & Narli, E. (2005). Effect of criteria on seakeeping performance assessment. *Ocean Engineering*, 1161-1173.
- Sayli, A., Alkan, A. D., Nabergoj, R., & Uysal, A. O. (2006). Seakeeping assessment of fishing vessels in conceptual design stage. *Ocean Engineering*, 724-738.
- SHIPFLOW. (2021). *Shipflow Motions*. Retrieved from Shipflow - Flowtech products: <https://www.flowtech.se/products/shipflow-motions>
- Tello, M., Silva, S., & Soares, C. (2011). Seakeeping performance of fishing vessels in irregular waves. *Ocean Engineering*, 763-773.
- Watanabe, Y., Inoue, S., & Murahashi, T. (1964). The modification of rolling resistance for full ships. *T West-Japan SNA*, 27.

Appendix A

Data obtained from ERA5, processed to obtain frequent wave characteristics for different geographical points (two in the North Sea and two in the Baltic Sea).

Table A-1: Sea characteristics. (part 01)

MONTH	WAVE PERIOD				WAVE HEIGHT			
2019	P. 01	P. 02	P. 03	P. 04	P. 01	P. 02	P. 03	P. 04
January	6.55	3.93	3.57	4.61	1.90	0.88	0.63	1.17
February	6.98	4.06	3.73	4.76	2.33	0.94	0.74	1.22
March	5.23	3.11	3.63	3.84	1.21	0.46	0.56	0.72
April	5.69	3.71	3.64	3.61	1.56	0.75	0.60	0.71
May	5.24	3.39	3.17	3.68	1.26	0.56	0.39	0.57
June	5.17	3.47	3.57	3.73	1.42	0.67	0.64	0.67
July	5.54	3.52	3.01	4.53	1.27	0.65	0.33	0.67
August	6.22	4.12	3.67	4.49	1.98	1.05	0.69	1.17
September	6.27	3.79	3.60	4.87	1.78	0.80	0.60	1.07
October	6.16	3.64	3.52	4.94	1.98	0.72	0.57	1.18
November	6.55	4.12	3.62	5.03	2.29	1.03	0.70	1.46
December	7.25	4.50	3.62	5.33	2.58	1.23	0.72	1.49
January	7.57	4.61	3.99	4.51	3.17	1.39	0.99	1.69
February	6.75	3.92	3.50	4.02	2.09	0.91	0.62	1.18
March	6.01	3.68	3.48	3.90	1.55	0.79	0.56	0.86
April	5.81	3.75	3.38	3.39	1.49	0.79	0.52	0.68
May	5.05	2.96	3.50	4.14	0.95	0.41	0.51	0.51
June	5.58	4.19	3.37	4.45	1.56	1.11	0.56	1.00
July	5.15	3.13	3.08	4.21	1.15	0.48	0.37	0.56
August	6.23	3.79	3.42	4.67	1.66	0.83	0.50	0.97
September	6.07	3.85	3.74	4.66	1.92	0.85	0.72	1.24
October	6.98	4.23	3.41	4.66	2.25	1.13	0.63	1.30
November	6.50	3.92	3.26	5.14	2.13	0.90	0.59	1.54
December	6.59	3.59	2.91	4.70	1.31	0.61	0.44	1.09
Mean	6.13	3.79	3.47	4.41	1.78	0.83	0.59	1.03
Most prob.	6.27	3.93	3.57	4.61	1.78	0.85	0.60	1.07

Table B-2: Sea characteristics. (part 02)

MONTH	WAVE DIRECTION				WAVELENGTH			
2019	P. 01	P. 02	P. 03	P. 04	P. 01	P. 02	P. 03	P. 04
January	233.21	228.54	237.14	225.07	66.98	24.11	19.90	33.18
February	271.60	246.85	262.58	232.97	76.07	25.74	21.72	35.38
March	122.29	160.24	100.09	128.79	42.71	15.10	20.57	23.02
April	256.53	242.95	201.41	175.15	50.55	21.49	20.69	20.35
May	208.41	210.94	177.48	185.54	42.87	17.94	15.69	21.14
June	242.45	248.76	212.67	218.27	41.73	18.80	19.90	21.72
July	228.58	220.89	204.61	173.95	47.92	19.35	14.15	32.04
August	234.06	221.41	217.00	212.76	60.40	26.50	21.03	31.48
September	238.94	211.48	189.40	213.16	61.38	22.40	20.23	37.03
October	140.86	145.74	147.68	162.44	59.24	20.69	19.35	38.10
November	238.08	218.74	224.20	207.85	66.98	26.50	20.46	39.50
December	254.01	240.81	253.98	232.39	82.07	31.62	20.46	44.36
January	245.10	228.70	239.22	233.05	89.47	33.18	24.86	31.76
February	244.54	217.72	178.82	183.65	71.14	23.99	19.13	25.23
March	256.20	267.39	205.85	224.86	56.47	21.14	18.91	23.75
April	280.51	265.50	226.48	195.07	52.70	21.96	17.84	17.94
May	215.99	207.91	137.71	112.20	39.82	13.68	19.13	26.76
June	274.79	252.10	253.00	216.75	48.61	27.41	17.73	30.92
July	229.54	207.92	149.53	175.33	41.41	15.30	14.81	27.67
August	248.27	213.94	182.20	208.32	60.60	22.43	18.26	34.05
September	200.75	185.59	170.81	180.32	57.53	23.14	21.84	33.90
October	236.27	215.92	211.15	211.10	76.07	27.94	18.16	33.90
November	201.99	173.36	173.98	184.97	65.97	23.99	16.59	41.25
December	260.96	191.71	197.65	202.98	67.80	20.12	13.22	34.49
Mean	231.83	217.71	198.11	195.71	59.44	22.69	18.94	30.79
Most prob.	242.45	228.54	205.85	202.98	61.38	24.11	19.90	33.18

Appendix B

Master's thesis in the Nordic Master in Maritime Engineering – Ship Design track / Design criteria for seakeeping and stability of fishing vessels in regular waves

SURVEY REGARDING STELLA NOVA IX(EX-CARMONA) BEHAVIOUR AND EFFECTS ON CREW ONBOARD.			
Made by:	Nestor Juan de Dios Gómez Rojas	Date	26/03/2021
Completed by:		Date	21/04/2021
		Date	
		Date	
Instructions: Please fill the following survey honestly and with the most accurate possible. The survey can be filled in groups with other skippers.			
Experience of the skipper (Brief description)			
<p>- Experience on fishing vessel operations. Previous skipper of Stella Nova IX (Ex-Carmona).</p>			
General questions			
What was the most frequent working conditions encountered during the operation on seas? (sea state, zone of operation) A brief description.			
<p>- The ship operates on the north Sea and on the Baltic sea.</p> <p>- The vessel normally encounters long length waves on the North sea and rough weather (Strong winds). The strong winds difficult the ship maneuvering only when coming from 0 deg.</p> <p>- The vessel normally encounters short length waves on the Baltic sea and short time calm weather</p>			
What was the most critical working conditions encountered during the operation on seas? (sea state, zone of operation) A brief description.			
<p>- The vessel normally encounters as critical conditions, according to the skipper experience, in the Baltic sea as the short wavelengths generate harsher responses on the ship. This condition complicates the ship's maneuvering (Rolling).</p> <p>- A particular condition that is avoided is when the ship has a considerable negative trimming angle (a deeper forward perpendicular draft than a aft perpendicular draft). This conditions makes the vessel really hard to maneuver on waves.</p>			
Regarding the ship			
Under frequent conditions		Under critical conditions	
1	Ship speed when leaving port	12	1 Ship speed when leaving port
2	Ship speed when trawling	4	2 Ship speed when trawling
3	Ship speed when returning	12	3 Ship speed when returning
			10

Regarding the crew						
Please qualify from 1 to 5 the following zones on the ship, being 1 no comfortable and 5 very comfortable.						
Working Condition		Frequent				
Zones on the ship		Calification				
		1	2	3	4	5
Habitability						
1	Quarters				X	
2	Common areas				X	
3	Bridge				X	
Working deck						
4	Aft					X
5	Mid ship					X
6	Forward				X	
Other zones						
7	Engine room			X		
8	Bow			X		
Working Condition		Critical				
Zones on the ship		Calification				
		1	2	3	4	5
Habitability						
1	Quarters				X	
2	Common areas				X	
3	Bridge				X	
Working deck						
4	Aft					X
5	Mid ship					X
6	Forward				X	
Other zones						
7	Engine room			X		
8	Bow			X		
Regarding equipment						
If you have any record or knowledge of the most commonly affected equipment on board and under which situation, please describe or attach on the mail						
Extra information (Any extra information is appreciated)						
<p>- Currently a new fishing vessel is being build following the same design provided by Jan-Erik Abrahamsson. With a modified bow, from a conventional bulbous bow to a vertical stem.</p>						

Appendix C

RBSMC

```
close all
% clear all
clc
```

RBSMC - Program details

```
% The computation is done by assuming that the ship is a rigid body.
% The program calculates the motions, velocities and accelerations by
% mapping the values over the coordinates of points on the decks.
% The deck evaluation is dependent of the input geometry.
% The zero height point corresponds to the lower vertical point of the geometry.
% Forward, upwards and port side are positives, along with their respective euler
% angles.

% The program stores the input variables after the first input and it is
% possible to load them again.

% RBSMC Ver 1.0 (Rigid Body Ship Motions Computations)
% Made by Nestor Juan de Dios Gomez Rojas.
% Nordic Master in Maritime Engineering - Ship Design track.
% Chalmers University of Technology
% Technical University of Denmark
```

Defining new variables name or loading variables from previous work

```
disp(' ')
prompt = 'Input N for new variables or L for loading variables : ';
l_n = input(prompt,'s');

if l_n == 'N'
```

Input Ship data

```
disp(' ')
disp('INPUT SHIP DATA')
disp(' ')
% Input file name for storing variables
filename = input('Input file name for storing variables : ','s');
disp(' ')
% Input length of the ship.
length = input('(1) Input length(Lbp) of the ship (m) : '); %43.3
% Input beam of the ship at midship.
beam = input('(3) Input beam at midship (m) : '); %11
% Input draft from lowest point.
draft = input('(4) Input draft from lowest vertical point (m) : '); %6.8
% Input ship model scale.
scale = input('(5) Input scale of the analysed model : '); %43.3
disp(' ')
disp('INPUT GEOMETRY AS CSV FILE (POINTS COORDINATES)')
disp(' ')
disp(' - The vertical coordinates must be in correlation with the amount of decks
```

```

to analyse')
disp (' - The file must be a 3 columns matrix x,y & z')
disp (' ')
% Input deck contour as .csv file.
DECKS = input('Write the name of the file with extension: ','s');
coordinates= readmatrix(DECKS);
% Input centre of gravity coordinates from aft perpendicular.
disp ('Input coordinates of the centre of gravity from floatation line and aft
perpendicular of the Ship. Coordinates must be in milimiters')
disp (' ')
xcg = input("(1) Input longitudinal coordinate of centre of gravity: "); %1-xcg
displayed by shipflow
ycg = input("(2) Input transversal coordinate of centre of gravity: "); %0
zcg = input("(3) Input vertical coordinate of centre of gravity: "); %-0.0462

```

Input resolution of analysing

```

disp (' ')
disp ('INPUT RESOLUTION PARAMETERS')
disp (' ')
% Input distance between longitudinal positions to analyze
x_l = input("(1) Input longitudinal distance for resolution (m): ");
% Input distance between transverse positions to analyze
y_l = input("(2) Input transversal distance for resolution (m) : ");
% Vertical positions to analyse (Related to distance between decks)
disp('The vertical separation is obtained from the geometry input')

```

Input result from SHIPFLOW

```

disp (' ')
disp ('INPUT RESULT DATA FROM SHIPFLOW')
disp (' ')
% Input Result data as .csv file
Shipflow_results = input('Write the name of the file with extension: ','s');
Motions_matrix= readmatrix(Shipflow_results);

```

Saving variables

```

save(filename, 'length', 'beam', 'draft', 'scale', 'coordinates', 'Motions_matrix', 'x_l', 'y_
l', 'xcg', 'ycg', 'zcg', '-v7.3', '-nocompression')

```

```

elseif l_n == 'L'

```

Loading variables %Activate for loading variables

```

disp (' ')
input_data = input('Input name of file containing the variables data with
extension : ','s');
load(input_data)

```

```

end

```

Breaking matrix

```

hull_x = coordinates(:,1);
hull_y = coordinates(:,2);

```

```

hull_z = coordinates(:,3);

T= Motions_matrix(:,2);
F = Motions_matrix(:,3:8);
R = Motions_matrix(:,9:14);
V = Motions_matrix(:,15:20);
A = Motions_matrix(:,21:26);

% Considerations
g = 9.81;
aft_l = 10/100*length;
bow_l = 110/100*length;
up_deck = max(hull_z)/1000;
b = beam/(2*scale);
decks = up_deck-draft;

```

Position analysis

```

z_l = unique(hull_z);
z_l = (z_l(2)-z_l(1))/1000;
cor_x = (-aft_l/scale:x_l/scale:bow_l/scale)';
cor_y = (-b:y_l/scale:b)';
cor_z = (-draft/scale:z_l/scale:decks/scale);

```

Time differentials

```

t = T(2)-T(1);

```

Motion

```

R_1 = R(:,1);
R_2 = R(:,2);
R_3 = R(:,3);
R_4 = R(:,4);
R_5 = R(:,5);
R_6 = R(:,6);

% Motion x, y & z
Pos_x_i = [];
Pos_y_i = [];
Pos_z_i = [];
for ll = 1: numel(cor_z)
    for kk = 1: numel(cor_y)
        for jj = 1: numel(T)
            for ii = 1: numel(cor_x)
                Pos_x_i(ll, kk, jj, ii) = R_1(jj) + (cor_x(ii)-xcg).*cos(R_6(jj))-(-cor_y(kk)+ycg)*sin(R_6(jj)) + (cor_x(ii)-xcg).*cos(R_5(jj))-(cor_z(ll)-zcg).*sin(R_5(jj)) - 2*(cor_x(ii)-xcg);
                Pos_y_i(ll, kk, jj, ii) = R_2(jj) + (cor_x(ii)-xcg)*sin(R_6(jj))+(-cor_y(kk)+ycg)*cos(R_6(jj)) + (-cor_y(kk)+ycg)*cos(R_4(jj))-(cor_z(ll)-zcg).*sin(R_4(jj)) - 2*(-cor_y(kk)+ycg);
                Pos_z_i(ll, kk, jj, ii) = R_3(jj) + (cor_x(ii)-xcg).*sin(R_5(jj))+(cor_z(ll)-zcg)*cos(R_5(jj)) + (cor_z(ll)-zcg).*cos(R_4(jj))+(-cor_y(kk)+ycg).*sin(R_4(jj)) - 2*(cor_z(ll)-zcg);
            end
        end
    end
end

```

```

end

% RMS x,y&z motion
RMS_R_x=[];
RMS_R_y=[];
RMS_R_z=[];
for ll = 1:numel(cor_z)
    for ii = 1:numel(cor_x)
        for jj = 1:numel(cor_y)
            RMS_R_x(ll,jj,ii) = rms(Pos_x_i(ll,jj,:,ii));
            RMS_R_y(ll,jj,ii) = rms(Pos_y_i(ll,jj,:,ii));
            RMS_R_z(ll,jj,ii) = rms(Pos_z_i(ll,jj,:,ii));
            RMS_Motion(ll,jj,ii) =
sqrt(RMS_R_x(ll,jj,ii)^2+RMS_R_y(ll,jj,ii)^2+RMS_R_z(ll,jj,ii)^2);
        end
    end
end
end

```

Velocity

```

% velocity x, y & z
v_1 = v(:,1);
v_2 = v(:,2);
v_3 = v(:,3);
v_4 = v(:,4);
v_5 = v(:,5);
v_6 = v(:,6);

vel_x_i=[];
vel_y_i=[];
vel_z_i=[];
for ll = 1:numel(cor_z)
    for kk = 1:numel(cor_y)
        for jj = 1:numel(T)
            for ii = 1:numel(cor_x)
                vel_x_i(ll,kk,jj,ii) = v_1(jj) + v_5(jj)*(cor_z(ll)-zcg) - v_6(jj)*(-
cor_y(kk)+ycg);
                vel_y_i(ll,kk,jj,ii) = v_2(jj) + -v_4(jj)*(cor_z(ll)-zcg) +
v_6(jj)*(cor_x(ii)-xcg);
                vel_z_i(ll,kk,jj,ii) = v_3(jj) + v_4(jj)*(-cor_y(kk)+ycg) -
v_5(jj)*(cor_x(ii)-xcg) ;
            end
        end
    end
end
end

% RMS x, y & z velocity
RMS_V_x=[];
RMS_V_y=[];
RMS_V_z=[];
for ll = 1:numel(cor_z)
    for ii = 1:numel(cor_x)
        for jj = 1:numel(cor_y)
            RMS_V_x(ll,jj,ii) = rms(vel_x_i(ll,jj,:,ii));
            RMS_V_y(ll,jj,ii) = rms(vel_y_i(ll,jj,:,ii));
            RMS_V_z(ll,jj,ii) = rms(vel_z_i(ll,jj,:,ii));
            RMS_velocity(ll,jj,ii) =
sqrt(RMS_V_x(ll,jj,ii)^2+RMS_V_y(ll,jj,ii)^2+RMS_V_z(ll,jj,ii)^2);
        end
    end
end

```

```

end
end

```

Acceleration

```

% Acceleration x, y & z
A_1 = A(:,1);
A_2 = A(:,2);
A_3 = A(:,3);
A_4 = A(:,4);
A_5 = A(:,5);
A_6 = A(:,6);

Acc_z_i=[];
for ll = 1:numel(cor_z)
    for kk = 1:numel(cor_y)
        for jj = 1:numel(T)
            for ii = 1:numel(cor_x)
                Acc_x_i(ll,kk,jj,ii) = A_1(jj) + (A_5(jj)*(cor_z(ll)-zcg)-A_6(jj)*(-
cor_y(kk)+ycg)) + ...
                    (V_5(jj)*(V_4(jj)*(-cor_y(kk)+ycg)-V_5(jj)*(cor_x(ii)-xcg)) -
V_6(jj)*(-V_4(jj)*(cor_z(ll)-zcg)+V_6(jj)*(cor_x(ii)-xcg)));
                Acc_y_i(ll,kk,jj,ii) = A_2(jj) + (-A_4(jj)*(cor_z(ll)-
zcg)+A_6(jj)*(cor_x(ii)-xcg)) + ...
                    (V_6(jj)*(V_5(jj)*(cor_z(ll)-zcg)-V_6(jj)*(-cor_y(kk)+ycg)) -
V_4(jj)*(V_4(jj)*(-cor_y(kk)+ycg)-V_5(jj)*(cor_x(ii)-xcg)));
                Acc_z_i(ll,kk,jj,ii) = A_3(jj) + (A_4(jj)*(-
cor_y(kk)+ycg)+A_5(jj)*(cor_x(ii)-xcg)) + ...
                    (V_4(jj)*(V_4(jj)*(cor_z(ll)-zcg)-V_6(jj)*(cor_x(ii)-xcg)) -
V_5(jj)*(V_5(jj)*(cor_z(ll)-zcg)-V_6(jj)*(-cor_y(kk)+ycg)));
            end
        end
    end
end

% RMS x, y & z Acceleration
RMS_A_x=[];
RMS_A_y=[];
RMS_A_z=[];
for ll = 1:numel(cor_z)
    for ii = 1:numel(cor_x)
        for jj = 1:numel(cor_y)
            RMS_A_x(ll,jj,ii) = rms(Acc_x_i(ll,jj,:,ii));
            RMS_A_y(ll,jj,ii) = rms(Acc_y_i(ll,jj,:,ii));
            RMS_A_z(ll,jj,ii) = rms(Acc_z_i(ll,jj,:,ii));
            RMS_Acceleration(ll,jj,ii) =
sqrt(RMS_A_x(ll,jj,ii)^2+RMS_A_y(ll,jj,ii)^2+RMS_A_z(ll,jj,ii)^2);
        end
    end
end
end

```

Shaping RMS on deck selected deck

```

disp(['There are ' num2str(numel(cor_z)) ' vertical positions to display'])
disp(' ')
n_d = input('Input deck number to show, 0 is the bottom, -1 ends the process : ');
while n_d > numel(cor_z)
    disp('This deck is not implemented in the coordinates system')

```

```

n_d = input('Input deck number to show, 0 is the bottom, -1 ends the process : ');
end

while n_d >= 0

% Sorting coordinates

indx = find(hull_z==(n_d)*1000);

plane_n_d = [hull_x(indx) hull_y(indx)];

Plane_n_d=[];
for ii = 1:numel(plane_n_d(:,2))
    if plane_n_d(ii,2) >= 0
        Plane_n_d = [Plane_n_d; plane_n_d(ii,:)];
    else
        Plane_n_d = [Plane_n_d; []];
    end
end

Plane_N_d = sortrows(Plane_n_d);

for ii = 2:round(numel(Plane_N_d(:,1))/2)
    if Plane_N_d(ii,1) == Plane_N_d(ii-1,1)
        if Plane_N_d(ii,2) < Plane_N_d(ii-1,2)
            ind1 = Plane_N_d(ii,2);
            ind2 = Plane_N_d(ii-1,2);
            Plane_N_d(ii,2) = ind2;
            Plane_N_d(ii-1,2) = ind1;
        end
        %         if Plane_N_d(1,2) == 0
        %             Plane_N_d(end,:) = [];
        %         end
    end
end

for ii = round(numel(Plane_n_d(:,1))/2):(numel(Plane_N_d(:,1))-1)
    if Plane_N_d(ii,1) == Plane_N_d(ii+1,1)
        if Plane_N_d(ii,2) < Plane_N_d(ii+1,2)
            ind1 = Plane_N_d(ii,2);
            ind2 = Plane_N_d(ii+1,2);
            Plane_N_d(ii,2) = ind2;
            Plane_N_d(ii+1,2) = ind1;
        end
        if Plane_N_d(end,2) == 0
            Plane_N_d(end,:) = [];
        end
    end
end

Plane_N_d;
Plane_N_d_x = Plane_N_d(:,1)/(scale*1000);
Plane_N_d_y = Plane_N_d(:,2)/(scale*1000);
aft_resv = 0;
bow_resv = Plane_N_d_x(end);
if Plane_N_d_y(1) == 0
    Plane_N_d_y(1) = [];
    aft_resv = Plane_N_d_y(1);
    Plane_N_d_x(1) = [];
end

```

```

end

n_cor_x = cor_x;

if max(cor_x)>max(Plane_N_d_x) && min(cor_x)<min(Plane_N_d_x)
    for ii = 1:numel(n_cor_x)
        if n_cor_x(ii) < Plane_N_d_x(1)
            n_cor_x(ii) = 0;
        end
        if n_cor_x(end-ii+1) > Plane_N_d_x(end)
            n_cor_x(end-ii+1) = 0;
        end
    end
    n_cor_x = [min(Plane_N_d_x),n_cor_x',max(Plane_N_d_x)];
end
n_cor_x = n_cor_x(n_cor_x~=0)';

% Interpolating coordinates according to resolution

Plane_N_d_x_forward = [];
for ii = 2:numel(Plane_N_d_x)
    if Plane_N_d_x(ii) == Plane_N_d_x(ii-1)
        Plane_N_d_x_forward = [Plane_N_d_x_forward ;Plane_N_d_x(ii)];
    end
end

if numel(Plane_N_d_x_forward) > 1
    Plane_N_d_x = Plane_N_d_x(1:(numel(Plane_N_d_x)-numel(Plane_N_d_x_forward)));
    Plane_N_d_y = flip(sort(Plane_N_d_y));
    Plane_N_d_y_forward = Plane_N_d_y(numel(Plane_N_d_x)+1:end);
    n_cor_y_forward = 0:y_l/scale:Plane_N_d_y_forward(1);
    n_cor_y_forward = flip(n_cor_y_forward');
    n_cor_y =
    interp1(Plane_N_d_x,Plane_N_d_y(1:numel(Plane_N_d_x)),n_cor_x,'spline');
    n_cor_y_s = [n_cor_y; n_cor_y_forward];
    n_cor_y_s = [-flip(sort(n_cor_y_s));sort(n_cor_y_s)];
    n_cor_x_forward = Plane_N_d_x_forward(end)*ones(numel(n_cor_y_forward),1);
else
    n_cor_y_forward = 0;
    n_cor_y = interp1(Plane_N_d_x(1:end-1),Plane_N_d_y(1:end-1),n_cor_x(1:end-
1),'spline');
    n_cor_y = [n_cor_y; Plane_N_d_y(end)];
    n_cor_y_s = [n_cor_y; n_cor_y_forward];
    n_cor_y_s = [-flip(sort(n_cor_y_s));sort(n_cor_y_s)];
    n_cor_x_forward = n_cor_x(end);
end

```

Deck plane - port side.

```

%   deck_folder_loc = 'D:\Simulations\Real_Conditions\Condition 01\Post_process_01';
%   [parentFolder, deepestFolder] = fileparts(deck_folder_loc);
%   deck_folder = sprintf('Deck%d',n_d);
%   newSubFolder = sprintf(deck_folder, deck_folder_loc, deepestFolder);
%   % mkdir(newSubFolder);   %create the directory
%   if ~exist(newSubFolder, 'dir')
%       mkdir(deck_folder_loc,newSubFolder);
%   end

```

```

deck_folder = sprintf('Deck_%d',n_d);
newSubFolder = sprintf(deck_folder);
if ~exist(newSubFolder, 'dir')
mkdir(newSubFolder);
end

figure()
plot([n_cor_x(1); n_cor_x; n_cor_x_forward],[0; n_cor_y;
n_cor_y_forward], 'b', 'Linewidth',1.5)
hold on
yline (0,'k--')
grid minor
xlabel ('x/Lpp')
ylabel ('y/Lpp')
title (['Deck plane ', num2str(n_d), '- Port side'])
x0=10;
y0=10;
width=1920;
height=400
set(gcf,'position',[x0,y0,width,height])
DeckFileName = sprintf('Deck_%d', n_d);
hold off

fulldestination = fullfile(newSubFolder, DeckFileName); %name file relative to
that directory
saveas(gcf,fulldestination,'png'); %save the file there directory

```

Interpolating RMS

```

% Interpolating RMS MOTION
rm_x = squeeze(RMS_R_x((n_d+1),:,:));
Rm_x = interp1(cor_x,rm_x,n_cor_x);
RM_x = interp1(cor_y,Rm_x',sort(n_cor_y_s));
rm_y = squeeze(RMS_R_y((n_d+1),:,:));
Rm_y = interp1(cor_x,rm_y,n_cor_x);
RM_y = interp1(cor_y,Rm_y',sort(n_cor_y_s));
rm_z = squeeze(RMS_R_z((n_d+1),:,:));
Rm_z = interp1(cor_x,rm_z,n_cor_x);
RM_z = interp1(cor_y,Rm_z',sort(n_cor_y_s));
rm = squeeze(RMS_Motion((n_d+1),:,:));
Rm = interp1(cor_x,rm,n_cor_x);
RM = interp1(cor_y,Rm',sort(n_cor_y_s));

% Interpolating RMS VELOCITIES
rv_x = squeeze(RMS_V_x((n_d+1),:,:));
Rv_x = interp1(cor_x,rv_x,n_cor_x);
RV_x = interp1(cor_y,Rv_x',sort(n_cor_y_s));
rv_y = squeeze(RMS_V_y((n_d+1),:,:));
Rv_y = interp1(cor_x,rv_y,n_cor_x);
RV_y = interp1(cor_y,Rv_y',sort(n_cor_y_s));
rv_z = squeeze(RMS_V_z((n_d+1),:,:));
Rv_z = interp1(cor_x,rv_z,n_cor_x);
RV_z = interp1(cor_y,Rv_z',sort(n_cor_y_s));
rv = squeeze(RMS_velocity((n_d+1),:,:));
Rv = interp1(cor_x,rv,n_cor_x);
RV = interp1(cor_y,Rv',sort(n_cor_y_s));

% Interpolating RMS ACCELERATIONS
ra_x = squeeze(RMS_A_x((n_d+1),:,:));

```



```

Ra_x = interp1(cor_x,ra_x,n_cor_x);
RA_x = interp1(cor_y,RA_x',sort(n_cor_y_s));
ra_y = squeeze(RMS_A_y((n_d+1),:,:))';
Ra_y = interp1(cor_x,ra_y,n_cor_x);
RA_y = interp1(cor_y,RA_y',sort(n_cor_y_s));
ra_z = squeeze(RMS_A_z((n_d+1),:,:))';
Ra_z = interp1(cor_x,ra_z,n_cor_x);
RA_z = interp1(cor_y,RA_z',sort(n_cor_y_s));
ra = squeeze(RMS_Acceleration((n_d+1),:,:))';
Ra = interp1(cor_x,ra,n_cor_x);
RA = interp1(cor_y,RA',sort(n_cor_y_s));

```

Setting coloured mapping

```

n_d = n_d+1;
deck_level = n_d*z_l/scale;
[X,Y] = meshgrid(n_cor_x,sort(n_cor_y_s));
X_s = [n_cor_x(1);n_cor_x;bow_resv;flip(n_cor_x(1:end));n_cor_x(1)];
complement = linspace(1,0,1/4*(numel(cor_x)-1))';
Y_s = [0;n_cor_y;0;-flip(n_cor_y(1:end));0];
Y_s_half = Y_s(2:(end-1)/2);
Y_s_half_s = [-Y_s_half;(Y_s_half)];

for ll = 1:numel(n_cor_x)
    for kk = 1:numel(n_cor_y_s)
        if Y(kk,ll) < 0 && Y(kk,ll) <= Y_s_half_s(ll)
            X(kk,ll)= NaN;
            Y(kk,ll)= NaN;
        elseif Y(kk,ll) > 0 && Y(kk,ll) >= -Y_s_half_s(ll)
            X(kk,ll)= NaN;
            Y(kk,ll)= NaN;
        end
    end
end
end

```

Scaling results to real size ship

```

scaling = input('Do you want to scale the result to ship size? Y/N : ','s');
if scaling == 'Y'

    deck_level = deck_level*scale;
    X = X*scale;
    Y = Y*scale;
    X_s = X_s*scale;
    Y_s = Y_s*scale;

    x_label = 'Length(m)';
    y_label = 'Beam(m)';
    z_label = 'Height(m)';

    RM_x = RM_x*length;
    RM_y = RM_y*length;
    RM_z = RM_z*length;
    RM = RM*length;
    title_m = '$m$';

    RV_x = RV_x*sqrt(length*g);
    RV_y = RV_y*sqrt(length*g);

```

```

RV_z = RV_z*sqrt(length*g);
RV = RV*sqrt(length*g);
title_v = '$m/s$';

RA_x = RA_x*g;
RA_y = RA_y*g;
RA_z = RA_z*g;
RA = RA*g;
title_a = '$m/s^2$';
elseif scaling == 'N'
title_m = '$\hat{r}$';
title_v = '$\hat{v}$';
title_a = '$\hat{a}$';

x_label = 'x/Lpp';
y_label = 'y/Lpp';
z_label = 'z/Lpp';

end

```

Plot with gradient colour for RMS on each direction

```

dir_2 = 'Deck_%d';
deck_folder_loc_2 = sprintf(dir_2,n_d-1);
[parentFolder, deepestFolder] = fileparts(deck_folder_loc_2);

if scaling == 'Y'
deck_folder = sprintf('Dimensionalised');
newSubFolder = sprintf(deck_folder) %, deck_folder_loc_2, deepestFolder);
% mkdir(newSubFolder); %create the directory

if ~exist(newSubFolder, 'dir')
mkdir(deck_folder_loc_2,newSubFolder);
end

elseif scaling == 'N'
deck_folder = sprintf('Normalised');
newSubFolder = sprintf(deck_folder) %, deck_folder_loc_2, deepestFolder);
% mkdir(newSubFolder); %create the directory

if ~exist(newSubFolder, 'dir')
mkdir(deck_folder_loc_2,newSubFolder);
end

end

% Motions
figure ()
subplot(3,3,1)
z = surf(X,Y,deck_level*ones(size(X)),RM_x)
hold on
set(z,'edgecolor','none')
plot3(X_s,Y_s,deck_level*ones(numel(X_s)),'k','Linewidth',1.5)
xlabel (x_label)
ylabel (y_label)
zlabel (z_label)
title ('Longitudinal RMS Motions')
h=colorbar;
title(h,title_m,'interpreter','latex')
grid on

```

```

subplot(3,3,2)
v = surf(X,Y,deck_level*ones(size(X)),RM_y)
hold on
set(v,'edgecolor','none')
plot3(X_s,Y_s,deck_level*ones(numel(X_s)),'k','Linewidth',1.5)
xlabel(x_label)
ylabel(y_label)
zlabel(z_label)
title('Lateral RMS Motions')
h=colorbar;
title(h,title_m,'interpreter','latex')
grid on

subplot(3,3,3)
a = surf(X,Y,deck_level*ones(size(X)),RM_z)
hold on
set(a,'edgecolor','none')
plot3(X_s,Y_s,deck_level*ones(numel(X_s)),'k','Linewidth',1.5)
xlabel(x_label)
ylabel(y_label)
zlabel(z_label)
title('Vertical RMS Motions')
h=colorbar;
title(h,title_m,'interpreter','latex')
grid on

% velocities
subplot(3,3,4)
z = surf(X,Y,deck_level*ones(size(X)),RV_x)
hold on
set(z,'edgecolor','none')
plot3(X_s,Y_s,deck_level*ones(numel(X_s)),'k','Linewidth',1.5)
xlabel(x_label)
ylabel(y_label)
zlabel(z_label)
title('Longitudinal RMS Velocities')
h=colorbar;
title(h,title_v,'interpreter','latex')
grid on

subplot(3,3,5)
v = surf(X,Y,deck_level*ones(size(X)),RV_y)
hold on
set(v,'edgecolor','none')
plot3(X_s,Y_s,deck_level*ones(numel(X_s)),'k','Linewidth',1.5)
xlabel(x_label)
ylabel(y_label)
zlabel(z_label)
title('Lateral RMS Velocities')
h=colorbar;
title(h,title_v,'interpreter','latex')
grid on

subplot(3,3,6)
a = surf(X,Y,deck_level*ones(size(X)),RV_z)
hold on
set(a,'edgecolor','none')
plot3(X_s,Y_s,deck_level*ones(numel(X_s)),'k','Linewidth',1.5)

```

```

xlabel (x_label)
ylabel (y_label)
zlabel (z_label)
title ('Vertical RMS velocities')
h=colorbar;
title(h,title_v,'interpreter','latex')
grid on

% Accelerations
subplot(3,3,7)
z = surf(X,Y,deck_level*ones(size(X)),RA_x)
hold on
set(z,'edgecolor','none')
plot3(X_s,Y_s,deck_level*ones(numel(X_s)),'k','Linewidth',1.5)
xlabel (x_label)
ylabel (y_label)
zlabel (z_label)
title ('Longitudinal RMS Accelerations')
h=colorbar;
title(h,title_a,'interpreter','latex')
grid on

subplot(3,3,8)
v = surf(X,Y,deck_level*ones(size(X)),RA_y)
hold on
set(v,'edgecolor','none')
plot3(X_s,Y_s,deck_level*ones(numel(X_s)),'k','Linewidth',1.5)
xlabel (x_label)
ylabel (y_label)
zlabel (z_label)
title ('Lateral RMS Accelerations')
h=colorbar;
title(h,title_a,'interpreter','latex')
grid on

subplot(3,3,9)
a = surf(X,Y,deck_level*ones(size(X)),RA_z)
hold on
set(a,'edgecolor','none')
plot3(X_s,Y_s,deck_level*ones(numel(X_s)),'k','Linewidth',1.5)
xlabel (x_label)
ylabel (y_label)
zlabel (z_label)
title ('Vertical RMS Accelerations')
h=colorbar;
title(h,title_a,'interpreter','latex')
grid on

sgt = sgtitle(['RMS COMPONENTS ON DECK ', num2str(n_d-1)])
sgt.FontSize = 15;
x0=10;
y0=10;
width=1920;
height=1080;
set(gcf,'position',[x0,y0,width,height])

DeckFigName = sprintf('RMS_comp_%d', n_d-1);
newSubFolder = strcat(DeckFileName,'\ ',newSubFolder);

```

```

fulldestination = fullfile(newSubFolder, DeckFigName); %name file relative to
that directory
saveas(gcf,fulldestination,'png'); %save the file there directory

% Plot with gradient colour for RMS magnitude
figure ()
subplot(1,3,1)
z = surf(X,Y,deck_level*ones(size(X)),RM)
hold on
set(z,'edgecolor','none')
plot3(X_s,Y_s,deck_level*ones(numel(X_s)),'k','Linewidth',1.5)
xlabel (x_label)
ylabel (y_label)
zlabel (z_label)
title ('RMS Motions')
h=colorbar;
title(h,title_m,'interpreter','latex')
grid on

subplot(1,3,2)
v = surf(X,Y,deck_level*ones(size(X)),RV)
hold on
set(v,'edgecolor','none')
plot3(X_s,Y_s,deck_level*ones(numel(X_s)),'k','Linewidth',1.5)
xlabel (x_label)
ylabel (y_label)
zlabel (z_label)
title ('RMS Velocities')
h=colorbar;
title(h,title_v,'interpreter','latex')
grid on

subplot(1,3,3)
a = surf(X,Y,deck_level*ones(size(X)),RA)
hold on
set(a,'edgecolor','none')
plot3(X_s,Y_s,deck_level*ones(numel(X_s)),'k','Linewidth',1.5)
xlabel (x_label)
ylabel (y_label)
zlabel (z_label)
title ('RMS Accelerations')
h=colorbar;
title(h,title_a,'interpreter','latex')
grid on

sgt = sgtitle(['RMS ON DECK ', num2str(n_d-1)])
sgt.FontSize = 15;
x0=10;
y0=10;
width=1920;
height=400
set(gcf,'position',[x0,y0,width,height])

DeckFigNameF = sprintf('RMS_%d', n_d-1);
% newSubFolder = strcat(DeckFileName,'\',newSubFolder);
fulldestination = fullfile(newSubFolder, DeckFigNameF); %name file relative to
that directory
saveas(gcf,fulldestination,'png'); %save the file there directory

```

```

disp('')
answer = input ('Do you want to visualise another deck? Y/N: ','s');
if answer == 'Y'
    disp('')
    n_d = input('Input deck number to show, 0 is the bottom, -1 ends the process :
');
    disp('')
    while n_d > numel(cor_z)
        disp('')
        disp('This deck is not implemented in the coordinates system')
        disp('')
        n_d = input('Input deck number to show, 0 is the bottom, -1 ends the
process : ');
    end
elseif answer == 'N'
    disp('')
    disp ('Process terminated')
    n_d = n_d -1;
    break
end
end
end

```

Published with MATLAB® R2019b

Code for parametric rolling evaluation

```
close all
clear all
clc
```

Input data

```
% Input ship data
% L = input ('Input ship length (m): ');
L = 46.303;
% B = input ('Input ship beam (m): ');
B = 11;
% disp = input ('Input the ship displacement (kg): ');
disp = 1562.8;
% V = input ('Input ship speed (m/s): ');
V = 12*0.514444;
% B_44 = input ('Input dimensional damping rolling coefficient : ');
B_44 = 1.35986E+04;
% gm_max = input ('Input maximum value of GM (m): ');
gm_max = 1.152;
% gm_min = input ('Input minimum value of GM (m): ');
gm_min = 0.352;

% Input wave characteristic
% Lambda = input ('Input wave length(m) : ');
Lambda = 24.11;
% w_dir = input ('Input Wave relative direction(deg) : ');
w_dir = 163.54

% Input simulation time ([50 0.05])
time = input ('Input the simulation time as [simulation_time time_step] :')
```

Determination of parameters of the differential equation for roll motion

Calculation of Added mas:

```
% Evaluation parameters
g = 9.81; % m/s^2
t = [time(2):time(2):time(1)]; % Time vector of analysis

w_period = (Lambda*2*pi/g)^0.5; % wave period
w = 2*pi/w_period; % wave frequency
w_e = abs(w-w^2/g*cos(deg2rad(w_dir))); % Angular wave frequency of encounter
tao = w_e*t; % Non-dimensional time

% GM evaluation
gm_a = 0.5*(gm_max-gm_min); % GM amplitude
gm_m = 0.5*(gm_max+gm_min); % Maximum GM
gm = gm_m+gm_a*cos(w_e*t); % Varying GM on time

% Initial Varying GM plot
figure ()
plot (t,gm)
hold on
grid on
xlabel ('time (s)')
```

```

ylabel ('GM (m)')
title ('Varying GM on time')

% Moment of inertia + added mass moment of inertia
k_44 = 0.4*B; % Estimated rolling radius of gyration
I_44 = disp*k_44^2; % Estimated rolling total moment of inertia

% Calculation of frequencies
w_m = sqrt((disp*g*gm_m)/(I_44)); % Mean changing GM frequency
w_m_bar = w_m/w_e; % Non-dimensional changing GM frequency
w_a = sqrt((disp*g*gm_a)/(I_44)); % Amplitude of changing GM frequency
w_a_bar = w_a/w_e; % Non-dimensional amplitude of changing GM frequency

% Damping coefficient
d = 0.5*(B_44/I_44); % Non-dimensional damping coefficient
mu = d/w_e; % 2nd Non-dimensional damping coefficient

```

Mathieu parameters

```

p = (w_m_bar^2-mu^2); % p coefficient
q = w_a_bar^2; % q coefficiente

% p = 0.15;
% q = 0.2;

```

Differential equation

```

% p = 0.15;
% q = 0.2;

syms x(tt)

% eqn = diff(x,tt,2)+(p+q*cos(tt))*x == 0;
% xSol = dsolve(eqn);

e = 2.71828;
[VV] = odeToVectorField(diff(x,tt,2)+(p+q*cos(tt))*x == 0);
M = matlabFunction(VV,'vars', {'tt','Y'})
sol = ode45(M,[0 160],[0.1 0]);
xxx=[0:0.005:160];
yyy = deval(sol,xxx,1);
phi=yyy.*(e.^(mu*xxx));
phi=rad2deg(phi);

figure ()
% fplot(x ,[0.000815793364136552 8.1579])
subplot(2,1,1)
fplot(@(x)deval(sol,x,1), [0, 160])
hold on
grid on
xlabel ('\tau')
ylabel ('x(\tau)')
title ('Mathieu Equation Solution')

subplot(2,1,2)
plot (xxx,phi)
hold on
xlim([0 160])

```



```

grid on
xlabel ('time (s)')
ylabel ('\phi(deg)')
title ('Rolling angle on time')

sgtitle('Parametric rolling with no damping')

```

Influence of damping and non-linearity

```

% GZ calculation
phi_0 = linspace(0,60,61);
phi_0r = deg2rad(phi_0);
idx = find(gm == min(gm));
scal = 5;

gm_0=[];
for ii=1:(idx)
gm_0(ii) = gm(scal*ii-(scal-1));
end
gz=[];
for ii = 1:numel(gm_0)
    gz = [gz; gm_0(ii).*phi_0r.*(1-phi_0r.^2)];
end

figure ()
plot(phi_0,gz)
hold on
grid on
xlabel ('\phi (deg)')
ylabel ('GZ (m)')
title ('Varying GZ on time')

```

Solving Differential equation

```

syms x(ttt)

% eqn = diff(x,tt,2)+(p+q*cos(tt))*x == 0;
% xSol = dsolve(eqn);

% mu = 0.2
% w_m_bar = sqrt(mu^2+p);
% w_a_bar = sqrt(q);

e = 2.71828;
[W] = odeToVectorField(diff(x,ttt,2)+(p+q*cos(ttt))*x-
(w_m_bar^2+(w_a_bar^2)*cos(ttt))*(x^3)*(e^(-2*mu*ttt)) == 0);
M = matlabFunction(W,'vars', {'ttt','Y'});
sol2 = ode45(M,[0 160],[0.1 0]);
xxx=[0:0.005:160];
yyy = deval(sol2,xxx,1);
phi=yyy.*(e.^(-mu*xxx));
phi=rad2deg(phi);

figure ()
% fplot(x,[0.000815793364136552 8.1579])
subplot(2,1,1)
fplot(@(x)deval(sol2,x,1), [0, 160])
hold on

```

```

grid on
xlabel ('\tau')
ylabel ('x(\tau)')
title ('Mathieu Equation Solution')

subplot(2,1,2)
plot (xxx,phi)
hold on
xlim([0 160])
grid on
xlabel ('time (s)')
ylabel ('\phi(deg)')
title ('Rolling angle on time')

sgtitle('Parametric rolling with damping')

```

Vulnerability criteria

```

% Frequency condition
% For 1st instability zone
p_b1 = 0.25+q/2;
p_b2 = 0.25-q/2;

if p > p_b2
    if p < p_b1
        sucept = 'Suceptibility encountered'
        S_pr = 1;
    else
        sucept = 'No suceptibility encountered'
        S_pr = 0;
    end
elseif p < p_b2
    sucept = 'No suceptibility encountered'
    S_pr = 0;
end

if S_pr == 1

% Damping condition
k_1 = 1-0.1875*q^2;
k_2 = 1.002*q+0.16*q+0.759;
k_3 = (q^2-16+sqrt(q^4+352*q^2+1024*p))/(16*q);
damp_tresh = q*k_1*k_2*sqrt(1-k_3^2);

end
w_0 = sqrt(g*gm_m/(k_44^2));
T_0 = 2*pi./w_0;

V_s1 = sqrt(g*L)*(1/sqrt(2*pi)-sqrt(2*L)./(T_0*sqrt(g)));
V_s2 = sqrt(g*L)*(1/sqrt(2*pi)-sqrt(6*L)./(T_0*sqrt(g)));

n = [1 2 3];
V_n = sqrt(g*L)*(1/sqrt(2*pi)*sqrt(Lambda/L)-2*Lambda./(n*T_0*sqrt(g*L)));

if w_e < 2*w_m
    txt = "Parametric rolling from head seas";
elseif w_e >= 2*w_m
    txt = 'Parametric rolling from following seas';
end

```

```

V_pr = (19.06*abs(2*w_m-w_e)/(w_e)^2)*0.5144;
V_sr = V; % Max service speed on the condition

if V_pr < V_sr
V_s = V_pr;
elseif V_pr > V_sr
V_s = V_sr;
end

```

Magnitude of stability change

```

nn = 4;

h = (w_a/w_m)^2;
a = 4*w_m_bar^2;
kappa = 0.25*sqrt(a^2*h^2-4*(a-1)^2);
epsilon = acos(2*(a-1)/(a*h))/2;

f = -(2^0.5)/2*exp(pi*nn*h/2-2*d*pi*nn/w_m).*sin(2*pi.*nn-pi/4);
GM_ratio = gm_a/gm_m;
value = 2*(log(f)+log(2))./(pi*nn)+4*d/w_m;
value_lim = 0.49;

if value_lim <= value
    txt_1 = "No parametric rolling suceptibility encountered"
else
    txt_1 = "Parametric rolling suceptibility encountered"
end

```

Parameters of the wave

```

% Considering Lambda = Ship length
Lambda_0 = L;

```

Published with MATLAB® R2019b

Code for triggering parametric rolling

```

close all
clear all
clc

```

Input data

The code can be modified to analyse possibility of parametric rolling or for estimating how to trigger the phenomenon. Input ship data

```

% B = input ('Input ship beam (m): ');
B = 11;

```

Variable vectors

```
% L = input ('Input ship length (m): ');
L_iii = [46.303*ones(4,1); 47.345*ones(2,1); 45.772*ones(6,1)];
% disp = input ('Input the ship displacement (kg): ');
disp_iii = [1562800*ones(4,1); 1574115*ones(2,1); 1998838*ones(6,1)];
% V = input ('Input ship speed (m/s): ');
V_iii = [12*ones(4,1); 3*ones(2,1); 11.75*ones(6,1)];
% B_44 = input ('Input dimensional damping rolling coefficient : ');
B_44_iii = 1000*[1.35986E+04 1.43941E+04 1.37284E+04 1.52724E+05 1.47325E+04
1.48585E+04 7.31975E+04 3.60312E+05 3.09703E+04 3.74148E+04
2.78664E+04 2.86528E+04];
% gm_max = input ('Input maximum value of GM (m): ');
gm_max_iii = [0.801416356
0.801416356
0.801416356
1.240442355
1.12558847
0.995
1.143416356
1.143416356
1.143416356
1.143416356
0.929436611
];
% gm_min = input ('Input minimum value of GM (m): ');
gm_min_iii = [0.801416356
0.801416356
0.801416356
0.785264866
0.689694144
0.995
1.143416356
1.143416356
1.143416356
1.143416356
0.772678071
];

% Input wave characteristic
% Lambda = input ('Input wave length(m) : ');
Lambda_iii = [24.11 24.11 19.9 19.9 61.38 33.18 61.38 24.11 24.11 19.9
19.9 33.18];
% w_dir = input ('Input wave relative direction(deg) : ');
w_dir_iii = [163.54 263.54 240.85 330.85 177.45 327.98 357.45 343.54 83.54
60.85 150.85 147.98];

for iii = 1:numel(L_iii)
```

Variable selection

```
% L = input ('Input ship length (m): ');
L = L_iii(iii);
% disp = input ('Input the ship displacement (kg): ');
disp = disp_iii(iii);
% V = input ('Input ship speed (m/s): ');
```

```

V = V_iii(iii)*0.514444;
% B_44 = input ('Input dimensional damping rolling coefficient : ');
B_44 = B_44_iii(iii);
% gm_max = input ('Input maximum value of GM (m): ');
gm_max = gm_max_iii(iii);
% gm_min = input ('Input minimum value of GM (m): ');
gm_min = gm_min_iii(iii);

% Input wave characteristic
% Lambda = input ('Input wave length(m) : ');
Lambda = Lambda_iii(iii);
% w_dir = input ('Input wave relative direction(deg) : ');
w_dir = w_dir_iii(iii);

% Input simulation time
% time = input ('Input the simulation time as [simulation_time time_step] :');
time = [150 0.05];

```

Determination of parameters of the differential equation for roll motion.

Calculation of Added mas:

```

% Evaluation parameters
g = 9.81; % m/s^2
t = [time(2):time(2):time(1)]; % Time vector of analysis

w_period = (Lambda*2*pi/g)^0.5; % wave period
w = 2*pi/w_period; % wave frequency
w_e = abs(w-w^2/g*v*cos(deg2rad(w_dir))); % Angular wave frequency of encounter
tao = w_e*t; % Non-dimensional time

% GM evaluation
gm_a = 0.5*(gm_max-gm_min); % GM amplitude
gm_m = 0.5*(gm_max+gm_min); % Maximum GM
gm = gm_m+gm_a*cos(w_e*t); % Varying GM on time

% Initial Varying GM plot
figure ()
plot (t,gm)
hold on
grid on
xlabel ('time (s)')
ylabel ('GM (m)')
title ('Varying GM on time')

% Moment of inertia + added mass moment of inertia
k_44 = 0.4*B; % Estimated rolling radius of gyration
I_44 = disp*k_44^2; % Estimated rolling total moment of inertia

% Calculation of frequencies
w_m = sqrt((disp*g*gm_m)/(I_44)); % Mean changing GM frequency
w_m_bar = w_m/w_e; % Non-dimensional changing GM frequency
w_a = sqrt((disp*g*gm_a)/(I_44)); % Amplitude of changing GM frequency
w_a_bar = w_a/w_e; % Non-dimensional amplitude of changing GM frequency

% Damping coefficient
d = 0.5*(B_44/I_44); % Non-dimensional damping coefficient
mu = d/w_e; % 2nd Non-dimensional damping coeficcient

```

Mathieu parameters

```
p = (w_m_bar^2-mu^2); % p coefficient
q = w_a_bar^2; % q coefficiente

% p = 0.15;
% q = 0.2;
```

Differential equation

```
p = 0.2;
q = 0.2;

syms x(tt)

% eqn = diff(x,tt,2)+(p+q*cos(tt))*x == 0;
% xSol = dsolve(eqn);

e = 2.71828;
[VV] = odeToVectorField(diff(x,tt,2)+(p+q*cos(tt))*x == 0);
M_1 = matlabFunction(VV,'vars', {'tt','V'});
sol = ode45(M_1,[0 320],[0.1 0]);

condition = max(sol.x);
if condition >= 320
    xxx = [0:0.005:320];
else
    xxx = [0:0.005:condition];
end

yyy = deval(sol,xxx,1);
phi=yyy.*(e.^(-mu*xxx));
phi=rad2deg(phi);

figure ()
% fplot(x ,[0.000815793364136552 8.1579])
subplot(2,1,1)
fplot(@(x)deval(sol,x,1), [0, 160])
% plot(x,sol(:,1),'-o',x,sol(:,2),'-.')
hold on
grid on
xlabel ('\tau')
ylabel ('x(\tau)')
title ('Mathieu Equation Solution')

subplot(2,1,2)
plot (xxx,phi)
hold on
xlim([0 160])
grid on
xlabel ('time (s)')
ylabel ('\phi(deg)')
title ('Rolling angle on time')

sgtitle('Parametric rolling with no damping')
```

Solving Differential equation

```
syms xx(ttt)

% eqn = diff(x,tt,2)+(p+q*cos(tt))*x == 0;
% xSol = dsolve(eqn);

% mu = 0.09;
w_m_bar = sqrt(mu^2+p);
w_a_bar = sqrt(q);

e = 2.71828;
[W] = odeToVectorField(diff(xx,ttt,2)+(p+q*cos(ttt))*xx-
(w_m_bar^2+(w_a_bar^2)*cos(ttt))*(xx^3)*(e^(-2*mu*ttt)) == 0);
M_2 = matlabFunction(W,'vars',{ 'ttt','Y' });
sol2 = ode45(M_2,[0 320],[0.1 0]);

condition = max(sol2.x);
if condition >= 320
    xxx = [0:0.005:320];
else
    xxx = [0:0.005:condition];
end

yyyy = deval(sol2,xxx,1);
phi = yyyy.*(e.^(-mu*xxx));
phi = rad2deg(phi);

figure ()
% fplot(x ,[0.000815793364136552 8.1579])
subplot(2,1,1)
% fplot(@(x)deval(sol2,x,1), [0, 160])
plot(xxx,yyyy)
hold on
grid on
xlabel ('\tau')
ylabel ('x(\tau)')
title ('Mathieu Equation Solution')

subplot(2,1,2)
plot (xxx,phi)
hold on
xlim([0 160])
grid on
xlabel ('time (s)')
ylabel ('\phi(deg)')
title ('Rolling angle on time')

sgtitle('Parametric rolling with damping')
```

Vulnerability criteria

```
% Frequency condition

p_b1 = 0.25+q/2;
p_b2 = 0.25-q/2-0.125*q^2+0.03125*q^3-q^4/384;

if p >= p_b2
    if p <= p_b1
```

```

    sucept = 'Frequency condition fulfilled'
    freq_sucep = 1
else
    sucept = 'Frequency condition not fulfilled'
    freq_sucep = 0
end
elseif p < p_b2
    sucept = 'Frequency condition not fulfilled'
    freq_sucep = 0
end

if freq_sucep == 1
% Damping condition

k_1 = 1-0.1875*q^2;
k_2 = 1.002*q+0.16*q+0.759;
k_3 = (q^2-16+sqrt(q^4+352*q^2+1024*p))/(16*q);
damp_tresh = q*k_1*k_2*sqrt(1-k_3^2);

if k_3 > 1
    damp_sucep = 0
    sucep = 'Damping criterion not satisfied'

elseif k_3 < 1 && mu*w_m/w_e > q*k_1*k_2*(1-k_3)^0.5
    damp_sucep = 0
    sucep = 'Unlikely parametric roll'

elseif k_3 < 1 && mu*w_m/w_e < q*k_1*k_2*(1-k_3)^0.5

    damp_sucep = 1
    sucep = 'Check Severity criterion'

end
end

```

```

w_0 = sqrt(g*gm_m/(k_44^2));
T_0 = 2*pi./w_0;

V_s1 = sqrt(g*L)*(1/sqrt(2*pi)-sqrt(2*L)./(T_0*sqrt(g)));
V_s2 = sqrt(g*L)*(1/sqrt(2*pi)-sqrt(6*L)./(T_0*sqrt(g)));

n = [1 2 3];
V_n = sqrt(g*L)*(1/sqrt(2*pi)*sqrt(Lambda/L)-2*Lambda./(n*T_0*sqrt(g*L)));

```

```

if w < 2*w_m
    txt = "Probable parametric rolling from head seas"
elseif w >= 2*w_m
    txt = 'Probable parametric rolling from following seas'
end

V_pr = (19.06*abs(2*w_m-w)/(w)^2);
V_sr = V; % Max service speed on the condition

if V_pr < V_sr
V_s = V_pr/0.5144444;
elseif V_pr > V_sr
V_s = V_sr/0.5144444;
end

```



```
% if v_pr > 15*0.51444
%     w_e = 5;
```

Magnitude of stability change

```
nn = 16;

h = (w_a/w_m)^2;
a = 4*w_m_bar^2;
kappa = 0.25*sqrt(a^2*h^2-4*(a-1)^2);
epsilon = acos(2*(a-1)/(a*h))/2;

f = -(2^0.5)/2*exp(pi*nn*h/2-2*d*pi*nn/w_m).*sin(2*pi.*nn-pi/4);
GM_ratio = gm_a/gm_m;
value = 2*(log(f)+log(2))./(pi*nn)+4*d/w_m;
value_lim = 0.49;

if value_lim >= value
    txt_1 = "No parametric rolling suceptibility encountered"
else
    txt_1 = "Parametric rolling suceptibility encountered"
end
end
```

Reaching parametric rolling

```
I_44 = 3.8698E+07;
B_44 = 1.373E+07;
w_e_new = 0.5*B_44/(damp_tresh*I_44);

syms ww

eqn1 = w_e_new == ww*(1+ww*11.75*0.51444444/g);
s1 = vpasolve(eqn1);
```

[Published with MATLAB® R2019b](#)

Appendix D

Criteria analyses

The presented analyses correspond to the conditions specified in Table 4-2.

Light ship working conditions

Condition 01

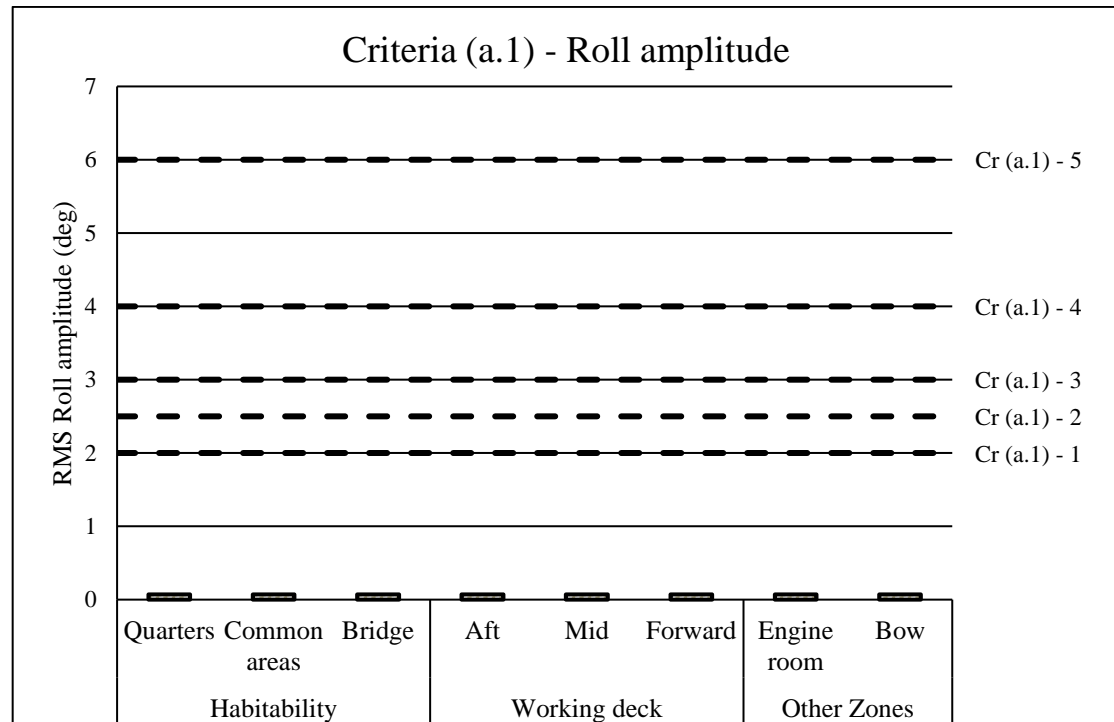


Figure D-0-1: Condition 01 – Roll amplitude criteria

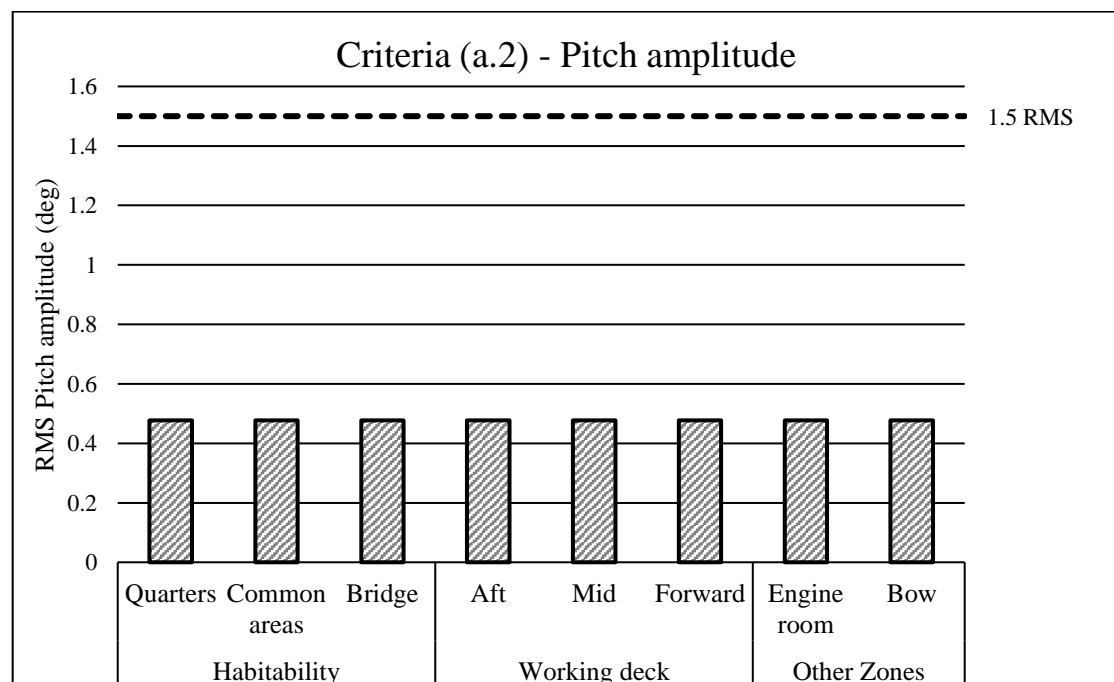


Figure D-2: Condition 01 – Pitch amplitude criteria

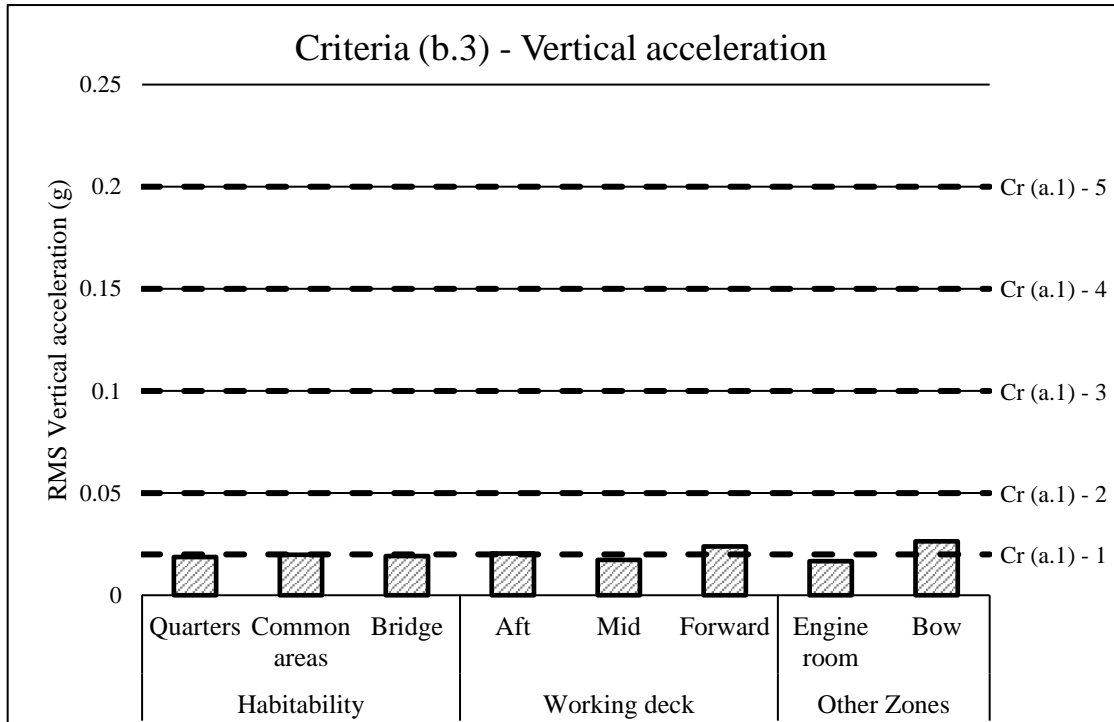


Figure D-3: Condition 01 – Vertical acceleration criteria

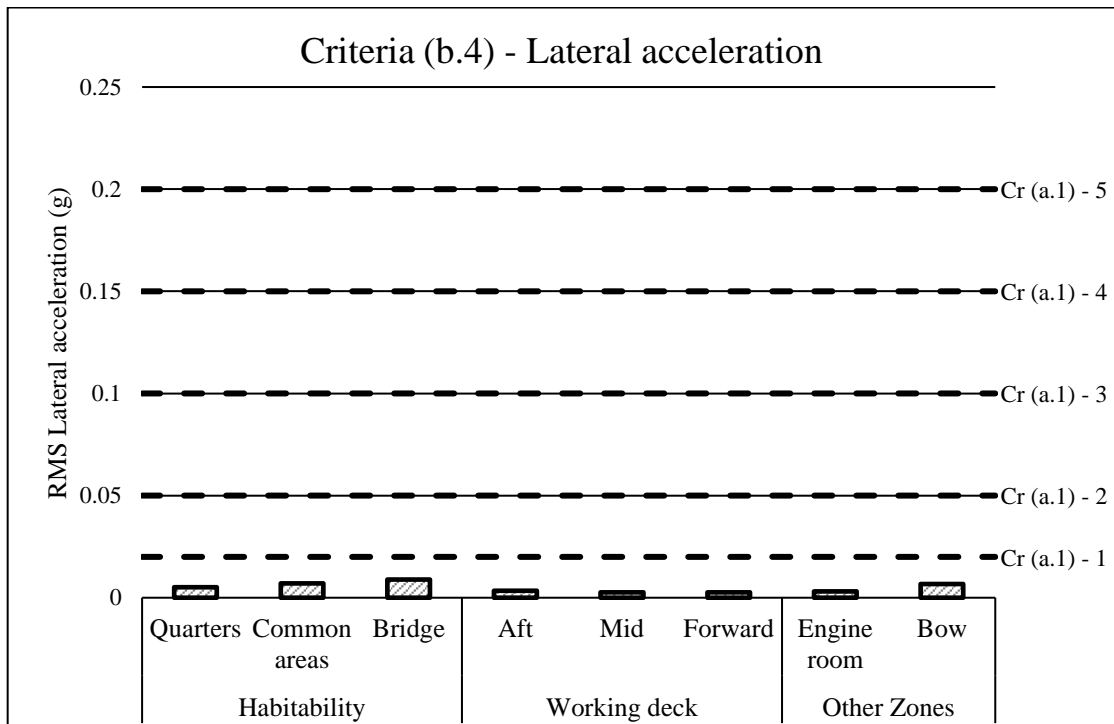


Figure D-4: Condition 01 – Lateral acceleration criteria

Condition 02

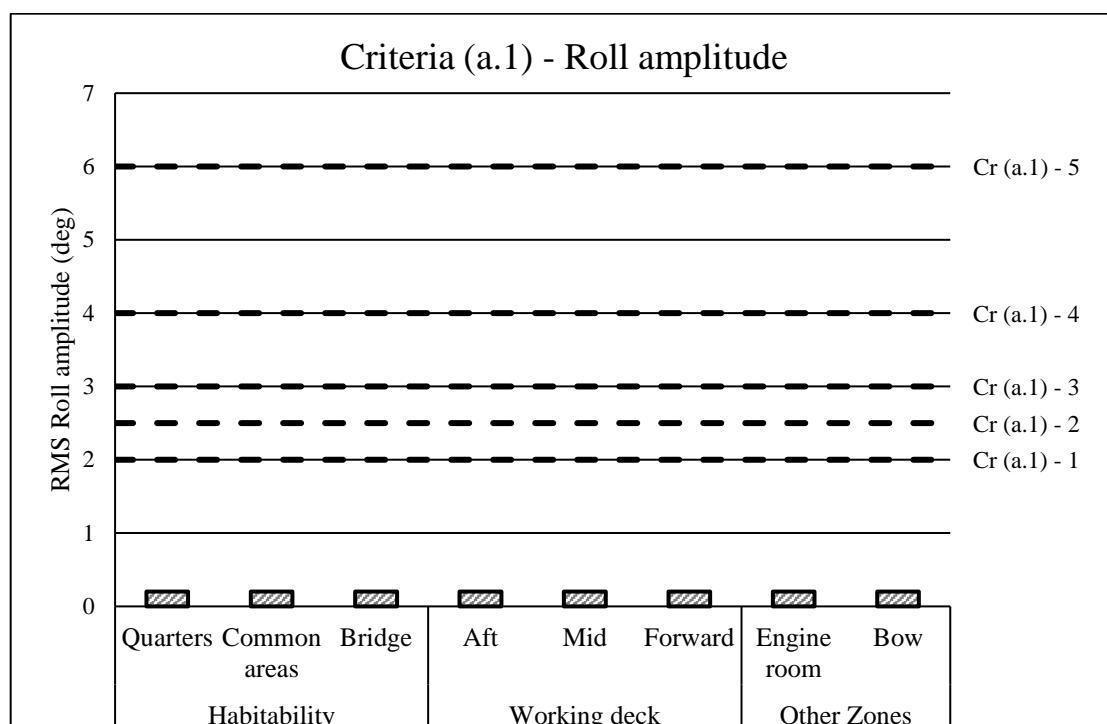


Figure D-5: Condition 02 – Roll amplitude criteria

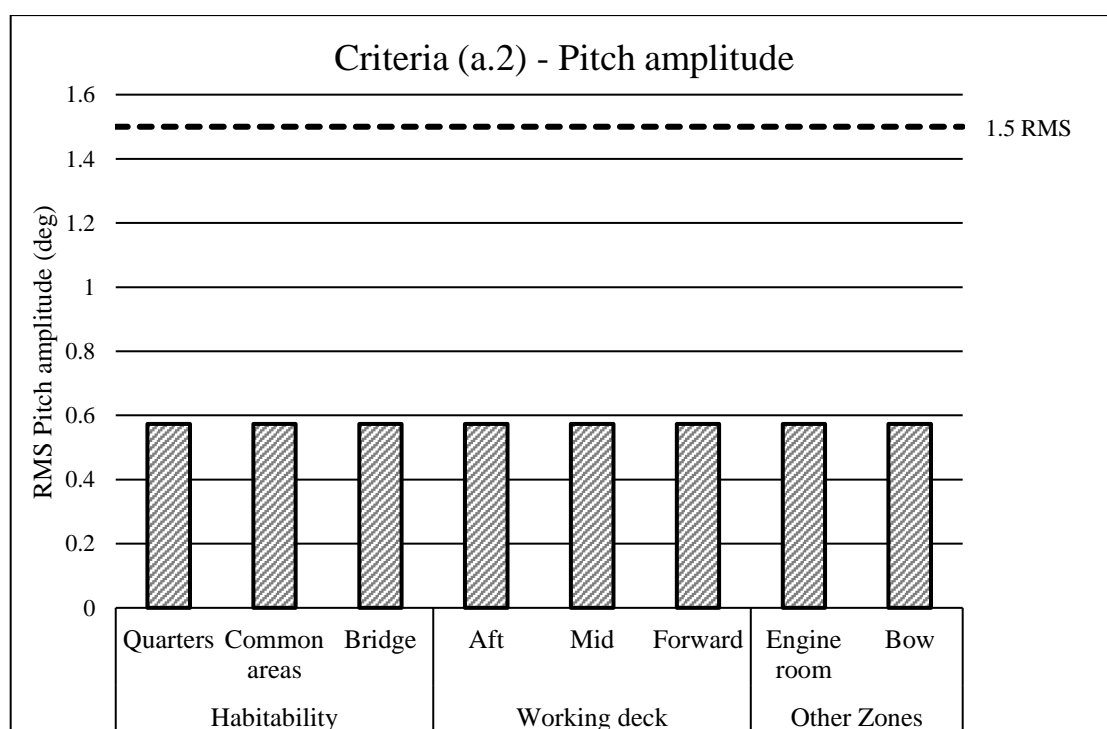


Figure D-6: Condition 02 – Pitch amplitude criteria

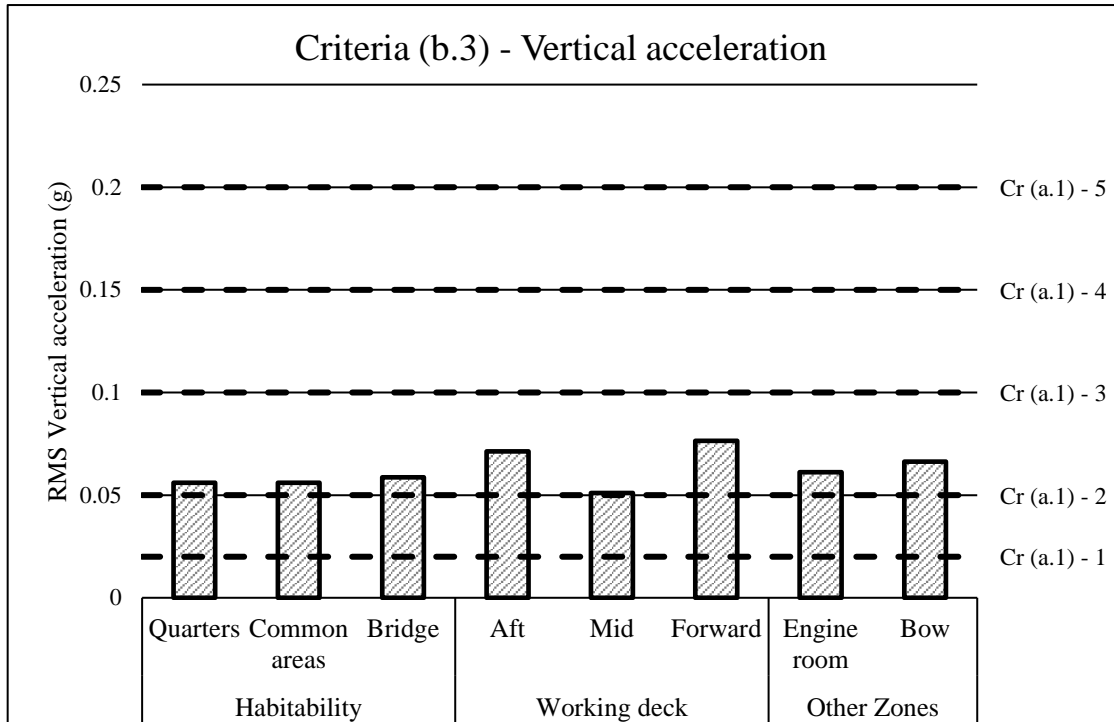


Figure D-7: Condition 02 – Vertical acceleration criteria

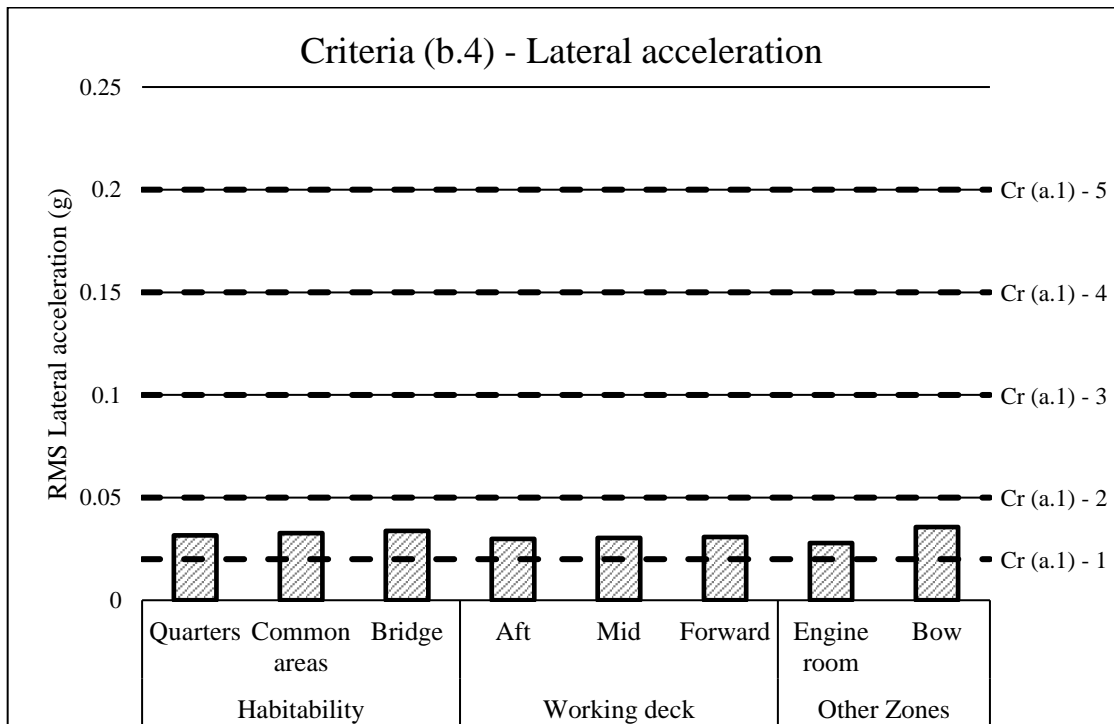


Figure D-8: Condition 02 – Lateral acceleration criteria

Condition 03

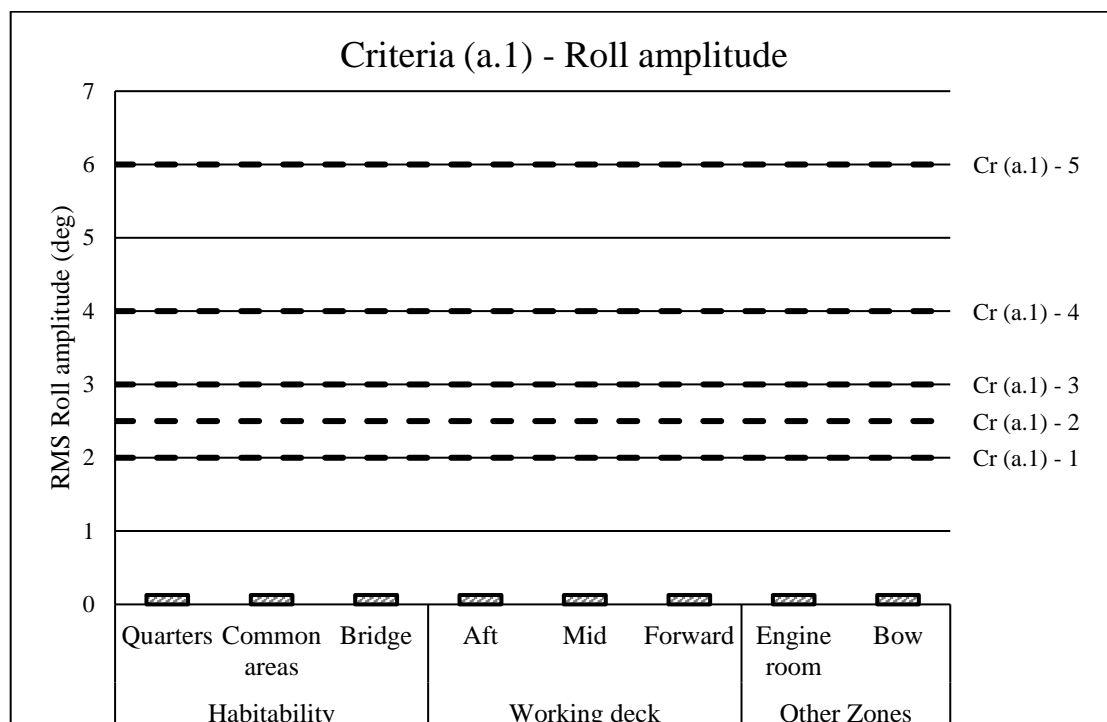


Figure D-9: Condition 03 – Roll amplitude criteria

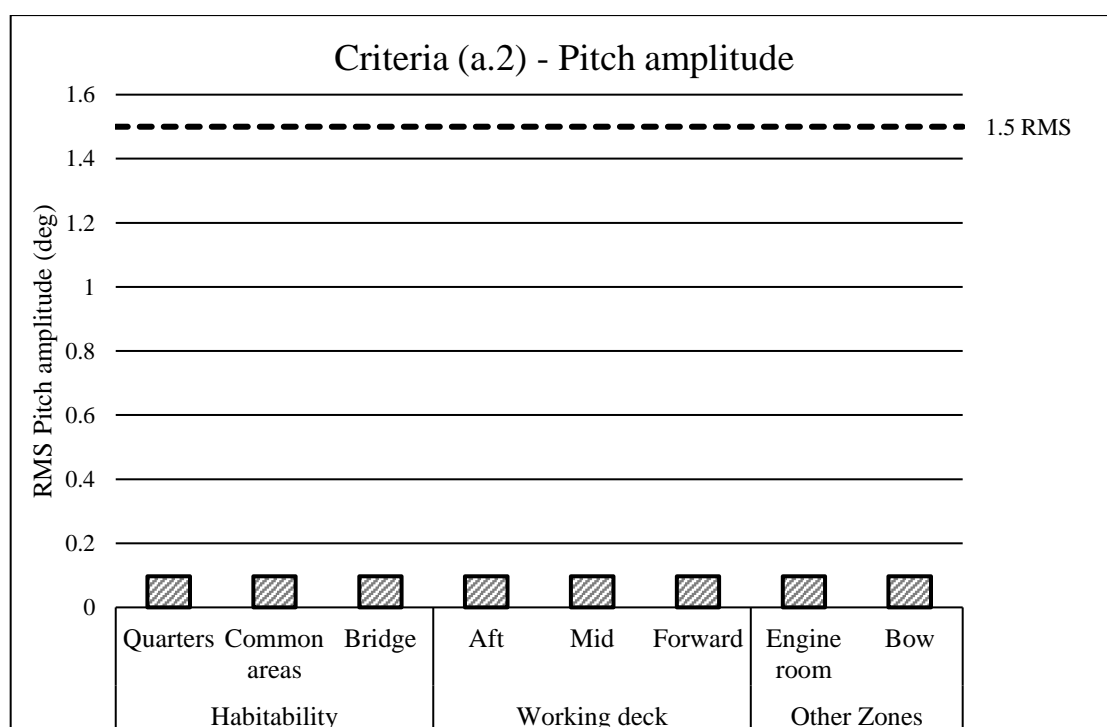


Figure D-10: Condition 03 – Pitch amplitude criteria

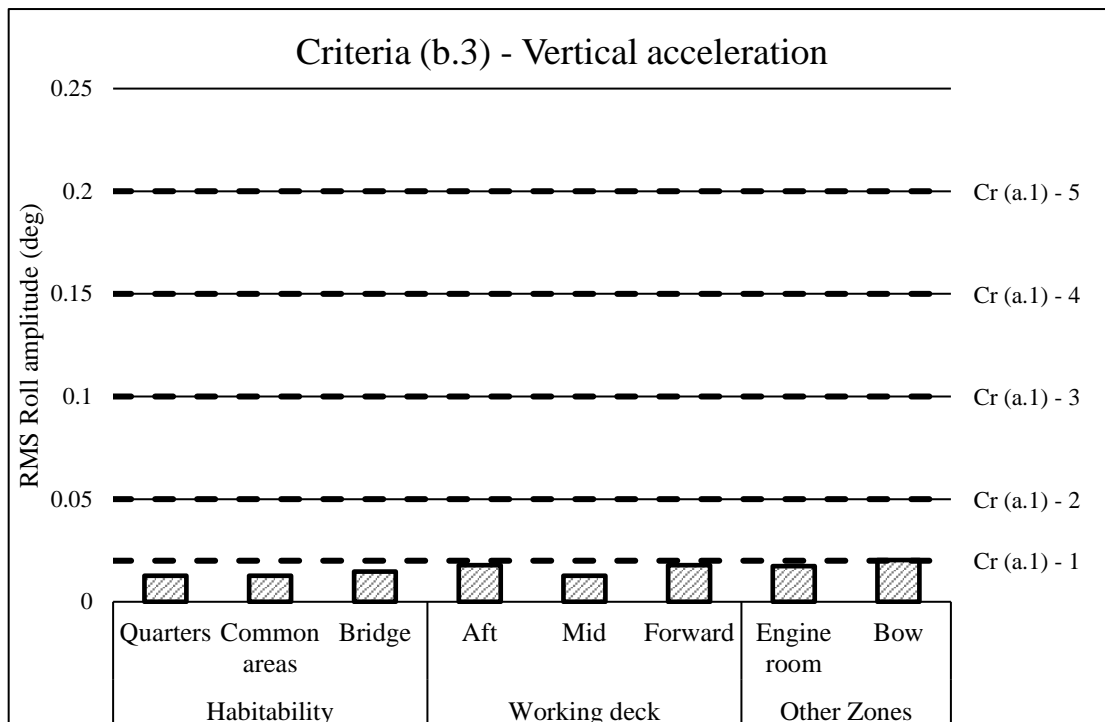


Figure D-11: Condition 03 – Vertical acceleration criteria

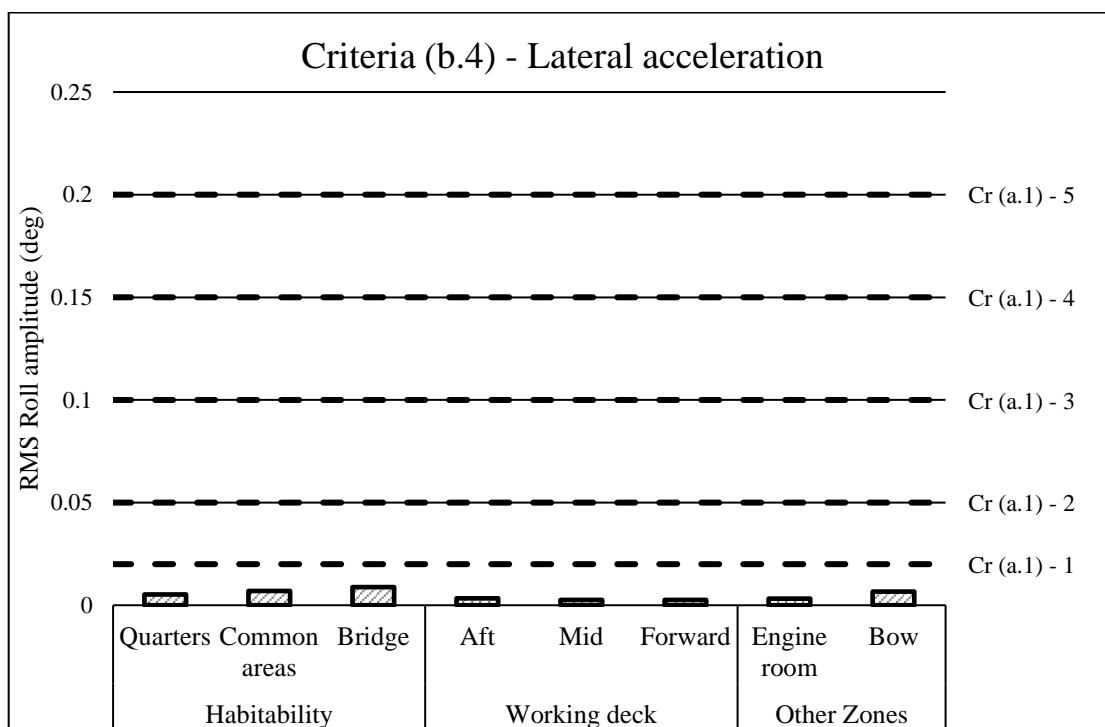


Figure D-12: Condition 03 – Lateral acceleration criteria

Condition 04

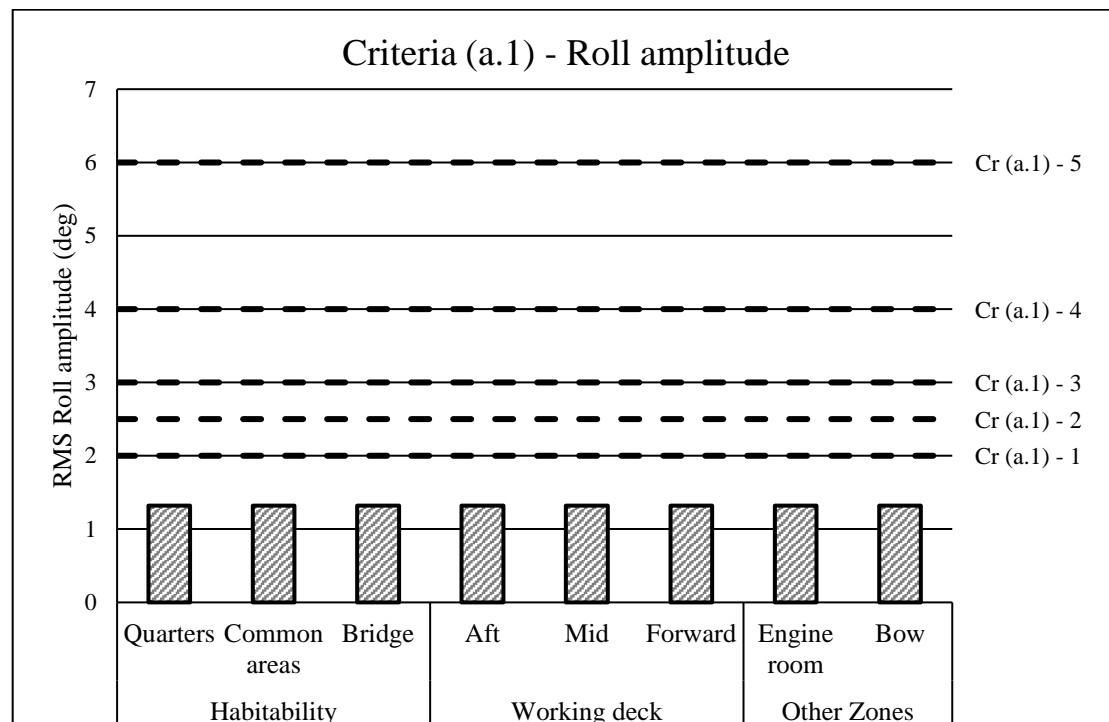


Figure D-13: Condition 04 – Roll amplitude criteria

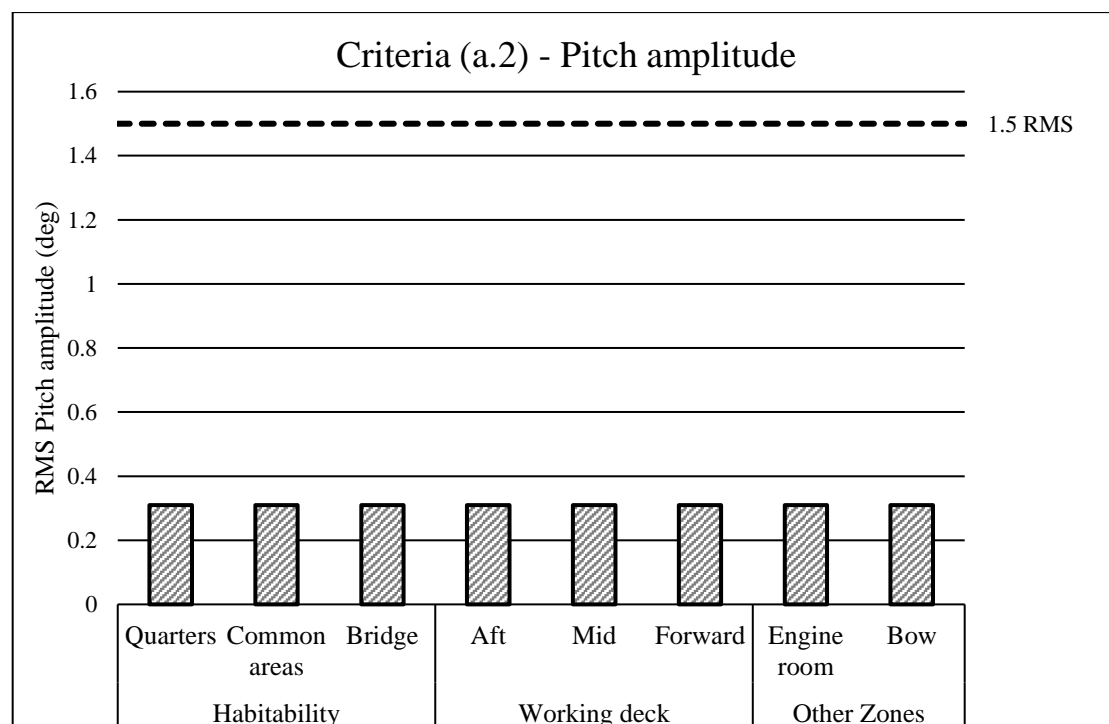


Figure D-14: Condition 04 – Pitch amplitude criteria

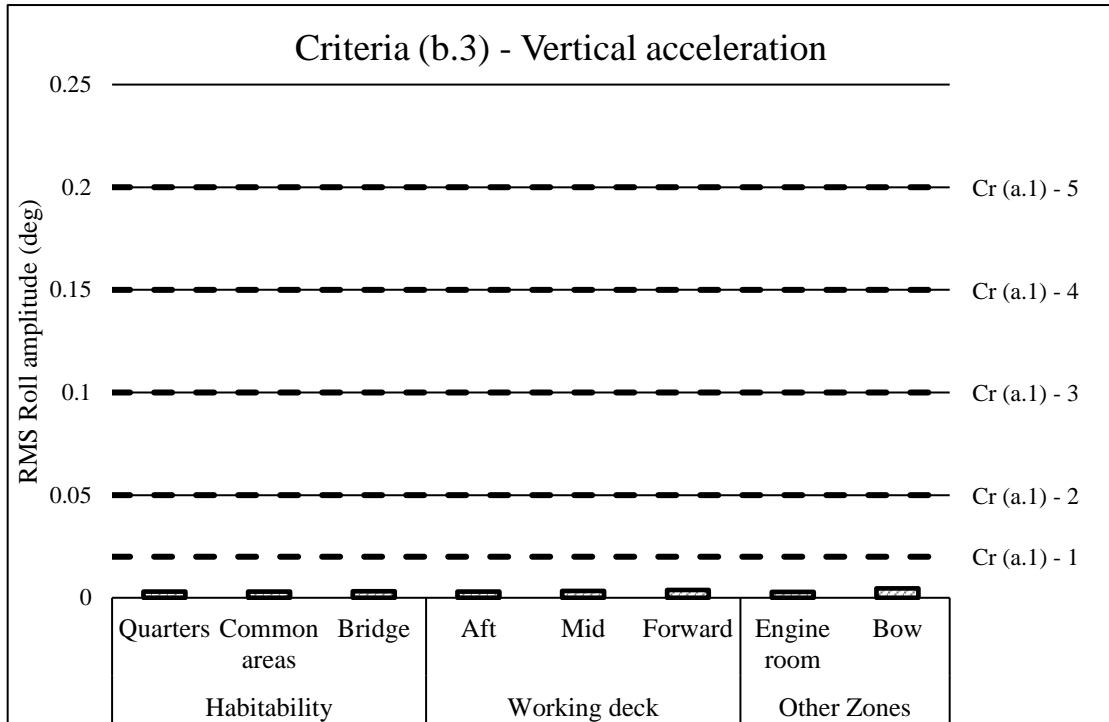


Figure D-15: Condition 04 – Vertical acceleration criteria

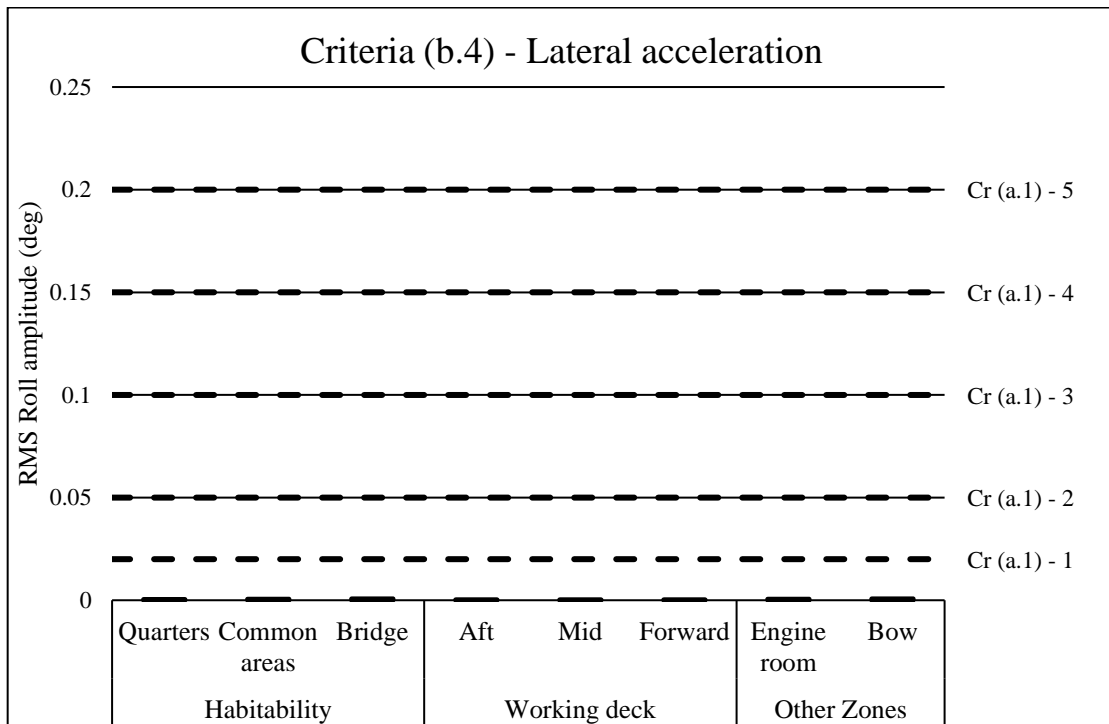


Figure D-16: Condition 04 – Lateral acceleration criteria

Trawling working conditions

Condition 05

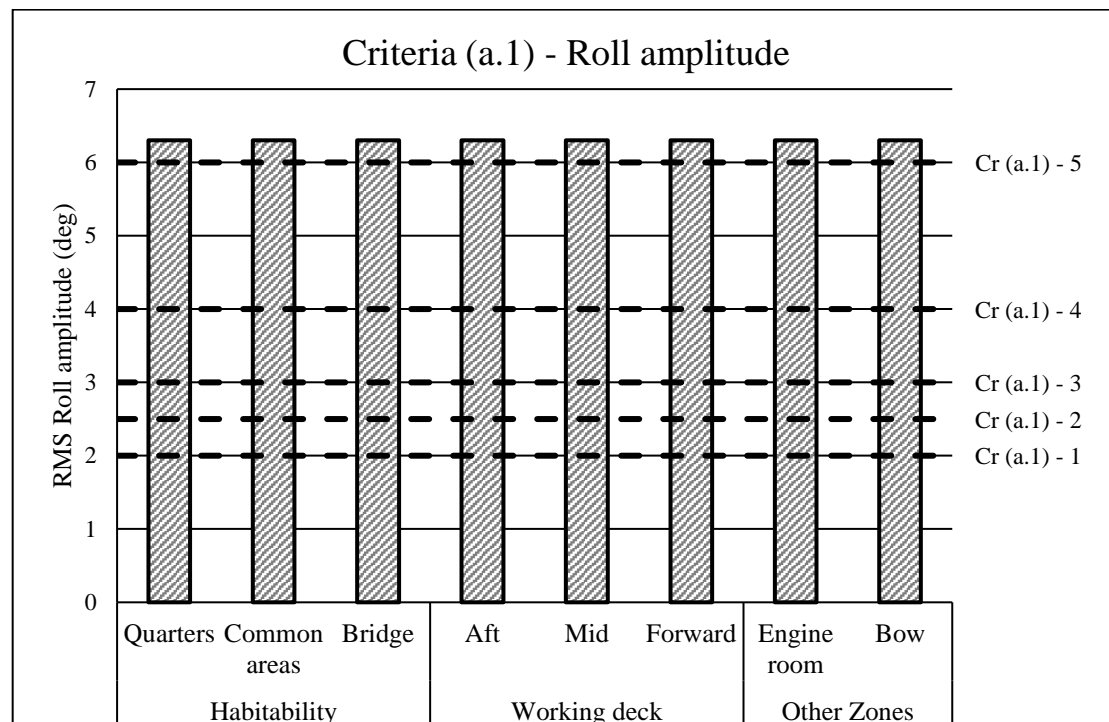


Figure D-17: Condition 05 – Roll amplitude criteria

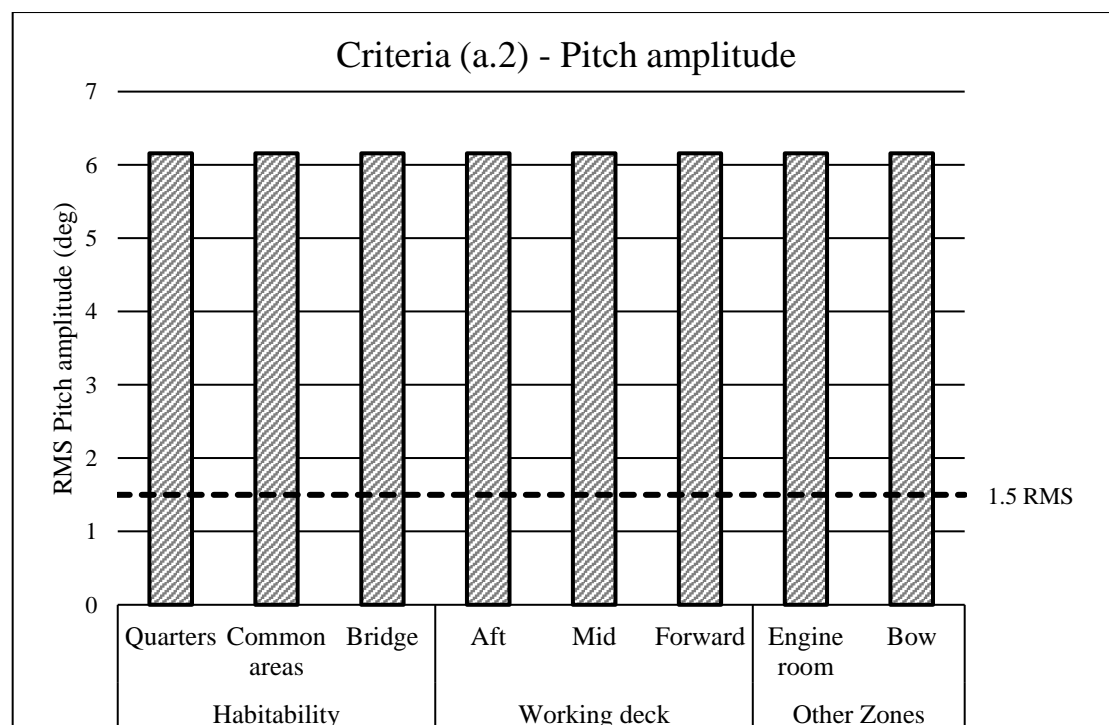
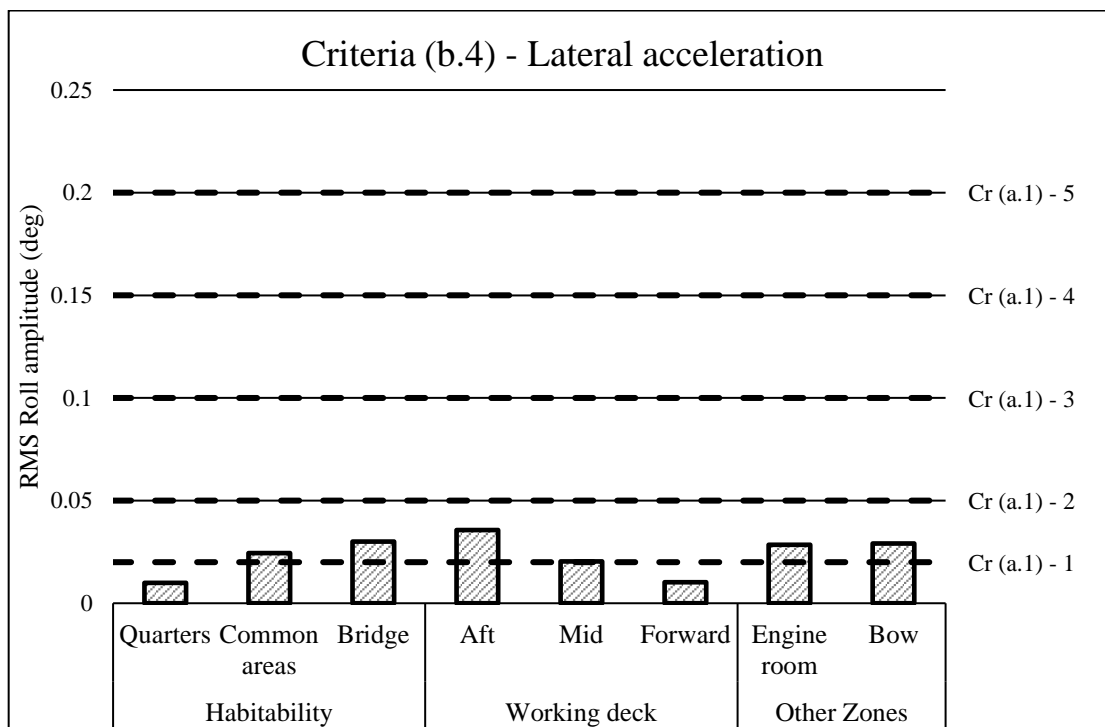
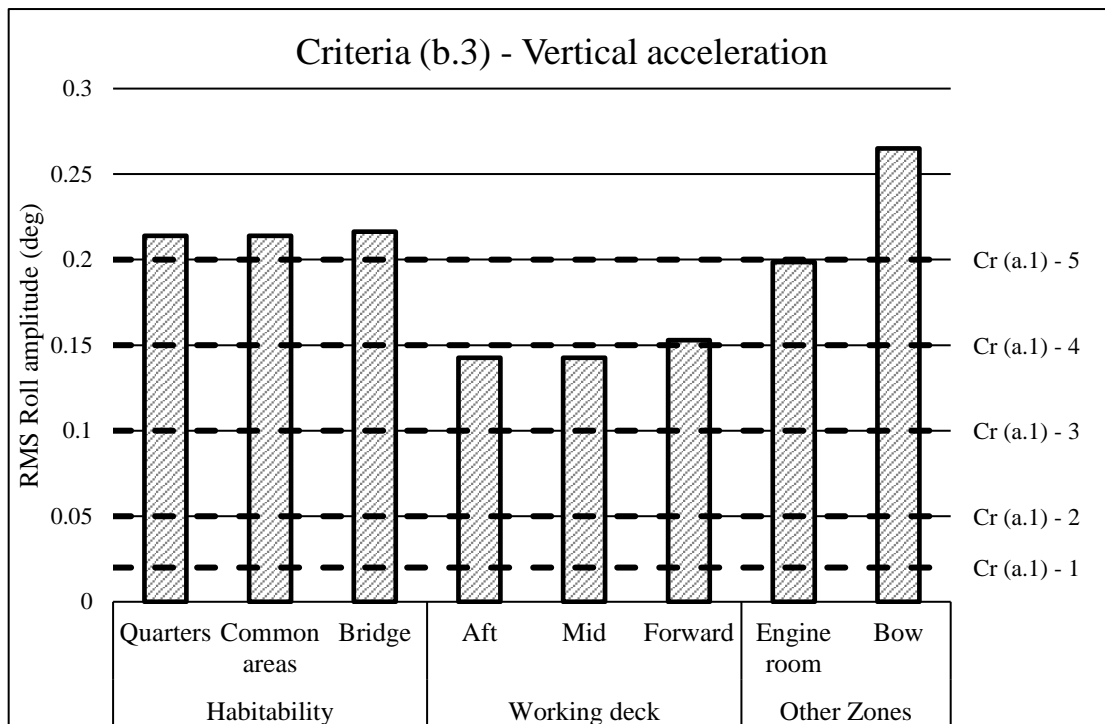


Figure D-18: Condition 05 – Pitch amplitude criteria



Condition 06

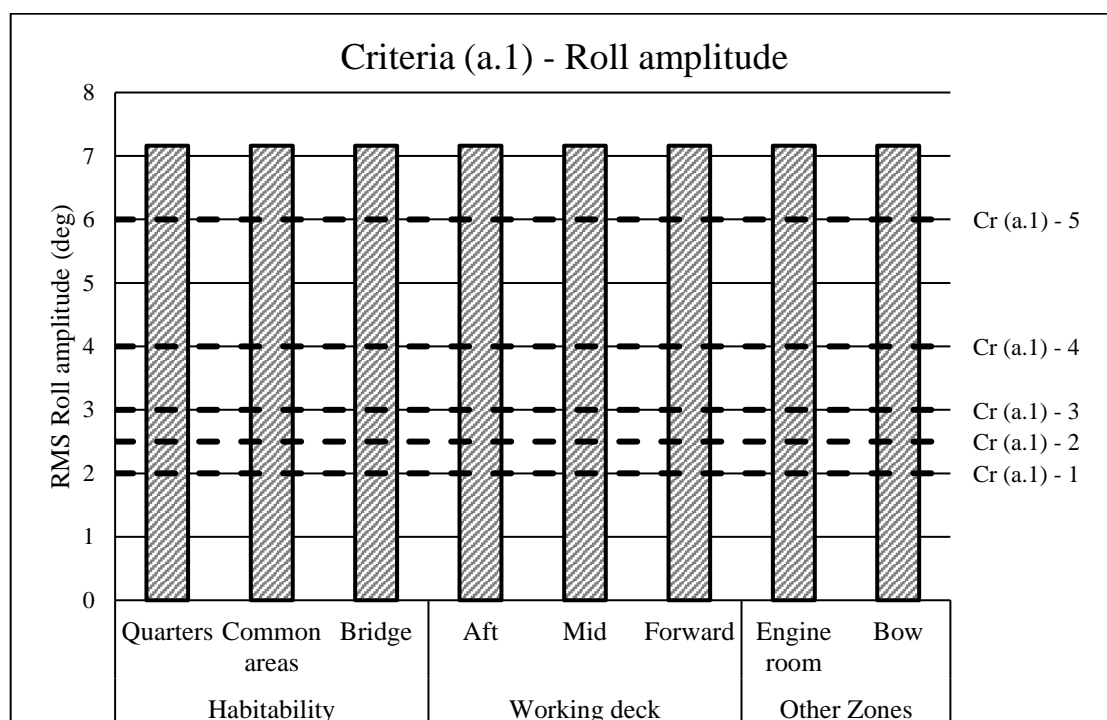


Figure D-21: Condition 06 – Roll amplitude criteria

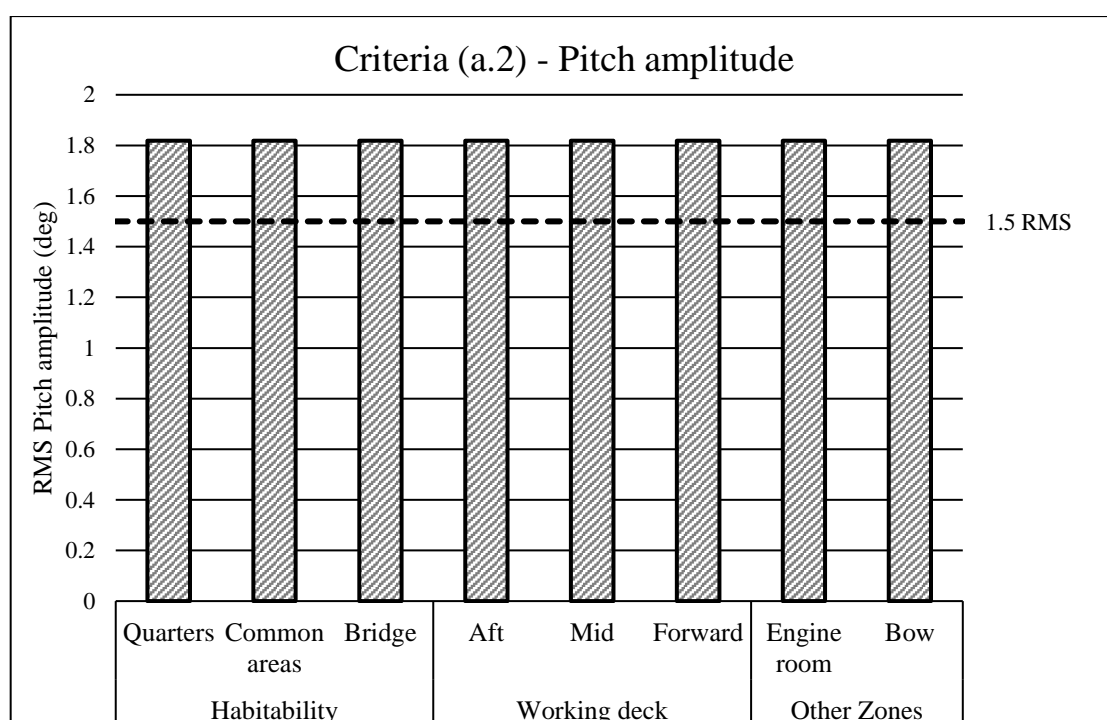


Figure D-22: Condition 06 – Pitch amplitude criteria

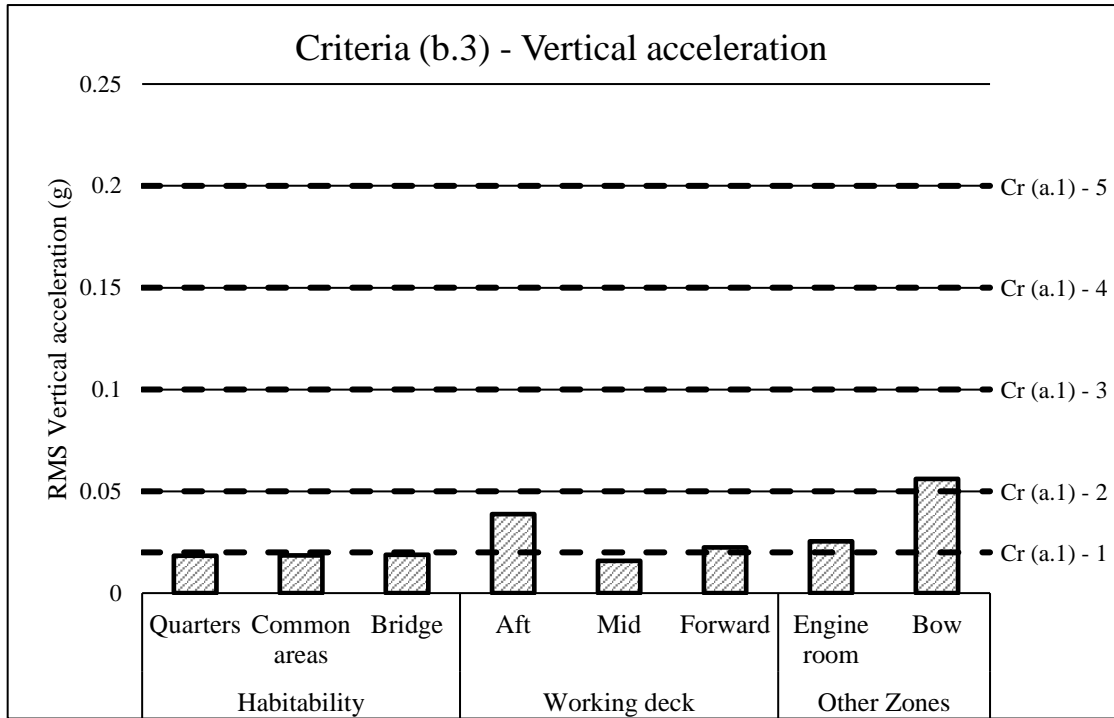


Figure D-23: Condition 06 – Vertical acceleration criteria

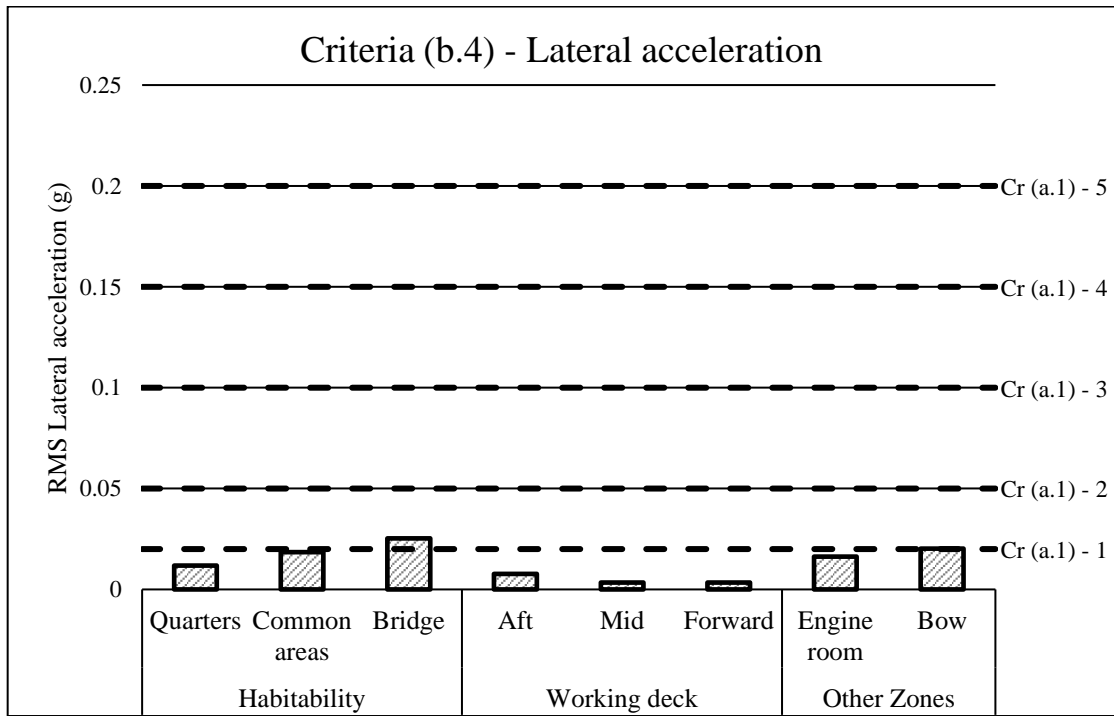


Figure D-24: Condition 06 – Lateral acceleration criteria

Fully loaded working conditions

Condition 07

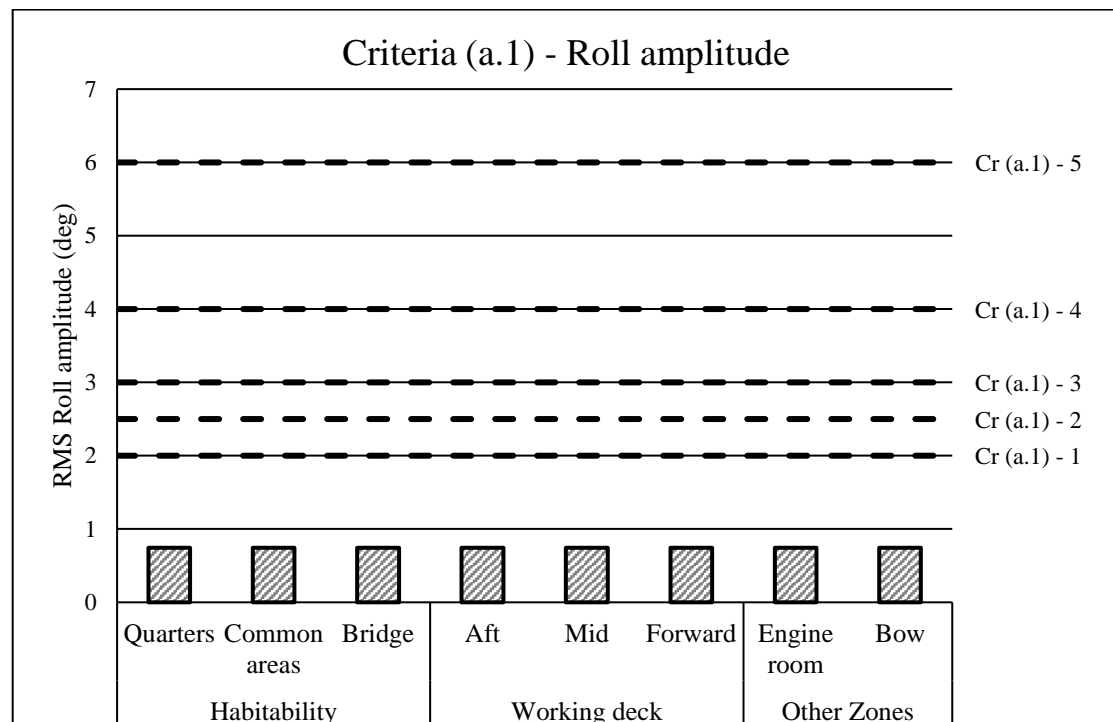


Figure D-25: Condition 07 – Roll amplitude criteria

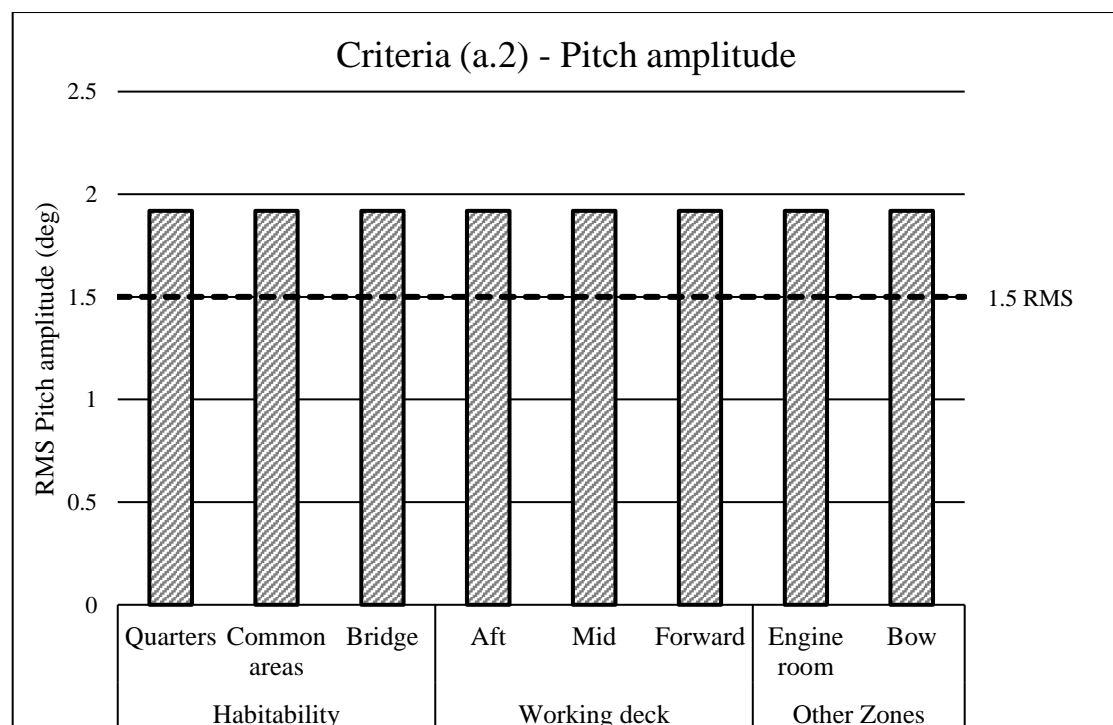


Figure D-26: Condition 07 – Pitch amplitude criteria

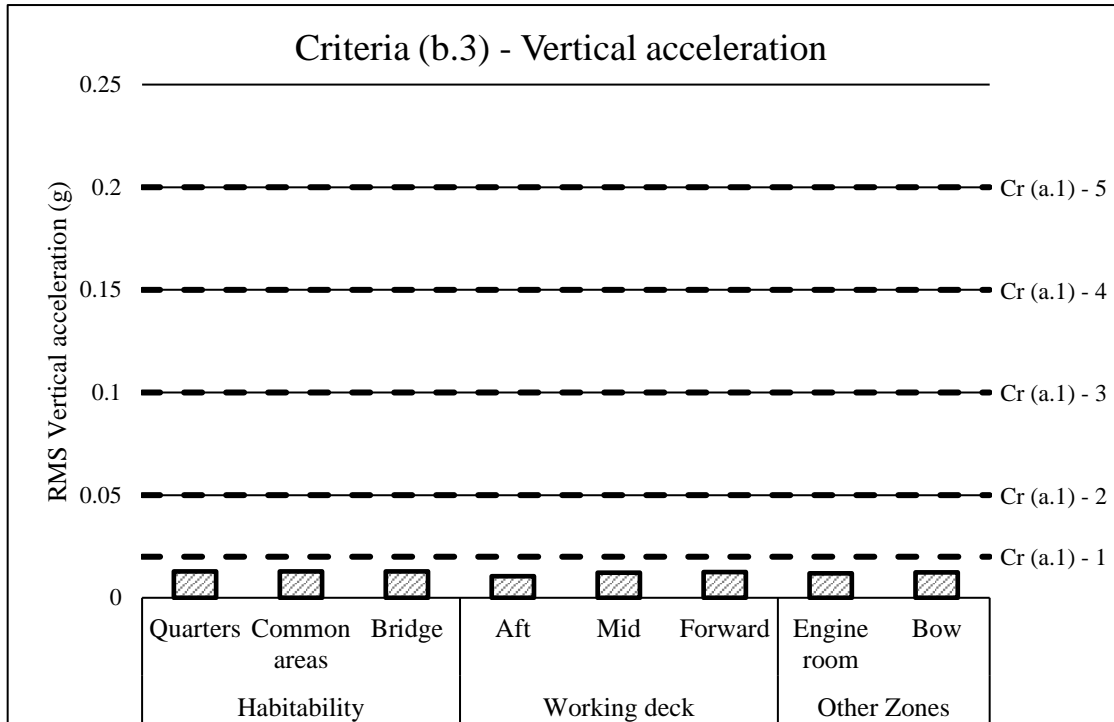


Figure D-27: Condition 07 – Vertical acceleration criteria

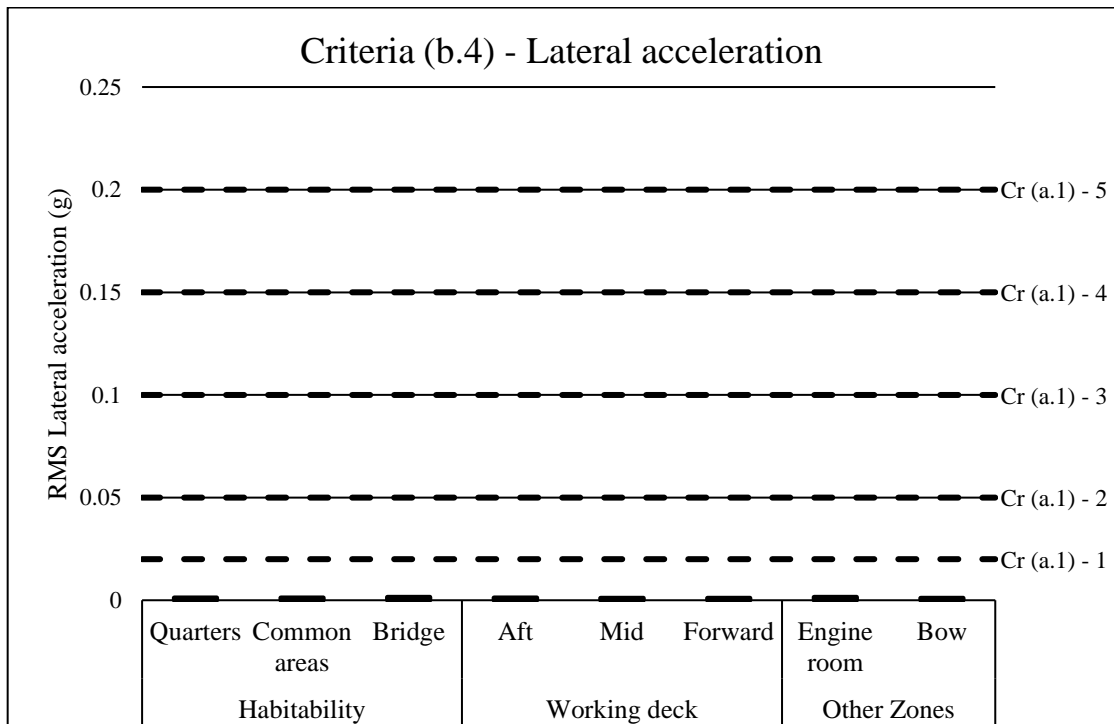


Figure D-28: Condition 07 – Lateral acceleration criteria

Condition 08

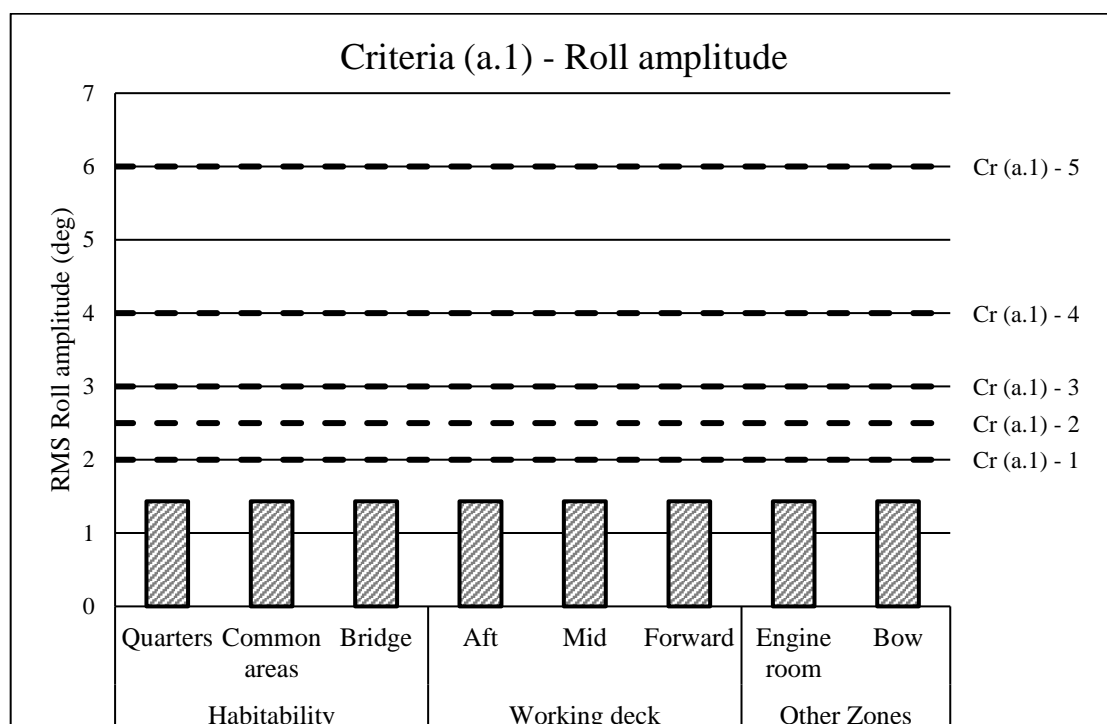


Figure D-29: Condition 08 – Roll amplitude criteria

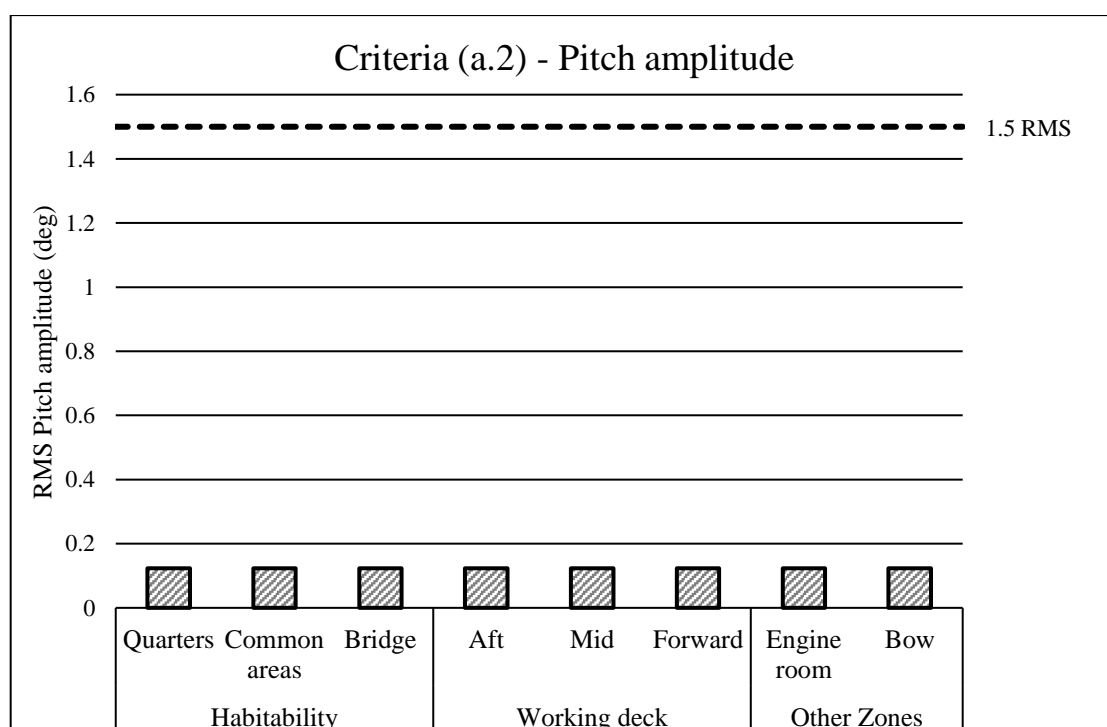


Figure D-30: Condition 08 – Pitch amplitude criteria

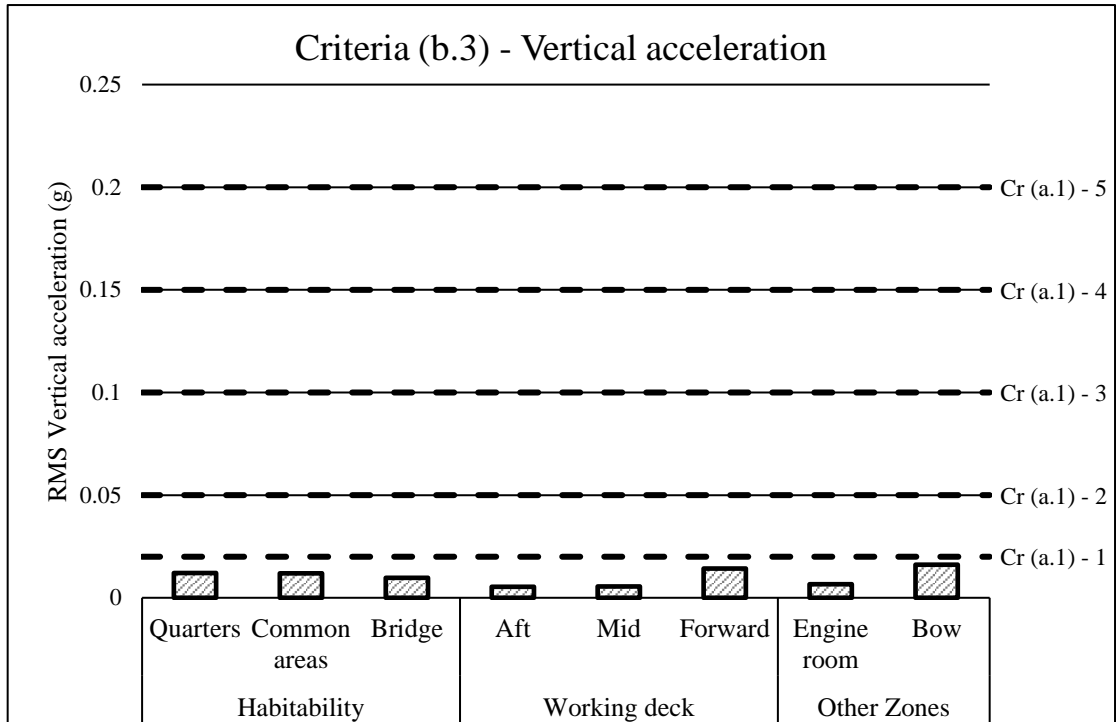


Figure D-31: Condition 08 – Vertical acceleration criteria

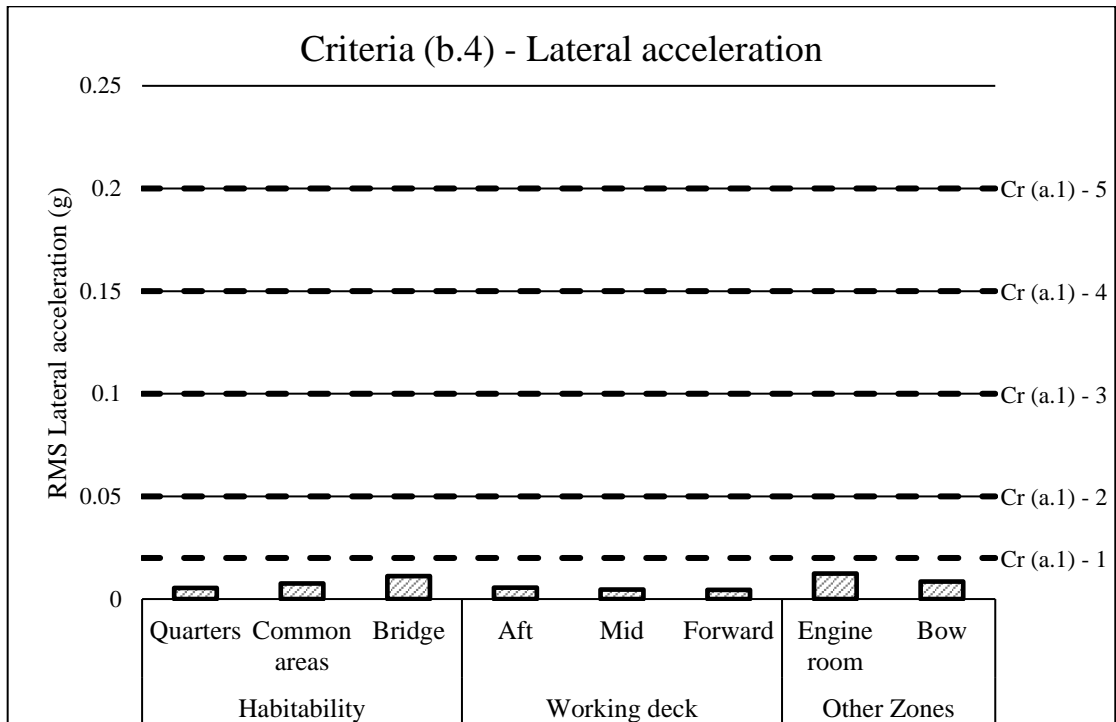


Figure D-32: Condition 08 – Lateral acceleration criteria

Condition 09

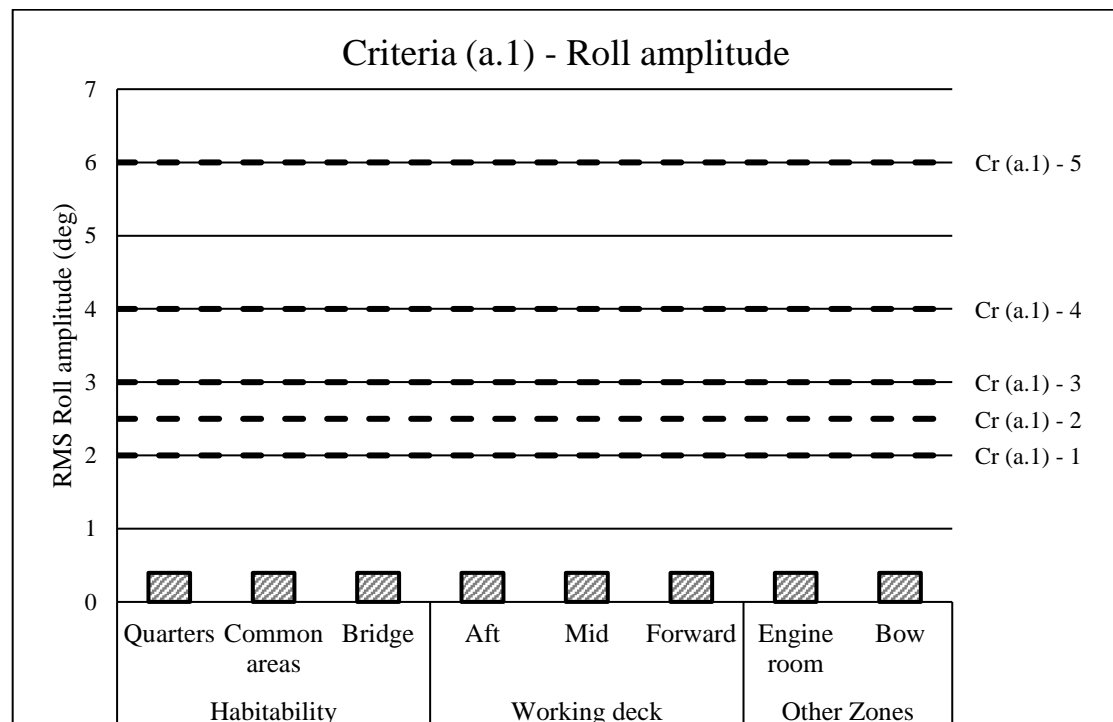


Figure D-33: Condition 09 – Roll amplitude criteria

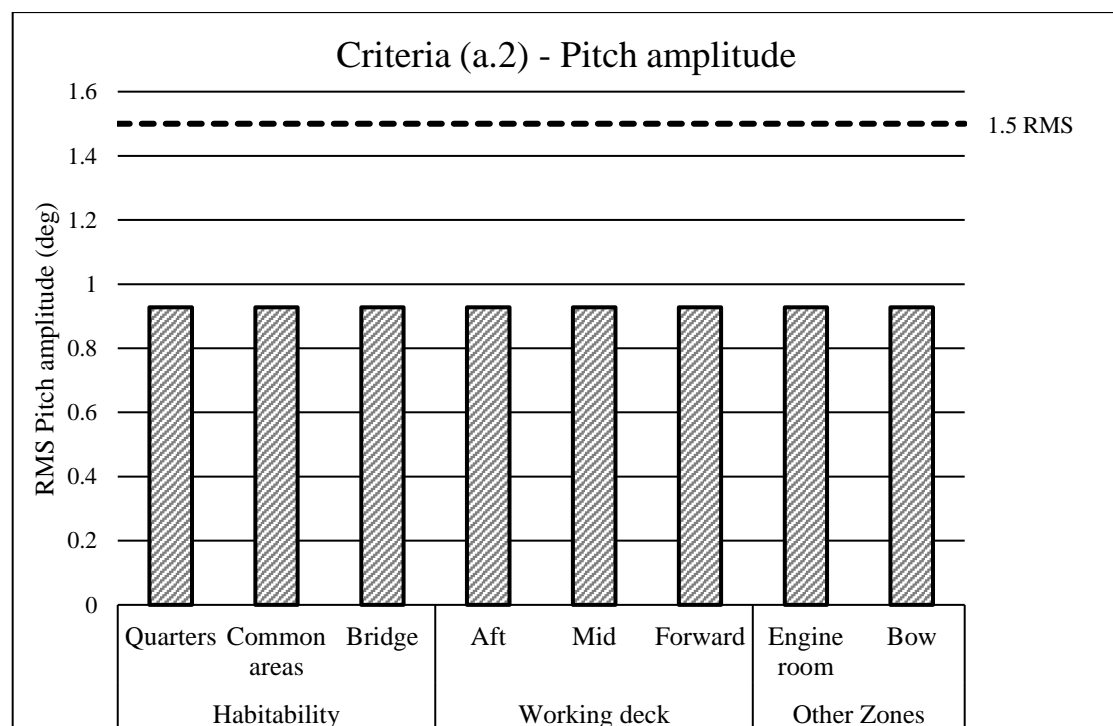


Figure D-34: Condition 09 – Pitch amplitude criteria

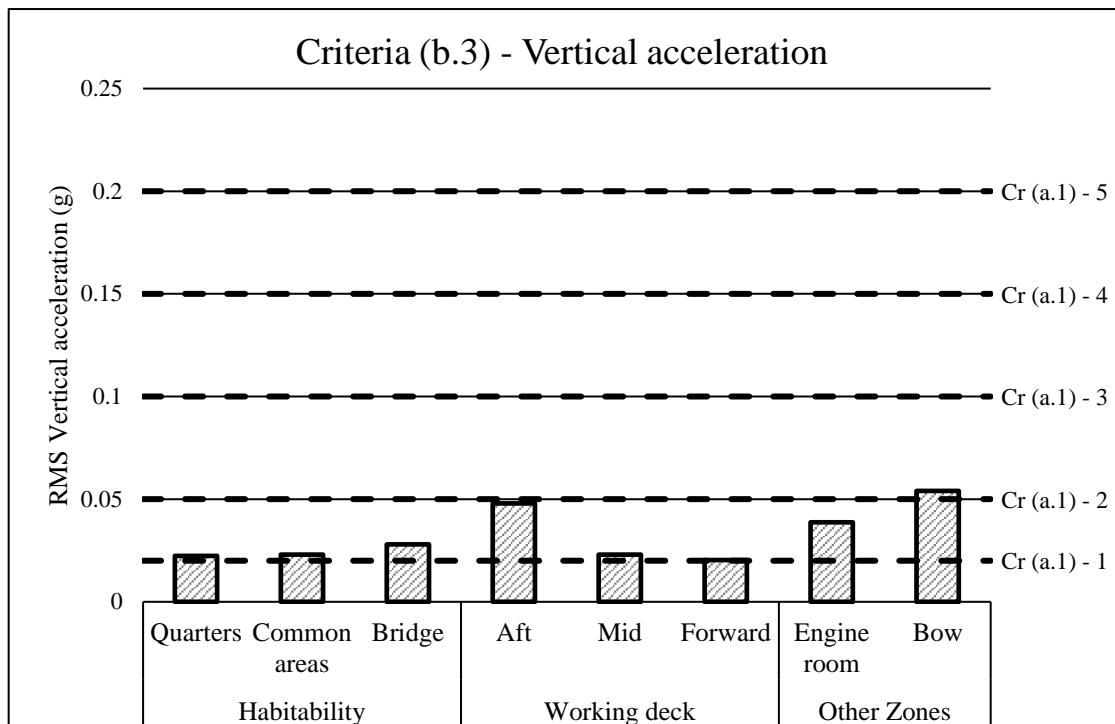


Figure D-35: Condition 09 – Vertical acceleration criteria

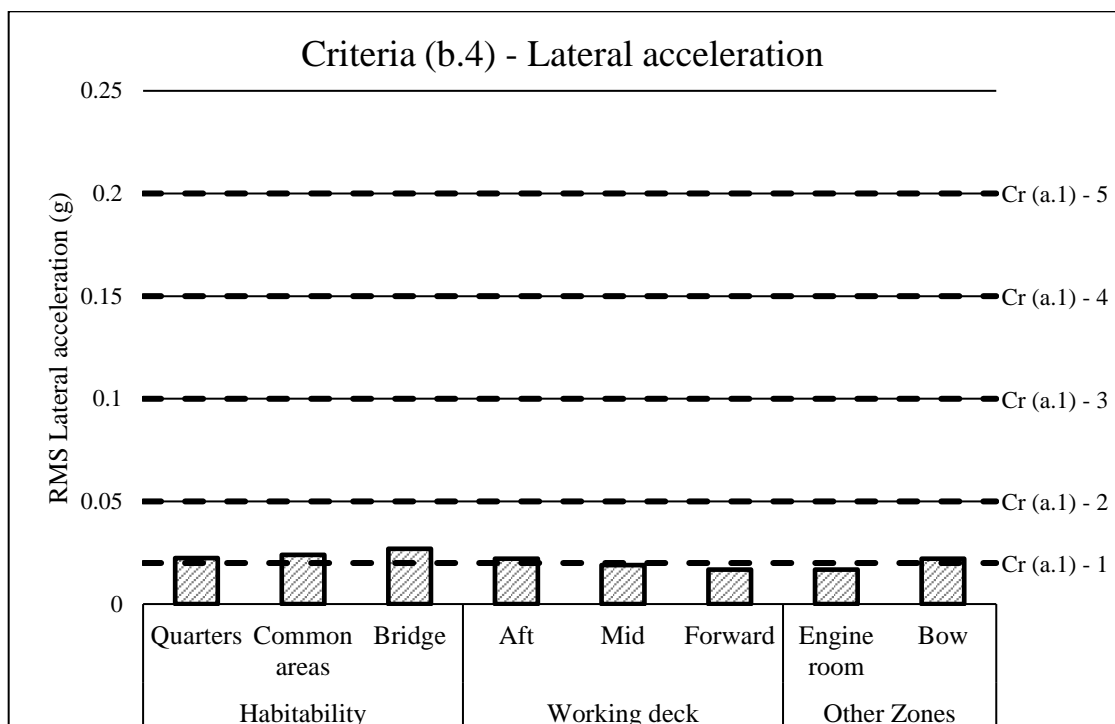


Figure D-36: Condition 09 – Lateral acceleration criteria

Condition 10

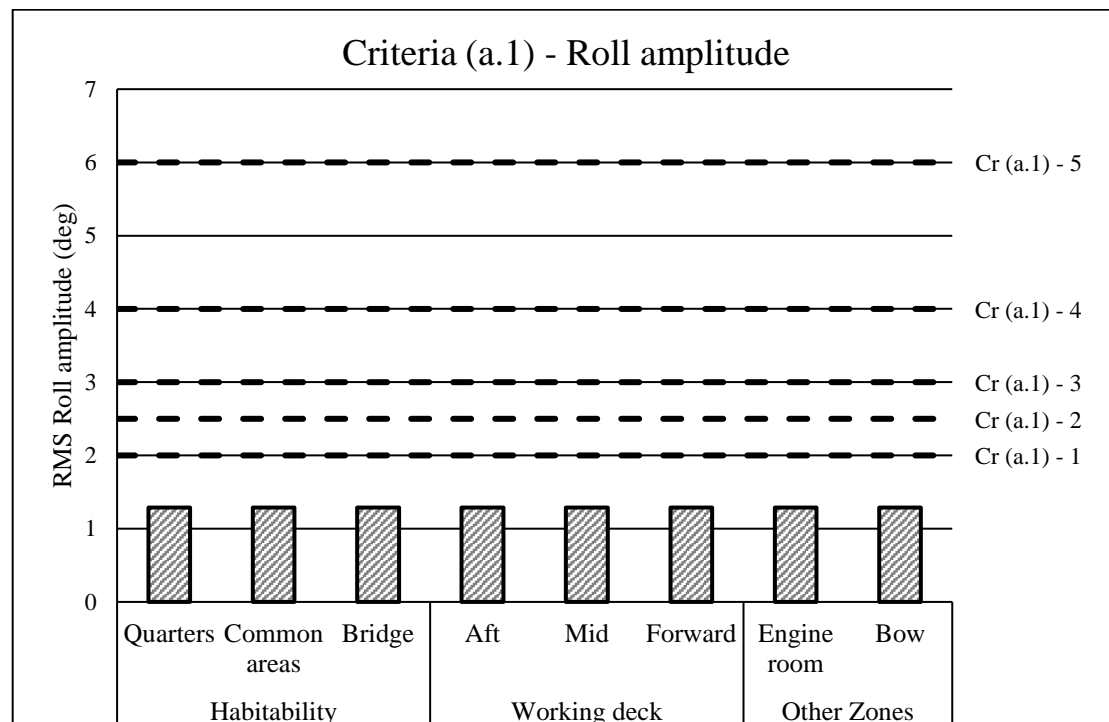


Figure D-37: Condition 10 – Roll amplitude criteria

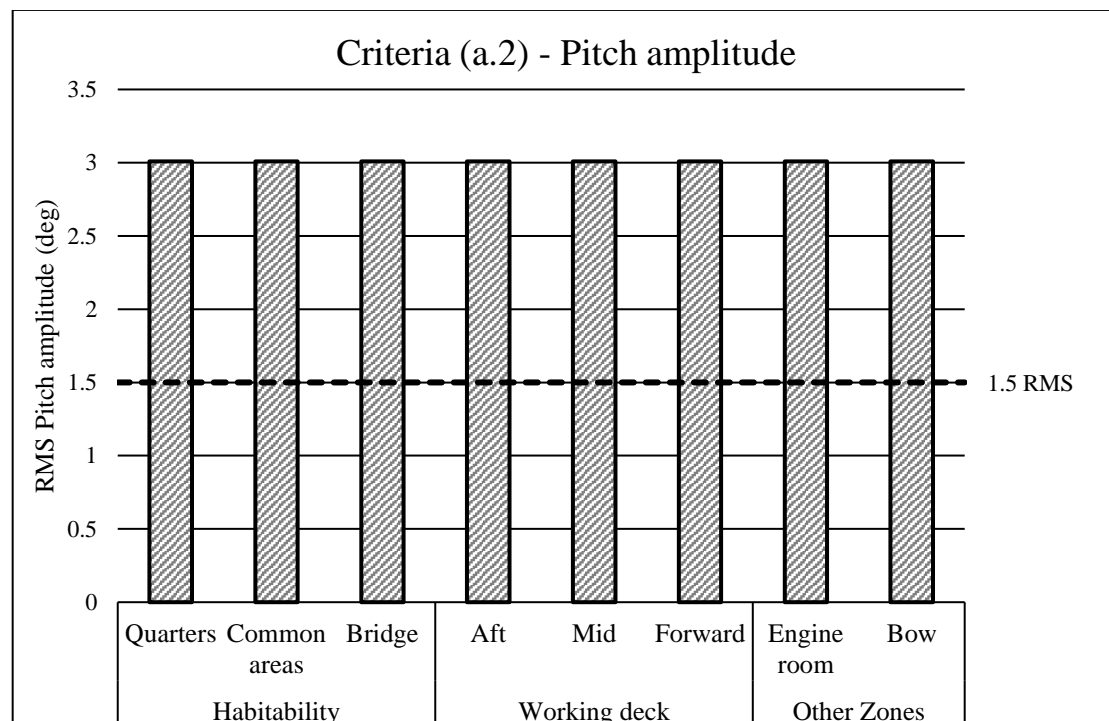


Figure D-38: Condition 10 – Pitch amplitude criteria

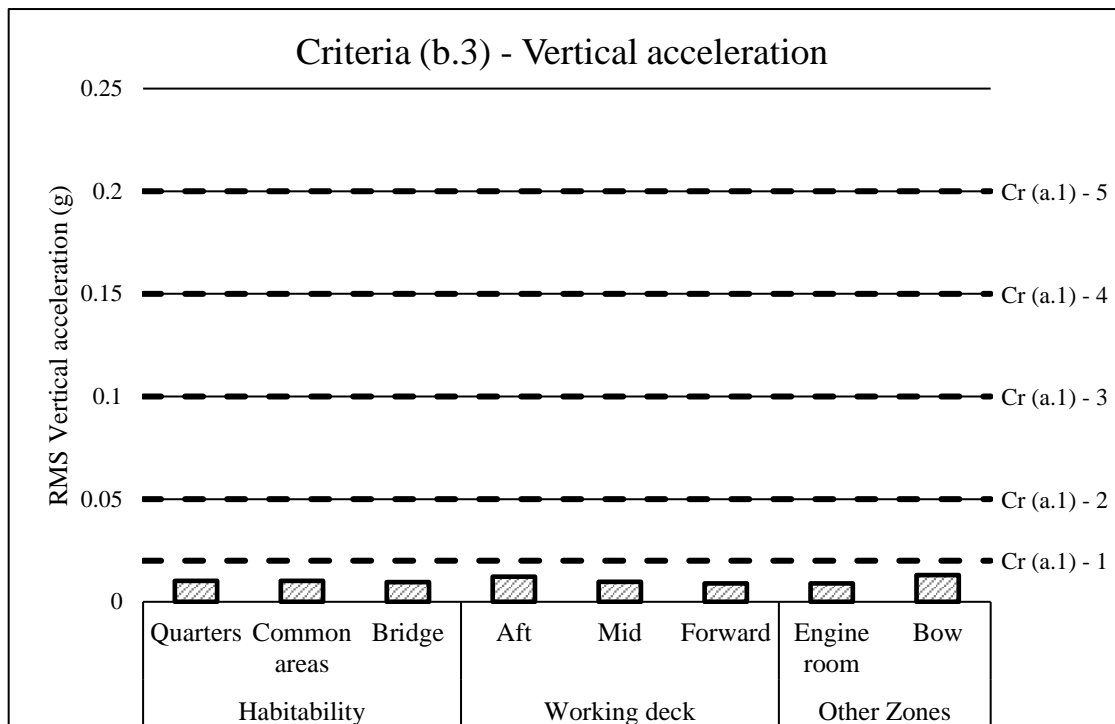


Figure D-39: Condition 10 – Vertical acceleration criteria

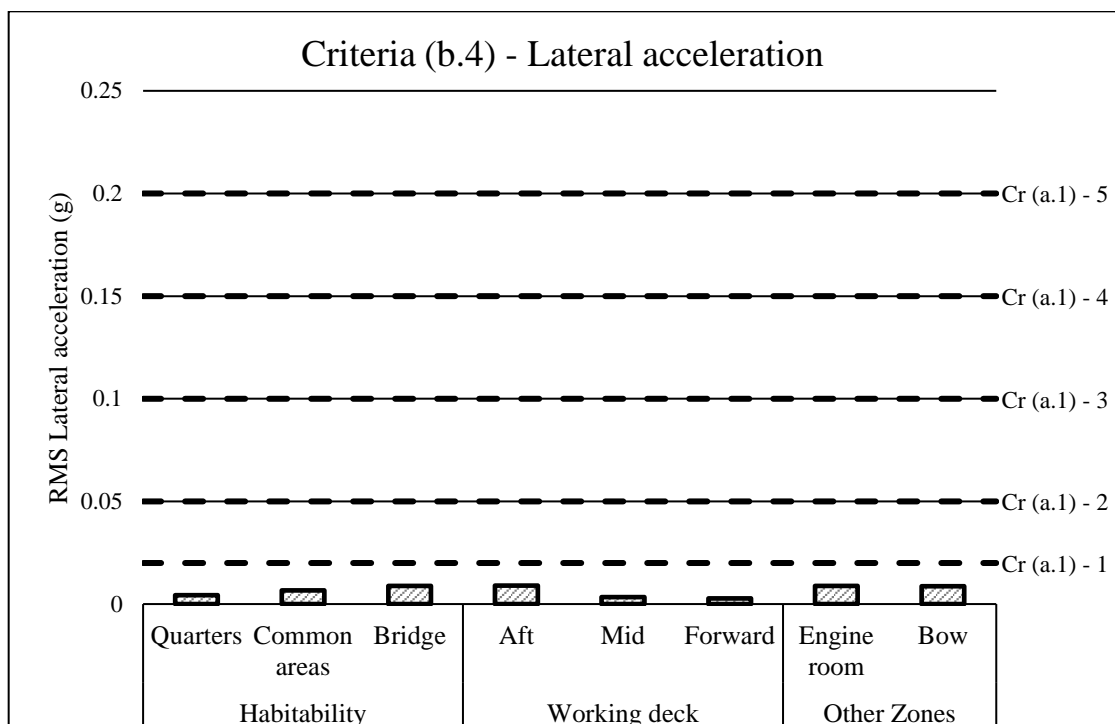


Figure D-40: Condition 10 – Lateral acceleration criteria

Condition 11

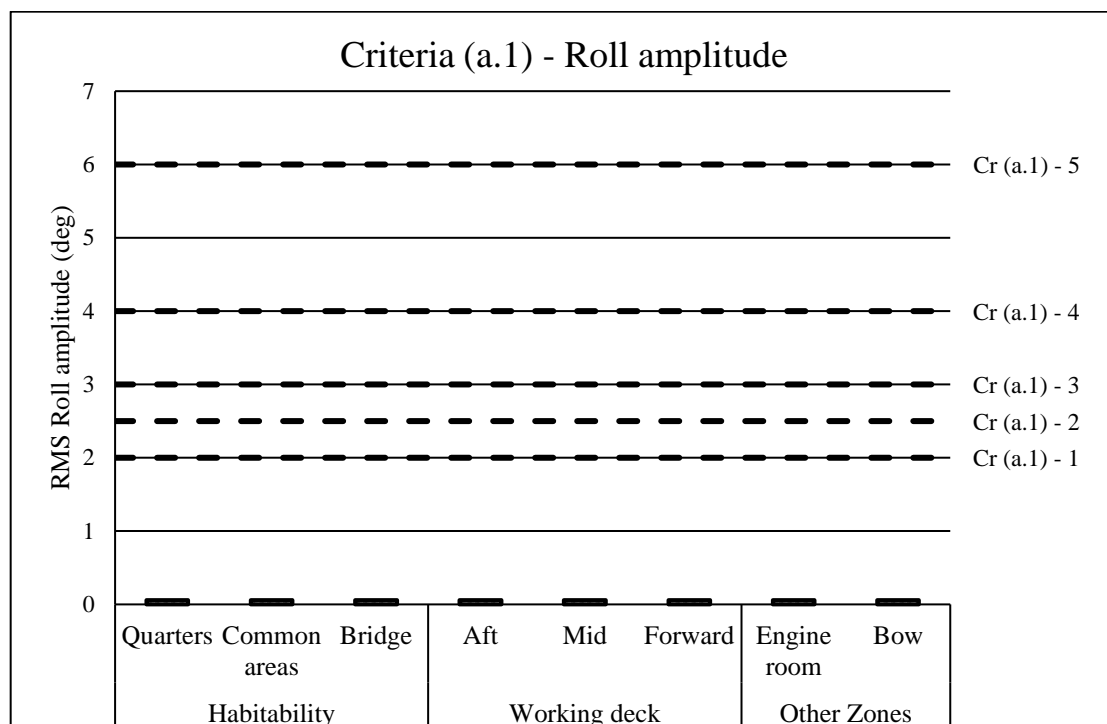


Figure D-41: Condition 11 – Roll amplitude criteria

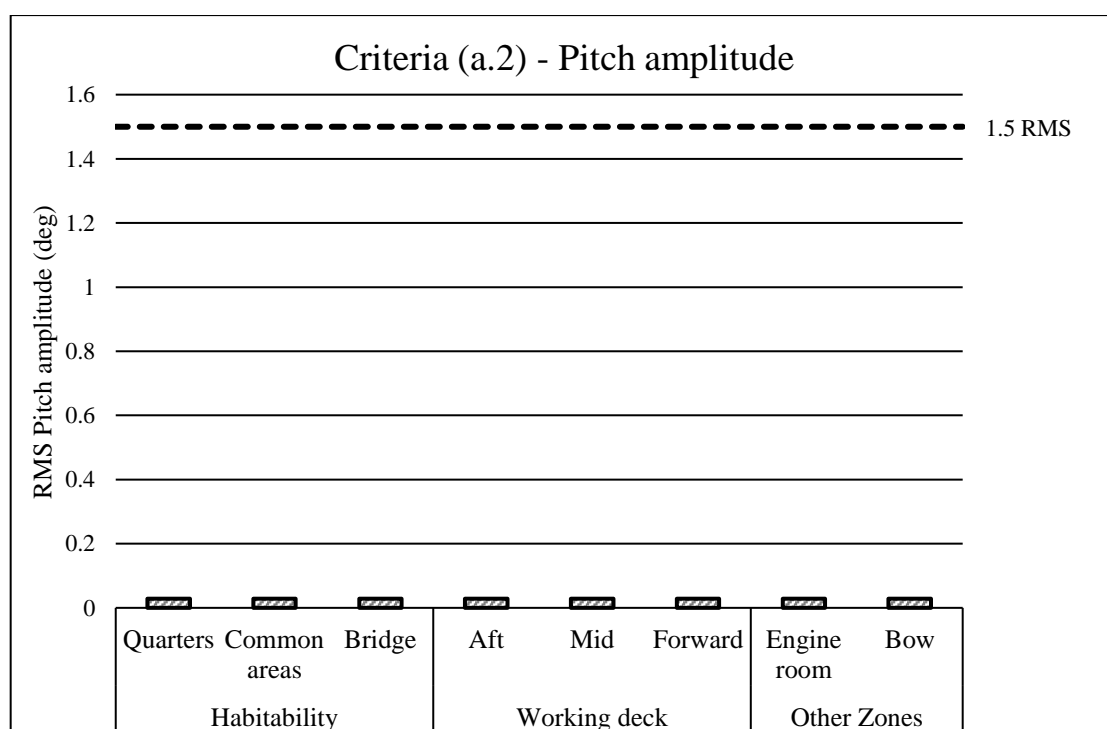


Figure D-42: Condition 11 – Pitch amplitude criteria

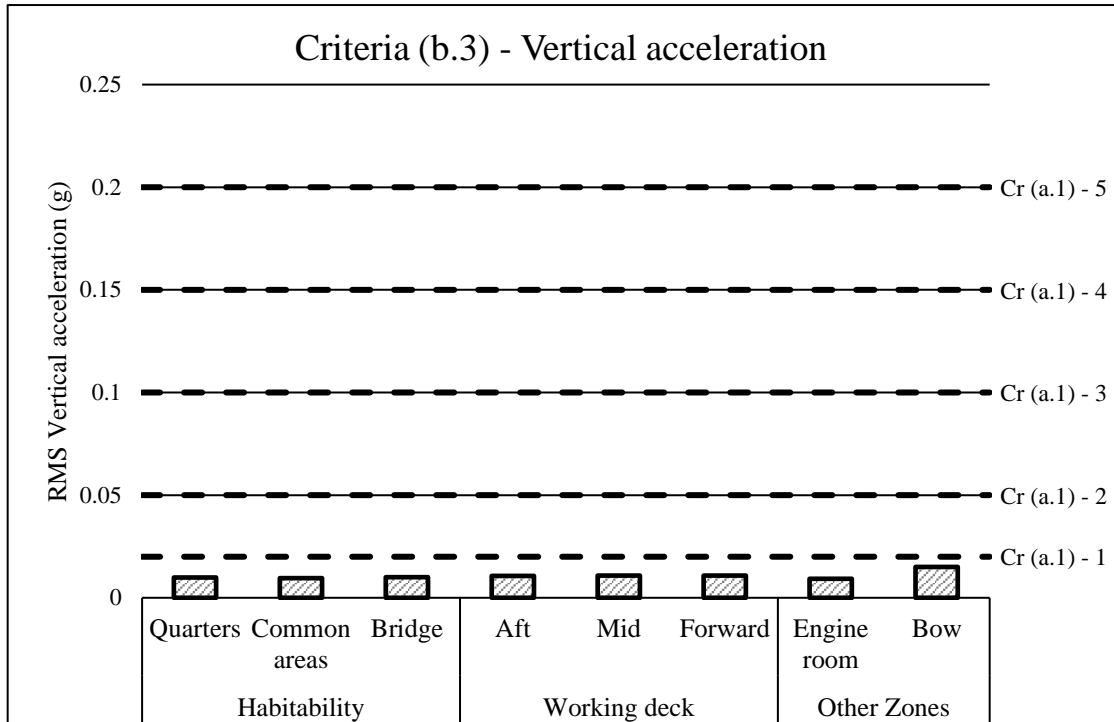


Figure D-43: Condition 11 – Vertical acceleration criteria

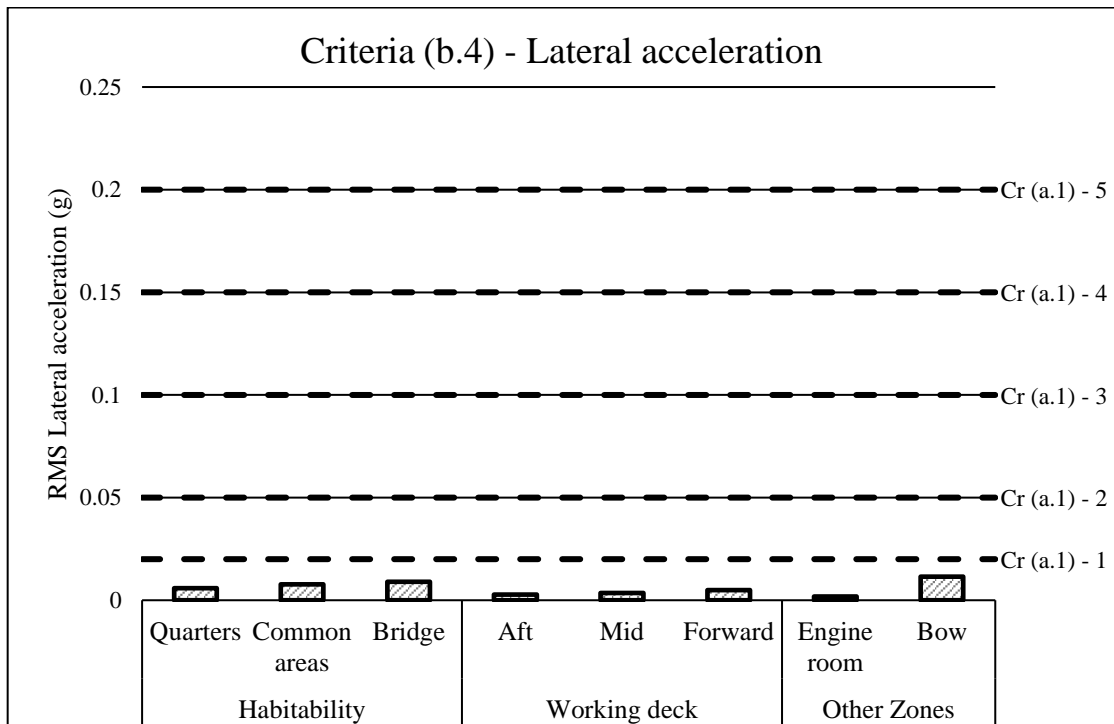


Figure D-44: Condition 11 – Lateral acceleration criteria

Condition 12

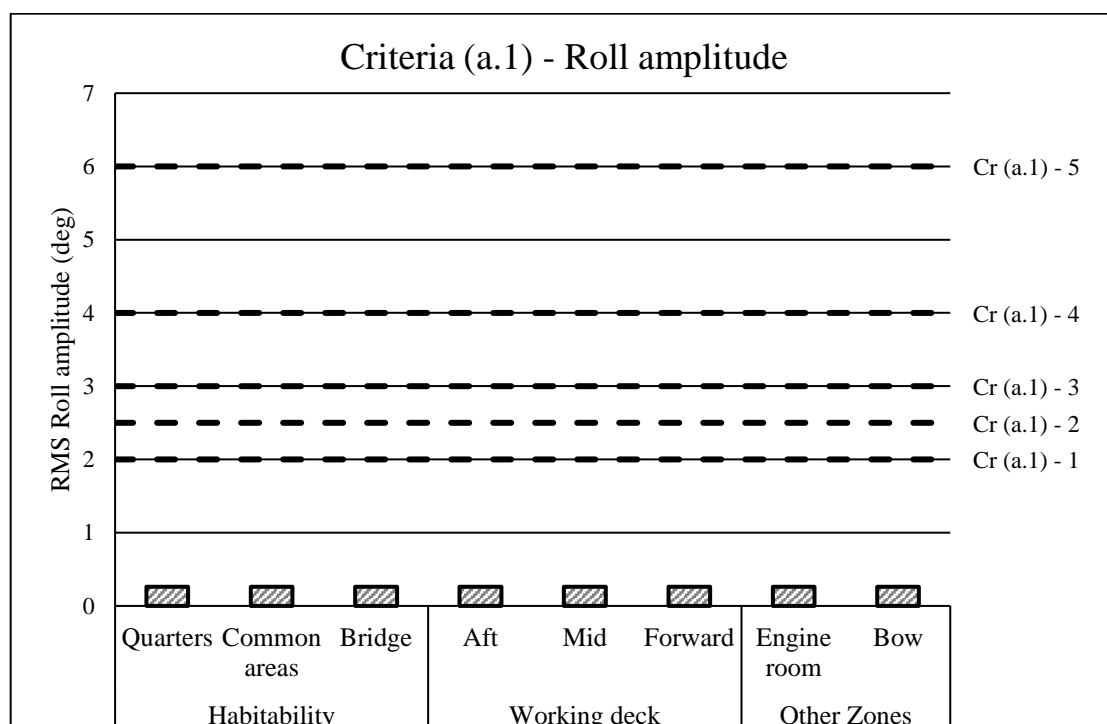


Figure D-45: Condition 12 – Roll amplitude criteria

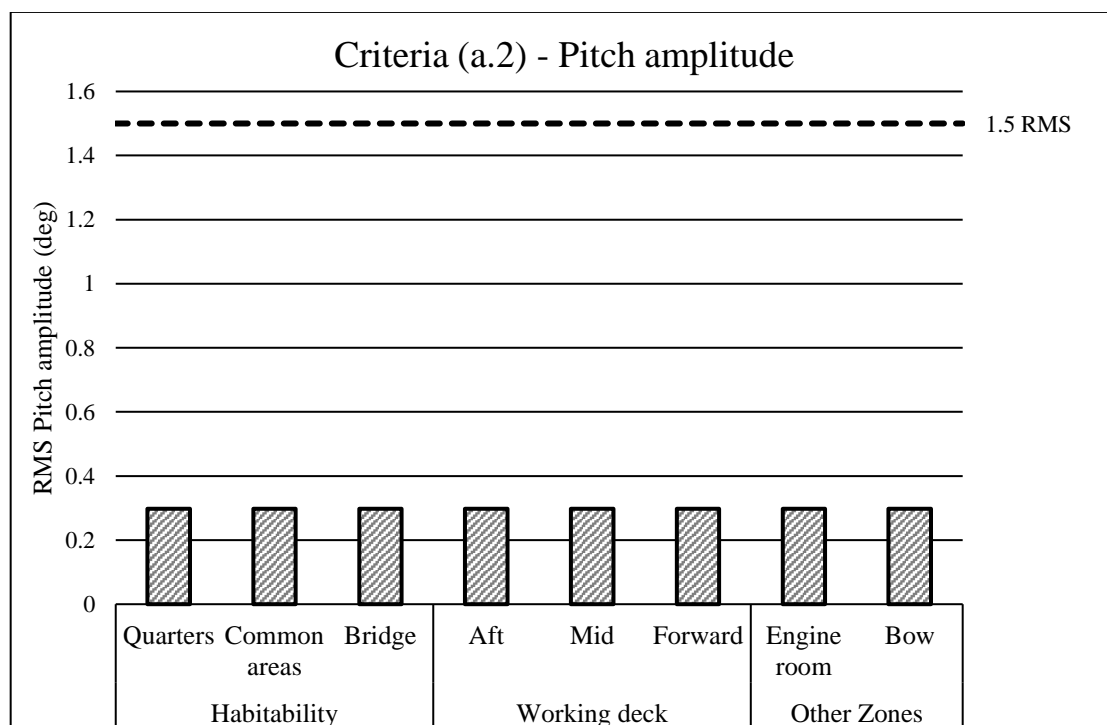


Figure D-46: Condition 12 – Pitch amplitude criteria

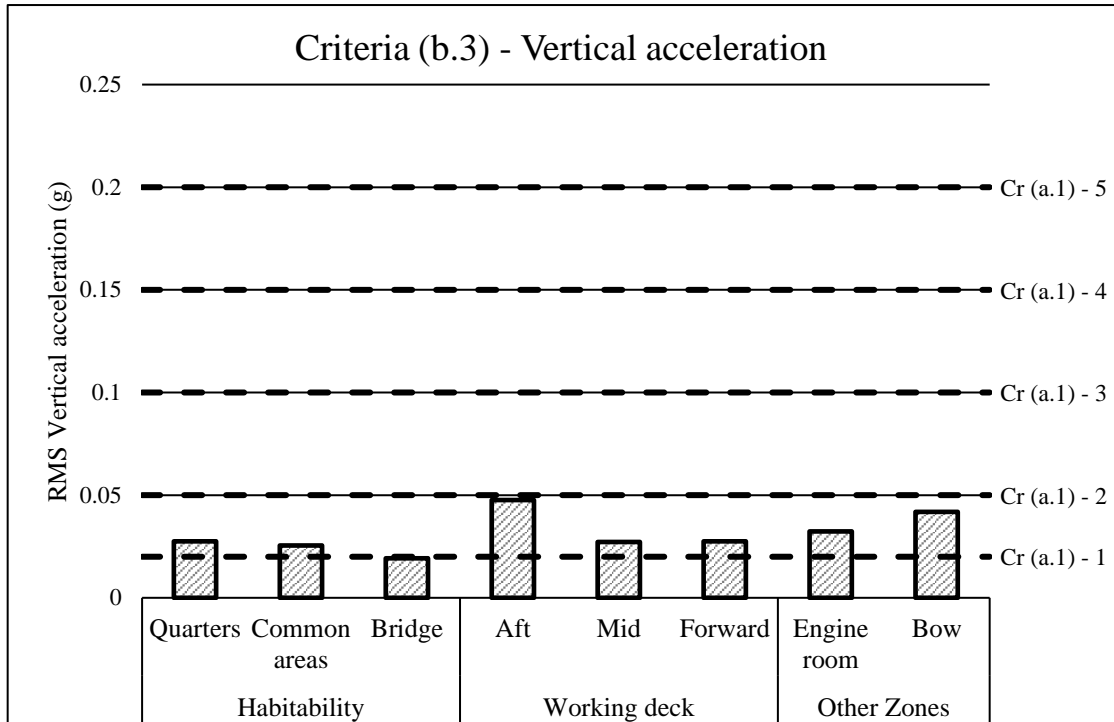


Figure D-47: Condition 12 – Vertical acceleration criteria

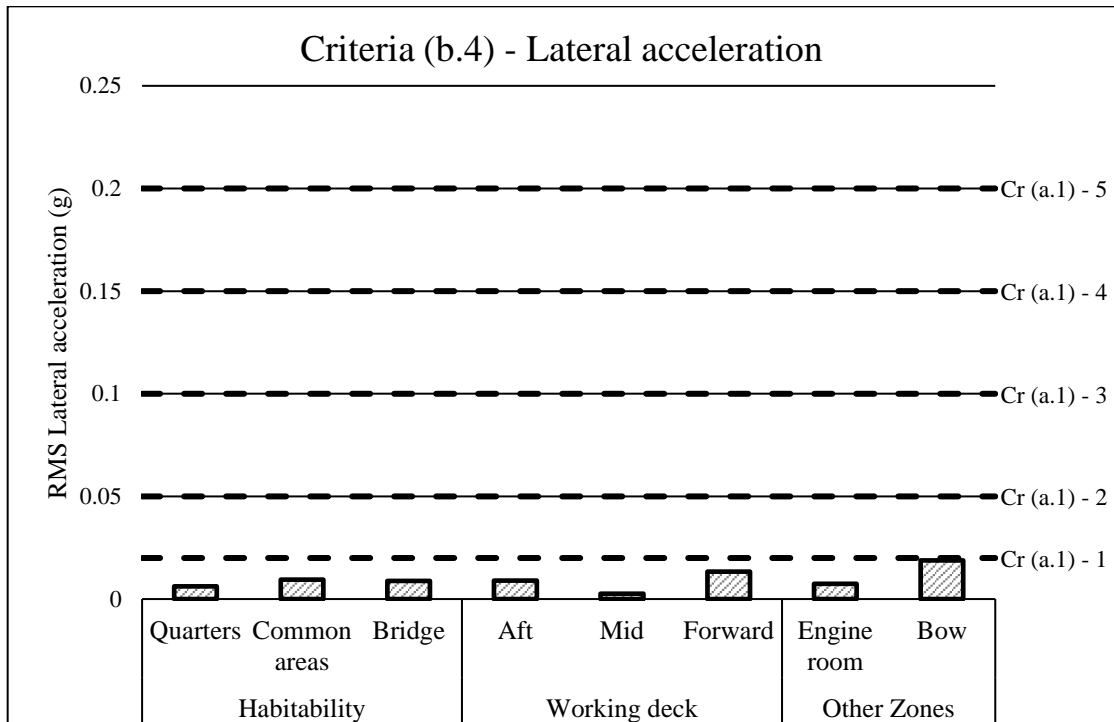


Figure D-48: Condition 12 – Lateral acceleration criteria

DEPARTMENT OF MECHANICS AND MARITIME SCIENCES

CHALMERS UNIVERSITY OF TECHNOLOGY

Gothenburg, Sweden 2021

www.chalmers.se



CHALMERS
UNIVERSITY OF TECHNOLOGY